석 사 학 위 논 문

Masters Dissertation

바이오폴리머를 처리한 세립토의 지반공학적 거동에 관한 연구

A Study on Geotechnical Behavior of Biopolymer Treated Fine Soils

2017

권 영 만 (權 寧 晩 Kwon, Yeong-Man)

한 국 과 학 기 술 원

Korea Advanced Institute of Science and Technology

석 사 학 위 논 문

바이오폴리머를 처리한 세립토의 지반공학적 거동에 관한 연구

2017

권 영 만

한 국 과 학 기 술 원

건설및환경공학과

바이오폴리머를 처리한 세립토의 지반공학적 거동에 관한 연구

권 영 만

위 논문은 한국과학기술원 석사학위논문으로
학위논문 심사위원회의 심사를 통과하였음

2017년 6월 5일

심사위원장 조 계 춘 (인)
심 사 위 원 이 승 래 (인)
심 사 위 원 김 동 수 (인)
심 사 위 원 권 태 혁 (인)

A Study on Geotechnical Behavior of Biopolymer Treated Fine Soils

Yeong-Man Kwon

Advisor: Gye-Chun Cho

A dissertation/thesis submitted to the faculty of
Korea Advanced Institute of Science and Technology in
partial fulfillment of the requirements for the degree of
Master in Civil and Environmental Engineering

Daejeon, Korea
June 5, 2017

Approved by

Gye-Chun Cho
Professor of Civil and Environmental Engineering

The study was conducted in accordance with Code of Research Ethics[1)].

1) Declaration of Ethical Conduct in Research**:** I, as a graduate student of Korea Advanced Institute of Science and Technology, hereby declare that I have not committed any act that may damage the credibility of my research. This includes, but is not limited to, falsification, thesis written by someone else, distortion of research findings, and plagiarism. I confirm that my dissertation contains honest conclusions based on my own careful research under the guidance of my advisor.

MCE 20154327

권영만. 바이오폴리머를 처리한 세립토의 지반공학적 거동에 관한 연구. 건설및환경공학과. 2017년. 97쪽. 지도교수: 조계춘. (영문 논문)

Yeong-Man Kwon. The micro interaction of biopolymer with clay materials. Department Civil and Environmental Engineering. 2017. 97 pages. Advisor: Gye-Chun Cho. (Text in English)

초 록

지난 20 세기 인류는 시멘트, 콘크리트 등의 신소재를 바탕으로 엄청난 성장을 일구어냈다. 그러나 시멘트 류의 소재는 지구 환경에 악영향을 끼쳤으며, 이로 인해 지반 공학을 포함한 토목 공학은 환경파괴의 주범으로 인식되는 실정이다. 이러한 문제를 해소하기 위해, 다양한 연구자들이 친환경 지반 신소재를 찾고자 하는 노력을 하고 있으며, 그 중 바이오폴리머가 친환경 지반보강재로 각광받고있다. 바이오폴리머는 사질토 지반을 코팅하거나 점토질과 전기적 작용을 하는 방법으로 흙 간의 결합을 향상시켜 강도를 증진하는 성능을 지니고 있으며, 지반의 투수성을 저감시키는 등의 역할을 할 수 있다는 선행연구가 있다. 본 학위논문에서는 특히 세립토에 집중하여, 바이오폴리머가 세립토에 처리 되었을 때 바이오폴리머의 거동을 확인하고 평가하고자 한다. 바이오폴리머 처리된 점토질의 액소성한계 등 토양 연경도의 변화를 살펴보았으며, 바이오폴리머의 점토 침전 성능을 평가했다. 또한 대표적인 세립토 환경 중 하나인 갯벌토를 활용해, 현장 함수비에서 갯벌토에 바이오폴리머를 처리했을 때의 성능 증진효과를 관측했다. 본 연구를 바탕으로 바이오폴리머의 전기적 작용에 관한 심층적 이해가 가능하다.

핵 심 낱 말 바이오폴리머, 세립토, 토양 연경도, 침전, 갯벌

Abstract

In the 20th century, humankind has made tremendous growth based on new materials such as cement and concrete. However, cement has adversely affected the global environment, and geotechnical engineering is being stigmatized as the main cause of environmental destruction. In order to solve these problems, various researchers have been trying to find new environmentally friendly new materials, among which biopolymers are attracting attention as eco-friendly ground reinforcements. Previous researchers found that biopolymers have the ability to improve the strength by increasing the bonding between the soil by coating the sandy soil and electrically acting with the clay, and can play a role of reducing the permeability of the ground. This dissertation evaluate the behavior of the biopolymer when the biopolymer is treated with fine soil. Changes in soil consistency such as liquid limit and plastic limit of biopolymer treated clay were examined and sedimentation performance of biopolymer treated fine soils was evaluated. In addition, this research observed the effect of biopolymer on improving the performance of the tidal flats, one of the representative soft ground environment consisted of fine soil. Based on this study, it is possible to understand in depth the electrical action of biopolymer.

Keywords Biopolymer, Fine soil, Soil consistency, Sedimentation, Tidal flat

Contents

List of Tables

List of Figures

Chapter 1. Introduction

1.1 Soft ground improvement

The field of improvement of the ground is one of the important construction fields that has been continuously developed since the beginning of humankind. Neolithic mankind in 3000 BC used technology to spread talc and harden with coal on soft ground, and bitumen or sticky rice mortars were also used as ground improvement materials from ancient times (Potts, 1997, Yang, Zhang and Ma, 2010).

Soft ground refers to the ground that does not have sufficient bearing capacity for the foundation so that it cannot support the upper structure. Generally, it is a term referring to the ground that is consisted of clay, organic soil and loose sandy soil. The term generally refers to clay, organic soil, and loose sandy soil with high shrinkage and low uniaxial compressive strength. Composition of soft ground generally consist of soft, compressible clay, silt, and peat with a standard cone penetration test N value of 0 to 4 and are found in many new alluvial deposits such as deltas, drowned valleys, and tidal flats. Also, loose sand of N <10 is classified as soft ground even when it has high water content, and there is a possibility of liquefaction due to dynamic load such as vibration or earthquake.

Typical methods of improving the ground developed in the history of geotechnical engineering include: 1) Mechanically stabilizing it by mixing soil with different particle size distribution to unevenly distributed sandy soil or applying vibration or impact to the sandy soil. 2) Ground improvement method by substitution that removes soft soil from the surface and replenishes with soil of good quality to improve ground. 3) Soil improvement by compaction drainage that compresses and dries moisture-rich clay soils to reduces water content and enhance the ground strength. 4) Ground improvement method by reinforcement that inserts geotextile etc. into the ground. 5) Improvement of ground by chemical cementation that improves soil strength by injecting chemical substance typified by cement into the ground.

Since the existing soft ground improvement method can detrimentally affect the environment such as global warming, groundwater pollution, and destruction of ecosystem, the demand for environmentally friendly soft ground improvement method is increasing.

1.2 Biopolymer

The biopolymer is a polysaccharide substance that occurs due to microbial metabolic activity. Biopolymers have little effect on the environment, and they improve the physical properties of soil through electrical bonding with clay particles. Thus, it has been attracting attention as eco-friendly ground reinforcements (Ayeldeen, Negm and El Sawwaf, 2016, Chang, Prasidhi, Im and Cho, 2015). Biomolecules with geotechnical potential include xanthan gum, gellan gum, agar, guar and ε-polylysine.

This study examines the possibility of improving soft ground using biopolymer. First, the behavior of biopolymer treated fine soils was analyzed at various pore fluid chemistry, and classified biopolymer treated fine soil using newly suggested classification system. In addition, a study on the coagulation and sedimentation efficiency of biopolymer by electrical reaction with clay was carried out. Finally, biopolymer treatment is applied to tidal flats, one of the soft ground types, to study the applicability of biopolymers to tidal flat enhancement through the enhancement of strength and sedimentation efficiency.

Chapter 2. Literature Review

2.1 Research background

Geotechnical engineering is a field of engineering that systemizes the theory and practice to improve the quality of human life, with soil as a natural substance. Structures such as beautiful and beautiful buildings, bridges, roads, railways, dams and tunnels cannot float in the air, and can function only if they rely on ground or soil. Thus, geotechnical engineering is the basis of civil engineering.

The field of improvement of the ground is one of the important construction fields that has been continuously developed since the beginning of humankind. Neolithic mankind in 3000 BC used technology to spread talc and harden with coal on soft ground, and bitumen or sticky rice mortars were also used as ground improvement materials from ancient times (Potts, 1997, Yang, Zhang and Ma, 2010).

Typical methods of improving the ground developed in the history of geotechnical engineering include: 1) mechanically stabilizing it by mixing soil with different particle size distribution to unevenly distributed sandy soil or applying vibration or impact to the sandy soil. 2) Ground improvement method by substitution that removes soft soil from the surface and replenishes with soil of good quality to improve ground. 3) Soil improvement by compaction drainage that compresses and dries moisture-rich clay soils to reduces water content and enhance the ground strength. 4) Ground improvement method by reinforcement that inserts geotextile etc. into the ground. 5) Improvement of ground by chemical cementation that improves soil strength by injecting chemical substance typified by cement into the ground.

Among the chemical soil improvement method, usage of Portland cement was developed in 1824 and it was used as a main soil improvement material after industrial revolution (Blezard, 1998). Portland cement is a binder made from the most abundant elements on earth. The main constituents of Portland cement, O2, Si, Al, Fe, and Ca, account for about 91% of the Earth element composition and if trace elements such as Na, K, Mg, H, S are included, it increases up to about 99% (Turekian and Wedepohl, 1961). In addition, it has various advantages such as high strength and durability. Thus, Portland cement played a role in driving industrial development as a ground material (Poon, Azhar, Anson and Wong, 2001). However, various environmental problems resulting from the use of cement have a great influence on spreading the perception that geotechnical engineering is one of the main causes of environmental destruction (Chen, Habert, Bouzidi and Jullien, 2010).

Various environmental problems caused by cement use

Portland cement industry is a high carbon dioxide (CO_2) emissions industry that produces about 0.4 tons of carbon dioxide (CO_2) per 1 ton of cement produced by calcination and combustion of coal fuels. Additionally, Hydration to form calcium carbonate (i.e., $5CaCO_3 + 2SiO_2 \rightarrow 3CaO{\cdot}SiO_2 + 2CaO{\cdot}SiO_2 + 5CO_2$) also produces 0.55 tons of CO_2 per 1 ton of cement produced. It accounts for about 5-7% of global CO_2 emissions (Larson, 2011).

Cement production worldwide is projected to reach 5 billion tons by 2030 (fig 2.1 (a)). Based on the generation of about 0.95 tons of carbon dioxide per ton of cement production, the cement industry is estimated to produce about 4.8 billion tons of CO_2 annually (Initiative, 2009) (Humphreys and Mahasenan, 2002) (fig 2.1 (b)). The enormous amount of carbon dioxide produced by cement is a major cause of global warming and, therefore, various studies have been conducted to reduce the use of cement.

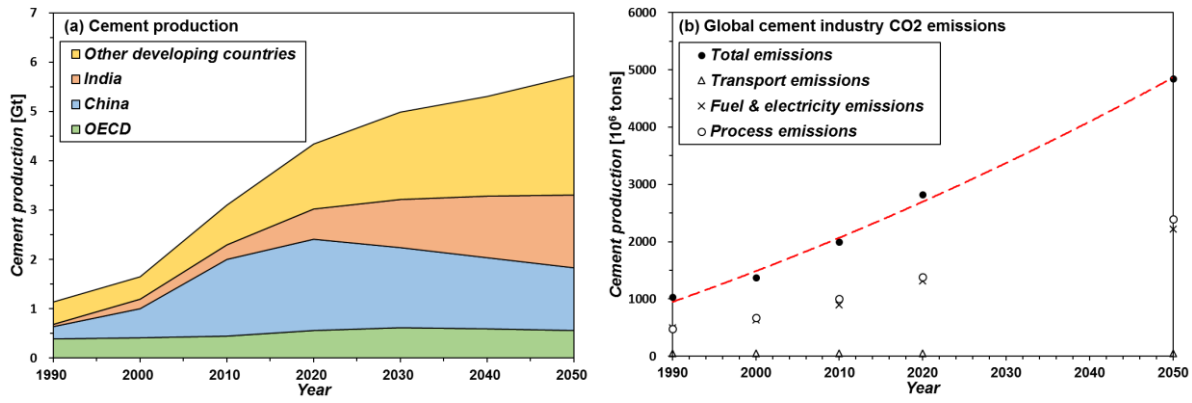

Figure 2.1 (a) Cement production in industrialized and developing countries based on Cement Sustainability initiative, 2009 and (b) CO2 emissions of cement industry based on Humbhreys, 2002.

In addition to global warming due to carbon dioxide emissions, cement causes various problems such as groundwater contamination, river pollution, and human hazards due to dust. Cement kiln contains heavy metals such as chromium and is included in the cement during production. These heavy metals have harmful effects on human body such as skin, bone, teeth disease, cancer. During the cement construction, heavy metals such as hexavalent chromium, which is a carcinogenic substance, leach out and pollute the ground water and soil environment and harm the human body (Hills and Johansen, 2007).

Also thereby during ground improvement process using the calcium oxide, lime reacts with the soil and increase the soil pH. When the pH is higher than 9.5 due to strong alkalinity, the ecosystem is adversely affected (Richman, Tucker and Koehler, 2006). Dust from cement also affects the respiratory system, causing pulmonary dysfunction such as pneumoconiosis. In addition, free silicate contained in cement dust causes lung cancer, pneumoconiosis, and chronic obstructive pulmonary disease. Furthermore, it causes inflammatory changes in the skin. It is caused by the allergic component (Cr, Nr, Co) and the irritant substance contained in the dust. Therefore, there is a growing demand for new environment friendly materials that can solve various side effects caused by cement use. (Doerr, 1952, Humans, Cancer and Organization, 1997).

In order to solve the environmental problems caused by the use of Portland cement, researches on the improvement of the ground using various eco-friendly materials have been conducted. In particular, researches on the improvement of the ground using the biopolymer have been continuously carried out.

Previous studies on the effect of biopolymer on soil improvement

The biopolymer is a polysaccharide substance that occurs due to microbial metabolic activity. Biopolymers have little effect on the environment, and they improve the physical properties of soil through electrical bonding with clay particles. Thus, it has been attracting attention as eco-friendly ground reinforcements (Ayeldeen, Negm and El Sawwaf, 2016, Chang, Prasidhi, Im and Cho, 2015).

Previous research data on the engineering properties of biopolymer treated soil are summarized visually in figure 2.2. Biopolymer increases the compressive strength of soil particles via binding soil particles by the direct interaction with fine soil particles. Previous researches proved that agar, starch, xanthan gum, guar gum, beta-glucan and gellan gum biopolymer increases the compressive strength of soil. Khatami and O'Kelly at 2012 conducted the triaxial compression tests using the Fontainebleau sand with particle size of 0.06 to 0.4mm (Khatami and O'Kelly, 2012). Result indicated that the unconfined compressive strength of the sand ranged from 158 to 487 kPa by agar with 1-4% BP/soil concentration and starch with 0.5-1% BP/soil concentration. Another studies also proved that the 3% concentration of agar gum can increase the unconfined compressive strength of soil up to 10 MPa (Chang, Prasidhi, Im and Cho, 2015). Gellan gum also enhances the compressive strength of soil. Chang et al at 2015 conducted the unconfined compression tests with gellan gum treated clayey soil and it was shown that the 3% gellan gum treated soil reaches 12.6 MPa of unconfined compressive strength (Chang, Prasidhi, Im and Cho, 2015). Additionally, gellan treated jumunjin sand, Korean representative sand, had higher unconfined compressive strength, which is 434 kPa than that of 12% cement treated sands (380 kPa). Ayeldeen et al at 2016 also measured the unconfined compressive strength of silt with xanthan gum, modified starch, guar gum (Ayeldeen, Negm and El Sawwaf, 2016). Result proved that the unconfined compression stress increased to 338kPa with xanthan gum, 570kPa with modified starch and 840kPa with guar gum. Latifi et al at 2016 conducted unconfined compression strength tests on xanthan gum, with the concentration of 1 and 1.5%, treated montmorillonite and kaolinite (Latifi, Horpibulsuk, Meehan, Abd Majid, Tahir and Mohamad, 2016). The 28-day UCS of 1% xanthan gum treated bentonite (2,580 kPa) increases 9 times higher than that of untreated bentonite (286 kPa). Additionally, the 28-day UCS of 1.5% xanthan gum treated kaolinite (1,180 kPa) is 8 times higher than that of untreated kaolinite (150 kPa). Beta-glucan biopolymer also can increases the compressive strength of soil. With a small amount of beta-glucan (0.25%), the compressive strength of soil reaches

2,650 kPa which is stronger than that of 10% cement mixed soil (2,170 kPa). Additionally, compressive strength 0.5% of beta-glucan treated soil reaches 4,310 kPa (Chang and Cho, 2012).

The shear strength is important for geotechnical engineering structures such as the stability of slope, foundations, earth retaining structures and embankments (Vanapalli, Fredlund, Pufahl and Clifton, 1996). Biopolymer can increases the shear strength of soil particles. It occurs due to the chemical bonding between biopolymer and soil. The adhesive forces between biopolymer and soil particles grip the soil particles and the cohesion increases. The biopolymer also has effect on the friction angle. Biopolymer covers soil particles and decreases the particle roughness. Thus, smoothed surface slightly decreases the friction angle. Previous research found that xanthan gum, modified starch, guar gum increases the shear strength of soil particles. Khatami and O'Kelly at 2012 computed shear parameters of agar and starch treated sand using the triaxial test datum. The result indicated that the cohesion increased from 0 (untreated sand) to 240 kPa (1% agar and 1% starch) and the friction angle decreased from 32.3 (untreated sand) to 17.5 degrees (1% agar and 0.5% starch) (Khatami and O'Kelly, 2012). Ayeldeen et al at 2016 estimated the effect of biopolymer (xanthan gum, modified starch, guar gum) on the shear strength of sand using the direct shear tests (Ayeldeen, Negm and El Sawwaf, 2016). The maximum cohesion (477 kPa) was measured with guar gum treated sand compared to the modified starch sample (309 kPa), xanthan gum treated sample (218 kPa). Latifi et al at 2016 also performed direct shear tests with montmorillonite and kaolinite (Latifi, Horpibulsuk, Meehan, Abd Majid, Tahir and Mohamad, 2016). The cohesion of BP treated samples increased by the curing time while the effect of curing time was smaller for friction angle. After 28 days of curing time, the cohesion of 1% xanthan gum treated montmorillonite (454 kPa) increases about 5 times than untreated montmorillonite (95 kPa). The 28-day cohesion of 1.5% xanthan gum treated kaolinite (316 kPa) increased about 6 times compared to the untreated soil. Friction angle slightly increased from 21 to 24 degrees for montmorillonite sample and 12 to 17 degrees for kaolinite specimen after 28 days of curing time. The existence of beta-glucan in soil enhances the shear stiffness. Previous research measured elastic wave velocity with beta-glucan treated Korean residual soil. The result proved that the existence of beta-glucan biopolymer increased the shear wave velocity and stiffness by enhancing the soil structure. However, the compressive wave velocity and stiffness were not drastically affected by beta-glucan biopolymer (Chang and Cho, 2012).

The soil at the liquid limit state has the undrained shear strength of 1.7-2.0 kPa. The undrained shear strength is affected by the water content. Thus, at the same water content, the soil with higher liquid limit has higher undrained shear strength than the soil with lower liquid limit (Watts, Tolhurst, Black and Whitmore, 2003). It indicates that the liquidity index of soil is important factor for shear resistance of soil. The biopolymer treatment in soil enhances the liquid limit of soil by the viscosity increase of pore fluid and the bonding characteristics of biopolymer with soil particles. Xanthan gum, guar gum can be applied to increases the liquid limit of soil. Additionally, the addition of cross-linking agents into biopolymers can drastically increases the liquid limit due to the enhancement of pore fluid viscosity (Nugent, Zhang and Gambrell, 2009). Guar gum showed more efficient effect on liquid limit and undrained shear strength than xanthan gum due to higher viscosity of guar gum solution than that of xanthan gum solution (Chen, Zhang and Budhu, 2013). Another previous research used the beta-glucan to analyze the effect of biopolymer on the liquid limit, plastic limit and plasticity index enhancements. The 0.8% concentration of beta-glucan in Korean residual soil increases the liquid limit up to 100% (46.3% increase compared to untreated soil). Plastic limit at the same concentration increased up to 52% from 37.4% of untreated sample (Chang and Cho, 2014).

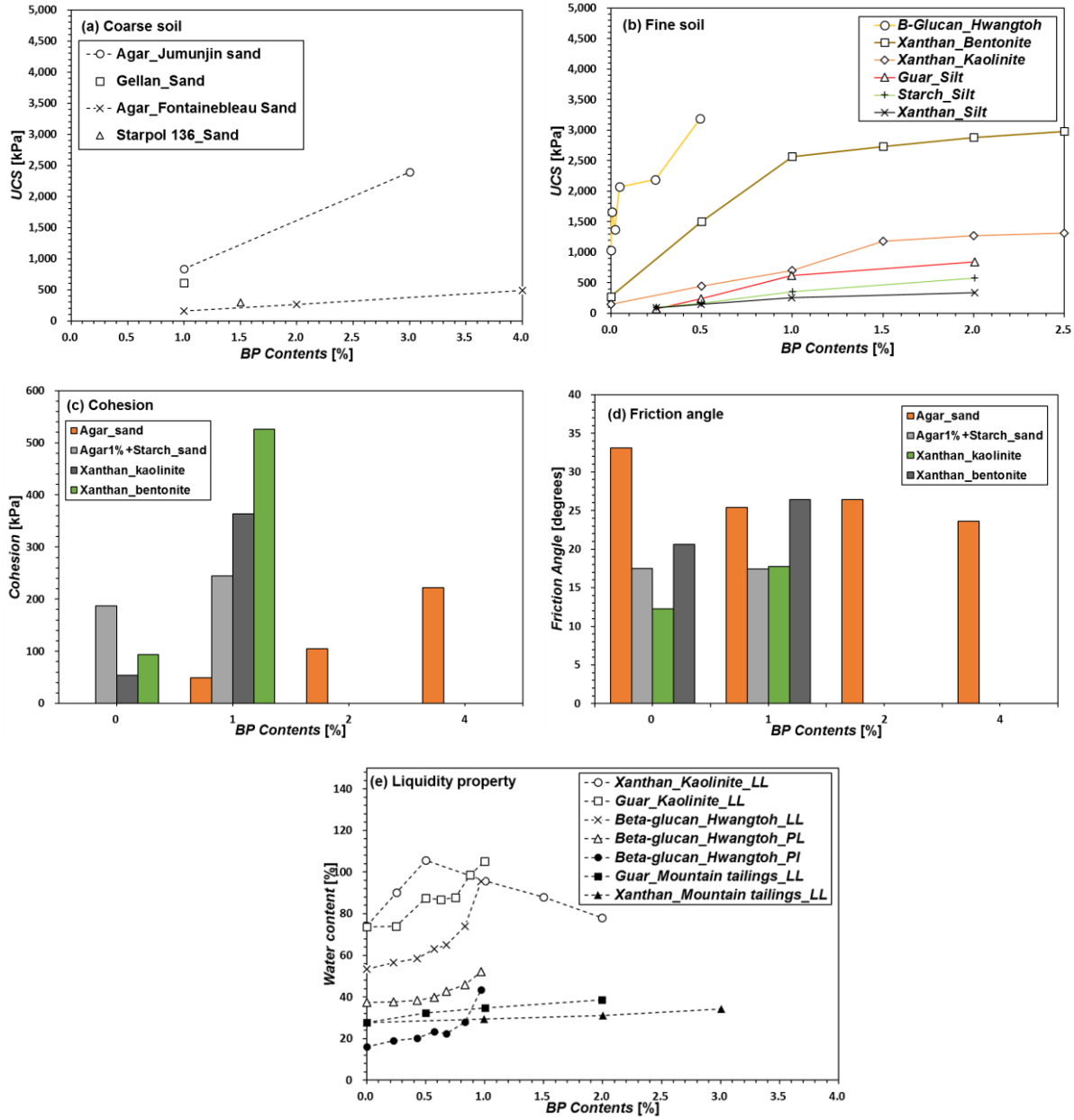

Figure 2.2 Previous studies on the effect of biopolymer on soil improvement. (a) and (b) show unconfined compressive strength changes of coarse soil and fine soil, respectively. (data obtained from Khatami and O'Kelly 2012, Chang et al. 2015, Ayeldeen et al. 2016, Latifi et al. 2016 and Chang and Cho 2012). (c) and (d) show shear strength parameters cohesion and friction angle change, respectively. (Data obtained from Vanapalli et al. 1996, Khatami and O'Kelly 2012, Ayeldeen et al. 2016, Latifi et al. 2016 and Chang and Cho 2012). (e) shows the change of liquid limit, plastic limit and plasticity index. (Data obtained from Nugent et al. 2009, Chen et al. 2013 and Chang and Cho 2014).

Previous studies on the effect of biopolymer on soil improvement

As shown in Figure 2.3, xanthan treatment price, which is a type of biopolymer, is about 3-7 times higher than that of cement. Although it is relatively expensive, there are various possibilities to secure the economic efficiency of xanthan. First, xanthan has regional advantages. The price of cement varies by region. Cement prices in Brazil are about $ 171 / ton and in South Korea it is $ 59 / ton (Kim, 2013). On the other hand, the price of xanthan is less affected by region due to the relatively stable supply of carbon sources. Additionally, to date, biopolymers are mainly produced for the purpose of food additives rather than construction objectives. To apply it in food industry, about 50% of the production cost is consumed in the purification process. However, xanthan gum for construction purposes can simplify the purification process (Chang, Jeon and Cho, 2015). Therefore, if the biopolymer production for the purpose of construction is put into practical use, sufficient economic efficiency can be secured.

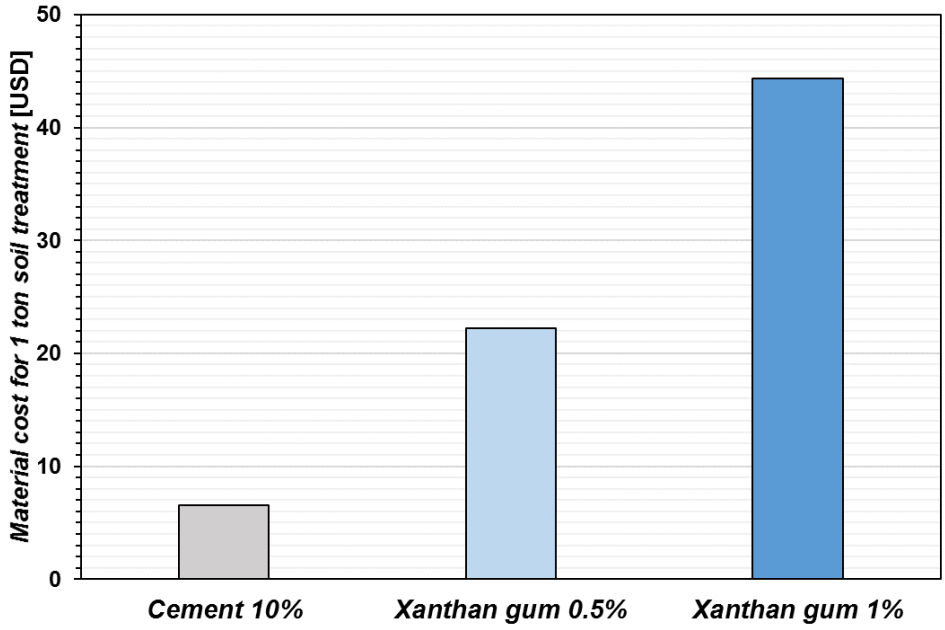

Figure 2.3 Estimated cost comparison for 1 ton soil treatment using cement (10%) and xanthan gum (0.5% and 1%)

2.2 Scope of the study

Previous researches found that the use of biopolymer increases the strength and stability of soils. However, research on biopolymers have only focused on the mechanical improvement of biopolymer such as strength and stability. This study researches on the interaction mechanisms between biopolymers and soil especially the fine soil. In depth study on the structure and the behavior of biopolymers with fine soil was provided via various experimental procedures and image analysis such as fall cone test, thread rolling test, sedimentation test, unconfined compressive strength measurement and scanning electrons microscope (SEM) analysis.

Chapter 2 analyzes the consistency variation of biopolymer treated clay with changes in fluid chemical properties and identifies the interaction mechanism between biopolymer and clay. This chapter studied the liquid limit and the plastic limit in fluid environments with different chemical properties such as permittivity and conductivity by treating kaolinite, clayey silt and montmorillonite, which are representative clay minerals, with biopolymer. Based on this, biopolymer treated clay is classified.

Chapter 3 identifies the sedimentation effects of biopolymers using the coagulation and flocculation-enhancing action of biopolymer treated clay. It has been confirmed that the use of a biopolymer having high surface charge properties improves the precipitation performance of the clay. This confirms the efficacy of the biopolymer in removal of groundwater contaminants and reclamation from biopolymers.

Chapter 4 analyzes the applicability of biopolymers in the tidal flats, which is a typical fine soil terrain. Through the laboratory vane shear test and the fall cone test, the possibility of undrained shear strength enhancement was examined. The sedimentation test for polylysine treated tidal flats were conducted to estimate the effect of biopolymer for the sedimentation of tidal flats. Finally, the unconfined compressive strength were measured to observe the effect of biopolymer treatment for compressive strength enhancement.

Finally, salient conclusions and recommendations for further study are summarized in Chapter 5.

Chapter 3. The effect of biopolymer on the consistency of fine soil

3.1 Introduction

According to the unified soil classification system (USCS), soil with particle size of less than 0.075 mm is determined as fine soil (Astm, 2011). Typically, fine soils were categorized as silt and clay materials.

Although, silt and clay are classified as fine soils, they have different features between them. In general, clay particles are much smaller than silt particles. They were divided by the particle size of 0.002 mm (Classification agency such as U.S. Department of Agriculture, International society of soil mechanics, MIT, AASHTO) or 0.005 mm (Federal Aviation Agency). However, particles definition based on particle size are not necessarily accurate. Clay has a much smoother surface compared to silt and therefore has lower angularity and less dilation. In addition, clay minerals have charge on the surface while silt does not charge on the surface. Charges on clay surface is electrically reacted with water to form a double layer and absorb water. Thus, in the wet state clay shows sticky and plastic behavior, silt shows silky and slimy surface.

Silt is one of the fine-grained soil that has mineral origin of quartz, feldspar and mica. Fine particles such as quartz, feldspar and mica does not develop plasticity when mixed with water and it does not compose liquid double layer. Thus, it has little or no plasticity compared to clay minerals. Thus, its liquid limit and plastic limit is lower than that of clay. USCS divide clay and silt soils by the difference of liquid limit and plastic limit (Astm, 2011). By setting the A-line on the plasticity chart as the boundary, fine soil classifies as the clay above the A-line and the silt below the A-line. Silt can be sub-classified as organic and inorganic silt. Silt has low permeability and is hard to drain water. Small change in moisture causes great change in dry density.

Clay minerals are composed of layers of aluminosilicates. Layers of clay mineral have negative charges on its surface (Schroth and Sposito, 1996, Sposito, Skipper, Sutton, Park, Soper and Greathouse, 1999). Thus, pore fluid chemistry such as the electrical conductivity and permittivity can affect the soil structure and mechanical properties of soils (Sridharan and Jayadeva, 1982, Di Maio, Santoli and Schiavone, 2004). Cations in pore fluid interact with clay particles and decrease the double layer thickness. Thus, the liquid limit of clay particles decreases.

The existence of organic fines also affect the soil consistency. Organic materials have high cation exchange capacity. Thus, it can absorb huge amount of water and increases liquid limits of soil. In contrast, organic materials aggregate clay particles and decreases the specific surface area. Therefore, organic materials can drops the liquid limits. In conclusion, organic fines functions as both liquid limit enhancer and reducer.

Biopolymers are polymers produced by the metabolism of living organisms (e.g., microbes) which come in various forms and properties (Van de Velde and Kiekens, 2002, Congress, 1993). Biopolymer researches have been ongoing in many fields of industry and numerous applications, such as food production, agriculture, cosmetics, medical treatment, and pharmaceuticals (Saha and Bhattacharya, 2010, Lorenzo, Zaritzky and Califano, 2012, Velde and Kiekens, 2002).

In the field of geotechnical engineering, previous studies have reported that biopolymers have promising effect on improving the strength and stability of soil aggregates (Orts, Roa-Espinosa, Sojka, Glenn, Imam, Erlacher and Pedersen, 2007, Ferruzzi, Pan and Casey, 2000). In one particular study performed by Orts et al. (2000), starch xanthate, cellulose xanthate, and chitosan were used to reduce soil runoff in agriculture farm lands (Orts, Sojka and Glenn, 2000). Other studies have investigated the strengthening behavior of polysaccharide biopolymers, such as beta-glucan and xanthan gum with different type of soils (Chang and Cho, 2012, Chang, Im, Prasidhi and Cho, 2015). Moreover, biopolymers synthesized from lignin, starch, and acrylamide are known to decrease the decomposition of plant residue (Awad, Blagodatskaya, Ok and Kuzyakov, 2012).

However, biopolymer application for soil treatment requires cautious concerns due to its rheology and strength dependency with soil water content and ionic characteristic of pore fluids. Chang et al. (2015b) observed the strengthening behavior of biopolymer-treated soils to be governed by the soil water content (Chang, Prasidhi, Im and Cho, 2015). Higher water content resulted in lower strengths, while lower water contents through dehydration resulted in higher strengths due to the formation of high tensile biofilms inside the particulate network. Especially, for biopolymer-treated sands, the moisture content directly defines the concentration (biopolymer to water ratio in mass) of biopolymer hydrogels, where the viscosity (shear stiffness) of biopolymer hydrogels become to most dominant factor on the entire strength. Meanwhile, another study shows the direct ionic bonding behavior between biopolymers and clayey particles, which induces remarkable strengthening results of biopolymer-treated clayey soils.(Chang, Im, Prasidhi and Cho, 2015). Moreover, it seems that the ‘biopolymer to

clay content (in mass)' becomes more important than the 'biopolymer to (total) soil content (in mass)' in strengthening purposes for biopolymer-treated soils (Chang and Cho 2017).

However, there have been no studies on the behavior of biopolymer treated soil, especially clay, by the above-described Pore fluid chemistry (electrical conductivity, permittivity, etc.). In order to utilize the biopolymer in various fields such as enhanced oil recovery (EOR) and the construction of the ground in the sea, prior studies on this part must be given priority. This chapter focuses on the effect of pore fluid on the consistency of fine soils mixed with cationic organic material, xanthan gum. Liquid limits and plastic limits of fine soils were obtained using a series of fall cone tests and plastic limit tests. From the liquid limit and plastic limit variations, the variation of soil consistency were observed. From additional experimental procedure such as scanning electron microscope, soil electrical conductivity and specific surface area measurement, the interaction between clay particles treated with organic fines and cations in pore fluid was taken shape.

Additionally, the classification of organic fines treated clay particles was performed using the unified soil classification system, USCS (Astm, 2011). However, it was proved that clay particles containing organic fines were not fitted well with USCS. To overcome the limitations of USCS, soils were classified by the classification based on the pore fluid chemistry that is recently suggested by Jang and Santamarina, 2016 (Jang and Carlos Santamarina, 2015). This method classifies fine soils by liquid limits measured with various pore fluid chemistry. Using the three chemically different fluids, this method reflects the surface charge of clay particles. From the classification, it was found that the clay particles containing organic fines could be widely classified by the organic contents.

3.2 Materials and Procedure

3.2.1 Materials

3.2.1.1 Soils

Kaolinite, montmorillonite were chosen for clay mineral and clayey silt were used to analyze the difference of surface charges between fine soils. Fine soils were mixed with silica sand to represent different soil types in this study.

Clay is fine-grained soil material that is composed of one or more clay minerals, complex silicates of aluminum, magnesium and iron. Two basic crystalline units form almost every type of clay minerals, silicon-oxygen tetrahedron and aluminum or magnesium octahedron as shown in Fig 3.1. Tetrahedron units in figure 3.1.a combine and form a silica sheet. Tetrahedron linkages leave one negative valence charge of the top oxygen atom. Combination of octahedron units in figure 3.1.b form a gibbsite sheet or brucite sheet with the main metallic atoms of aluminum and magnesium respectively. Silica sheet and gibbsite sheet combines and stacked as the oxygen atoms in silica sheets replace the hydroxyls in gibbsite and forms clay minerals.

Two types of clay minerals (kaolinite, montmorillonite) were used in this study to estimate the effect of specific surface area, cations exchange capacity on the soil consistency.

Kaolinite is one of the most common clay minerals and its chemical formula is $Al_2Si_2O_5(OH)_4$. Kaolinite minerals consist of repeating 1:1 layer structure of gibbsite and silica sheets (Fig 3.2.a). Kaolinite layers bonds each other through hydrogen bonding and do not permit water to enter the lattice (Bear, 1964). Hydrogen bonding between kaolinite layers forms strong structure (Devidal, Dandurand and Gout, 1996). Thus, kaolinite mineral forms stable structures and does not expand by fluids. Bintang kaolinite (Belitung Island, Indonesia) is used in this study.

Illite and montmorillonite minerals consist of repeating layer sheets of two silica sheets and a gibbsite sheet (Fig 3.2.b and c).

Montmorillonite is a member of smectite group and it is chemically hydrated sodium calcium aluminium magnesium silicate hydroxide, $(Na,Ca)_{0.33}(Al,Mg)_2(Si_4O_{10})(OH)_2 \cdot nH_2O$. Montmorillonite minerals have negative charge on its surface due to isomorphous substitutions within the clay structures. Thus, it has high cation exchange capacity (Sondi, Bišćan and Pravdić, 1996). Montmorillonite particles absorbs water and swells (Hensen and Smit, 2002). It has the largest liquid double layer among three

clay minerals and has the highest liquid limits due to its high surface charge. This study used bentonite (Sigma Aldrich Co., Ltd) as a representative montmorillonite material.

Jumunjin sand, standard sand in Korea, which is classified as SP (poorly graded sand) is used for silica sand. Its average particle size, D_{50}, is 0.61 mm, the coefficient of uniformity is 1.54 and the coefficient of curvature is 0.96. Silica sand has no charge on its surface nor an absorbed double layer. Therefore, silica sand has low liquid limits compared to silt and clay minerals. Additionally, those properties are not greatly altered by pore fluid chemistry.

In order to represent various soil types, fine soils and sand were mixed with the mass ratios (sand:fine soil) as 0:100, 50:50, 80:20 which indicate pure fine soil, 50% fine soil and 20% fine soils respectively. Pure fine soil reflects only the effect of clay or silt particles. 50% fine soil is the minimum fine amount to be classified as fine soils based on the USCS. 20% fine soil represents fine mixed sand materials. Figure 3.3 shows the particle size distribution of soils used for this study.

Particle size distribution curves of soils used were plotted in figure 3.3. Basic soil informations were displayed in table 3.1.

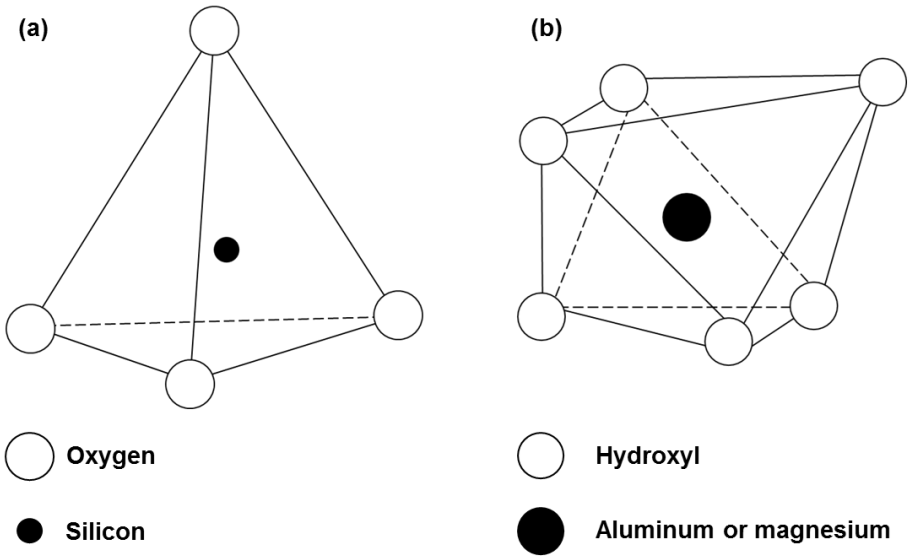

Figure 3.1 (a) Silicon-Oxygen tetrahedron unit and (b) Aluminum or magnesium octahedral unit

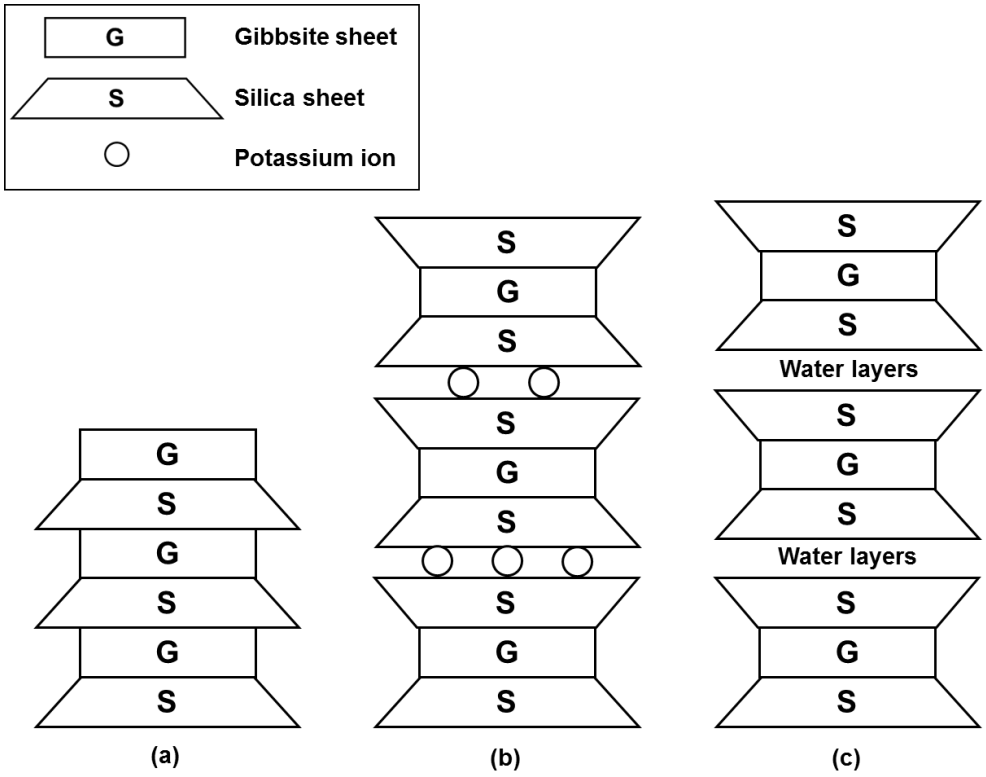

Figure 3.2 Symbolic structures of (a) kaolinite, (b) illite and (c) montmorillonite

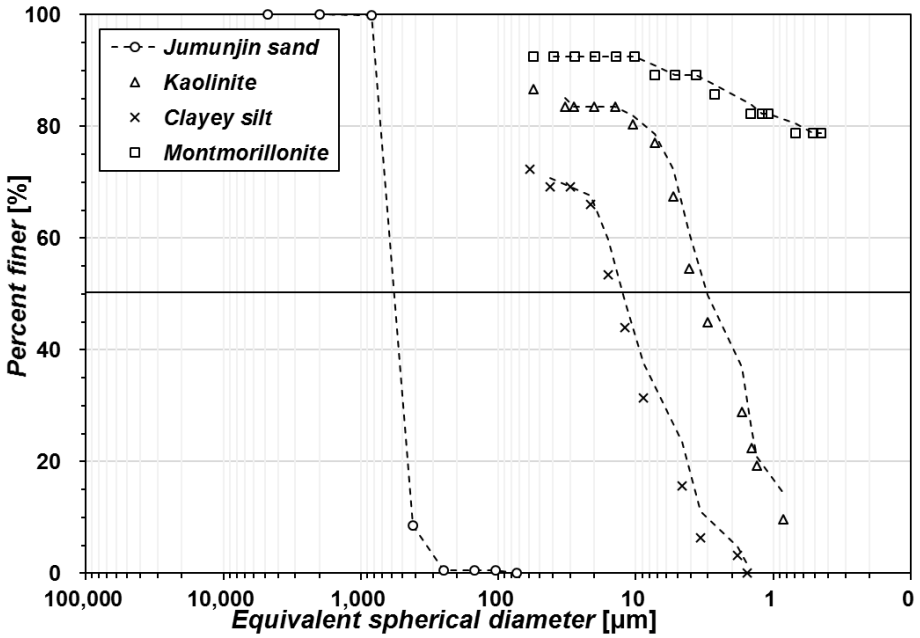

Figure 3.3. Particle size distribution of soils, jumunjin sand, kaolinite, clayey silt and montmorillonite.

Table 3.1 Basic properties of soils used

Soil description	Mean particle size D_{50} [μm]	Plastic limit [%]	Liquid limit			USCS	Proposed class	
			Deionized water	Brine	Kerosene		Plasticity	Sensitivity S_E
Jumunjin sand	421	-	-	-	-	SP	-	-
Kaolinite	2	45.21	69.76	50.90	93.15	CH	I	H
Clayey silt	9	16.67	30.41	28.80	32.12	ML	N	L
Bentonite	0.07[1)]	68.18	398.48	87.53	60.52	CH	H	H

[1)] Plashke et al., 2001

3.2.1.2 Organic matter: Xanthan gum Biopolymer

Biopolymers are organic materials produced by the metabolic action of microorganisms. This study used biopolymers as an organic material to analyze the effect of organic components on the soil consistency. Among the biopolymers, xanthan gum biopolymer was chosen for this study. Xanthan gum is an anionic bipolymer that is produced by the *Xanthomonas compestris* bacterium. Due to its high viscosity when dissolved in water, xanthan gum solution is widely used as a thickener in food, farming, and oil industries (Garcıa-Ochoa, Santos, Casas and Gomez, 2000). Recent researchs have attempted to apply xanthan gum in geotechnical area as a soil strengthening agents (Chang, Im, Prasidhi and Cho, 2015). Studies have shown that xanthan gum interacts with clay particles forming a structured matrix between the clay particles, and these increased interactions have been shown to be capable of increasing the strength of the clay material and undrained shear strength (Latifi, Horpibulsuk, Meehan, Abd Majid, Tahir and Mohamad, 2016) (Ayeldeen, Negm and El Sawwaf, 2016) (Chang, Im, Prasidhi and Cho, 2015). Other researches have focused on the decrease of soil permeability by forming impervious barriers (Martin, Yen and Karimi, 1996). The research observed that the permeability was decreased by a factor of 100 or greater. Additionally, due to its aggregation effect and fluid thickening effect, xanthan gum can affect the liquid limit of clay soils (Nugent, Zhang and Gambrell, 2009). Nugent et al applies xanthan gum only to kaolinite minerals and analyzed only the liquid limit variation with deionized water. Additionally, Nugent et al focuses on the liquid limit variation at high xanthan concentration. However,

high xanthan concentration is limited to applied in real field application due to the economic feasibility. Thus, this study focuses on the low to medium concentration of xanthan gum and uses various pore fluid chemistry.

3.2.1.3 Pore fluids

Pore fluids have different permittivity κ' and electrical conductivity σ_{el} and these chemical differences call for distinct electrical fluid-particle interactions. Three disticive fluids, deionized water (highest $\kappa' = 80$, $\sigma_{el} = 10^{-6}$ S/m), brine ($\kappa' = 55$, highest $\sigma_{el} = 12$ S/m) and kerosene (lowest $\kappa' = 2$, lowest $\sigma_{el} = 10^{-11}$ S/m), were chosen to explore the different chemical behaviors of organic materials on the pore fluid chemistry. Deionized water was produced through the reverse osmosis process, and it has highest relative permittivity among the fluids. Brine was produced by dissolving 2M of NaCl into deionized water. It has the highest electrical conductivity. Kerosene has the lowest relative permittivity and the lowest electrical conductivity. Thus, the comparison of consistency between deionized water and kerosene means the effect of permittivity on the soil consistnecy and the comparison between brine and kerosene represents the effect of electrical conductivity on the soil liquid limit.

3.2.2 Experimental Program

3.2.2.1 Soil-BP Mixture preparation

First, fine soil (kaolinite, clayey silt and montmorillonite) and jumunjin sand was dried in the oven at 90℃ to remove the moisture in the soils. Afterwards, the fully dried sand and fine soils were mixed by three different ratios, 20:80, 50:50, 100:0 respectively. Finally, dry xanthan gum powder was directly mixed into the soil sample with varying proportions to the soil weight between 0-2%.

3.2.2.2 Plastic limit and liquid limit determination

Plastic limit of soils were determined using thread rolling test. Plastic limit-Rolling device produced based on the ASTM D 4318-05 was used to increase the reliability of results (ASTM). A device made of acryl was depicted in figure 3.4. Unglazed papers attached to the top and bottom plate absorb the fluid in soil and does not add foreign substance. Top plates were moved back and forth to decrease the water content of soil until the thread were broken at the thread thickness of 3.2mm and the

water content at this state was determined as plastic limit. Same procedure was repeated twice to reduce the error.

The liquid limits were determined by the fall cone tests instead of the ‘casagrande cup’ method, due to its high reliability (Koumoto and Houlsby, 2001, Casagrande, 1958). The fall cone equipment used for this study conforms to the British Standard BS 1377 (BS1377, 1990). A cone with a weight of 80g and an angle of 30° was allowed to penetrate soil specimens for 5 seconds at various water contents. The penetration depth was measured using a dial gauge with a precision within 0.01mm. Liquid limits for each sample were determined as the water content when the cone penetrated 20mm into the soil sample. For one soil sample, an average of 12 different measurements, 4 different water content and 3 repeated penetration at same water content, were taken to obtain credible penetration depth-water content line.

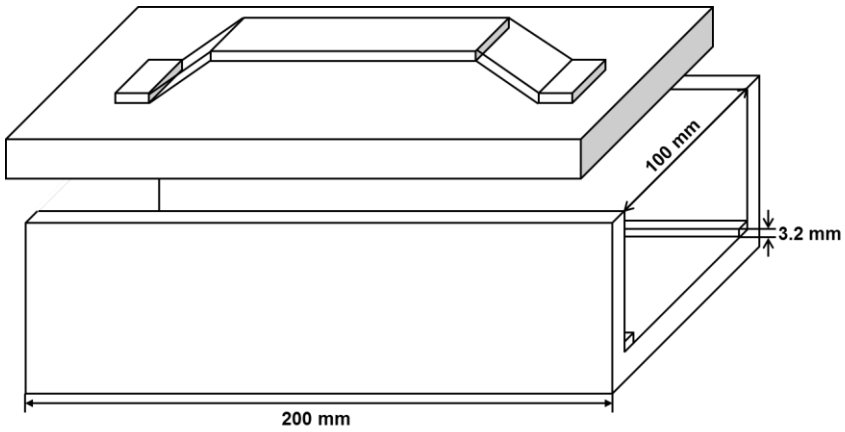

Figure 3.4 Schematic diagram of plastic limit rolling device

3.2.2.3 Microscopic observation (Scanning Electron Microscopy: SEM)

Microscopic observations using the scanning electron microscope (SEM; SU8230, S4800) was performed to visually analyze the behavior among organic materials (i.e. xanthan gum), clay minerals or silt, and the pore fluid chemistry. The soil with the water content near the liquid limit were sampled after the fall cone tests. Then, soil samples were dried in room temperature to maintain the interaction of soil with organic material and cations in pore fluids. The target samples were coated in an Osmium coating for 10 seconds before images were taken for specimen to get the enough conductivity. The images were then used to better clarify the internal structure of the mixtures.

3.2.2.4 Specific surface area

The specific surface areas of kaolinite, clayey silt and montmorillonite were determined by methylene blue absorption measurements. Methylene blue (MB), $C_{16}H_{18}ClN_3S$, has been used to determine the specific surface area of clay or silt minerals. In aqueous solution, the cationic parts of methylene blue, $C_{16}H_{18}N_3S^+$, interact with negatively charged clay particles. Thus, the specific surface area can be obtained by the amount of methylene blue that clay particle can absorb.

For this experiment, commercial methylene blue powder produced by Samchun Pure Chemical Co., LTD. It has molecular weight of 313.87 g/mol and it is assumed that one molecule of methylene blue covers 130 $Å^2$ (1 $Å^2 = 10^{-20}$ m^2).

The procedure is as follows. (i) Methylene blue solution (0.5 wt% to deionized water) is prepared. (ii) Then, the soil suspension (0.3 wt% to deionized water) is prepared. (iii) Methylene blue solution prepared in step (i) is added to soil suspension in 0.5 mL increments. (iv) Soil suspension and methylene blue solution are mixed for 1 minute and (v) a small drop of mixed suspensions were placed on Fisher brand filter paper P5. (vi) If the unabsorbed methylene blue is remained in the suspension, a permanent light blue halo is found and it means that all of the clay minerals were coated by MB and reaches the “end point”.

To increase the reliability of experiment procedure, those procedure was repeated 3 times for each clay minerals and average number of increments were determined as “end point”.

From the volume of MB solution increments, the specific surface area of clay minerals can be obtained using the equation below

$$S_s = \frac{1}{319.87} \times 0.005 \times (0.5N) A_v A_{MB} \frac{1}{M_{soil}}$$

Where N is the number of MB increments, A_v is Avogadro’s number (6.02×10^{23}/mol), A_{MB} is the area covered by one MB molecule, 130 $Å^2$, and M_{soil} is the mass of soil in suspension.

Through this technique, the specific surface area of expansive clay such as bentonite can be correctly because this experiment is performed in water suspension. However, due to the negative charge of xanthan gum itself, it can absorb MB. Thus, it does not reflect the bondage between xanthan gum and clay particles. Due to this reason, only the specific surface area of pure clay were determined.

3.3. Results and Observations

3.3.1 Surface area and Electrical conductivity

From the methylene blue absorption measurements, the specific surfaces of each fine soils were obtained. The results were summarized in table 3.2. Clayey silt has shown the minimum specific surface, 2.20 m^2/g, which is in the range of silt material and the smallest among the fines used. Expanding layer silicates such as bentonite have higher specific surface area than that of un-expanding clay minerals such as kaolinite and illite (Carter, Mortland and Kemper, 1986). Experimental results proved that the specific surface of bentonite, 220.63 m^2/g, is 10 times higher than that of kaolinite minerals.

Additionally, the result of methylene blue absorption measurements has relationship with cation exchange capacity of clay minerals because this measurement was based on the electrical interaction between the negative charge of clay surface and the cationic part of MB (Hang and Brindley, 1970). The result indicates the cation exchange capacity of bentonite is much higher than kaolinite and clayey silt. It was proved that the surface charge of clayey silt is the smallest among three fines. Thus, it can be estimated that montmorillonite absorb the most amount of water and forms the largest liquid double layer. Clayey silt can absorb the smallest amount of water and forms the smallest liquid double layer. Thus, the liquid limit and plastic limit will be the highest for montmorillonite and the lowest for clayey silt.

Table 3.2 Specific surface of clay minerals used.

	Clayey silt	Kaolinite	Montmorillonite (Bentonite)
Specific surface area (m^2/g)	2.20	22.06	220.64

3.3.2 Cone penetration

The results of the fall cone test using kaolinite, montmorillonite and clayey silt as fine soils are shown in Fig 3.5, 3.6 and 3.7, respectively.

In each figure, Fig. a, b, and c show the effects of increased biopolymer content on the soil penetration with varying pore fluids for pure fine soils, while fig d, e and f are for 50: 50 sand-fine mixtures and fig g, h and I show the results at 20:80 sand-fine mixtures. For all fine soils, if the figures

are compared in the vertical direction, it can be seen that with the addition of sand particles, the penetration depth of the soil is reduced, which is as expected due to the absence of plasticity for sands.

At the same penetration depth, it was confirmed that the higher water content was observed in the order of montmorillonite, kaolinite and clayey silt. This is due to the difference in surface charge density, as demonstrated by the particle size distribution and specific surface area comparison described above. The size of the double layer formed by the clay minerals determines the amount of water absorption of fine soils.

Cone penetration results of kaolinite-sand mixtures

When deionized water is used as the pore fluid (Fig. 3.5 a, d and g), slight fluctuations in the penetration curves with increasing biopolymer content can be observed with varying water contents. This is especially seen in the pure clays where a peak in the liquid limit is observed at 0.5% xanthan gum concentration. With the brine mixtures (Fig. 3.5 b, e, h), the penetration curves increased with an increase in the biopolymer concentration. This mechanism shows the hydrophilic properties of xanthan gum biopolymers and its high capabilities of water absorption. In the case of the kerosene samples (Fig. 3.5 c, f, i), no alterations in the penetration curves were observed with an increase in the xanthan gum biopolymers. As such, it can be said that due to the low electrical charge density of the kerosene molecules, the xanthan gum biopolymers have no significant interactions with the kerosene resulting in no change in the pore fluid characteristics.

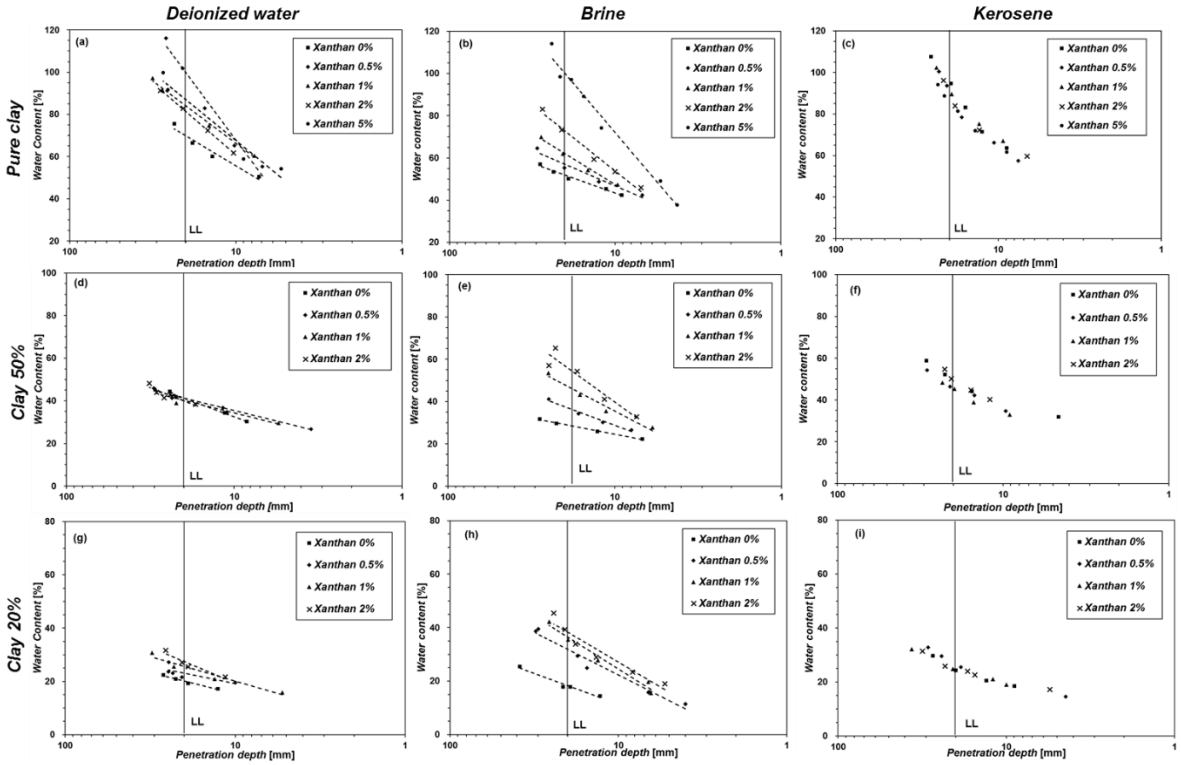

Figure 3.5 Penetration depth against water content relationship for pure kaolinite (a, b & c), 50% kaolinite and 50% jumunjin sand (d, e & f) and 20% kaolinite and 80% jumunjin sand (g, h & i) with deionized water (a, d & g), 2M NaCl brine (b, e & h) and kerosene (c, f & i)

Cone penetration results of clayey silt-sand mixtures

The cone penetration behavior of clayey silt-sand mixture is similar to that of kaolinite at lower water content than kaolinite. In deionized water (Fig. 3.6 a, d, g), the liquid limit tended to increase and then to decrease. Especially, peak liquid limit of pure clayey silt is obtained at the 0.1% xanthan content. In the Brine (Fig. 3.6 b, e, h) environment, the liquid limit of untreated clayey silt decreased compared to deionized water state. However, the liquid limit was steadily increased due to the water absorption capacity of xanthan. Likewise, it was confirmed that there was almost no change due to the xanthan content during kerosene treatment. Since the specific surface area of clayey silt used is lower than that of kaolinite, behavior of clayey silt is similar to kaolinite but at lower xanthan content. It occurs because xanthan does not interact with silt particles but the clay fraction in clayey silt.

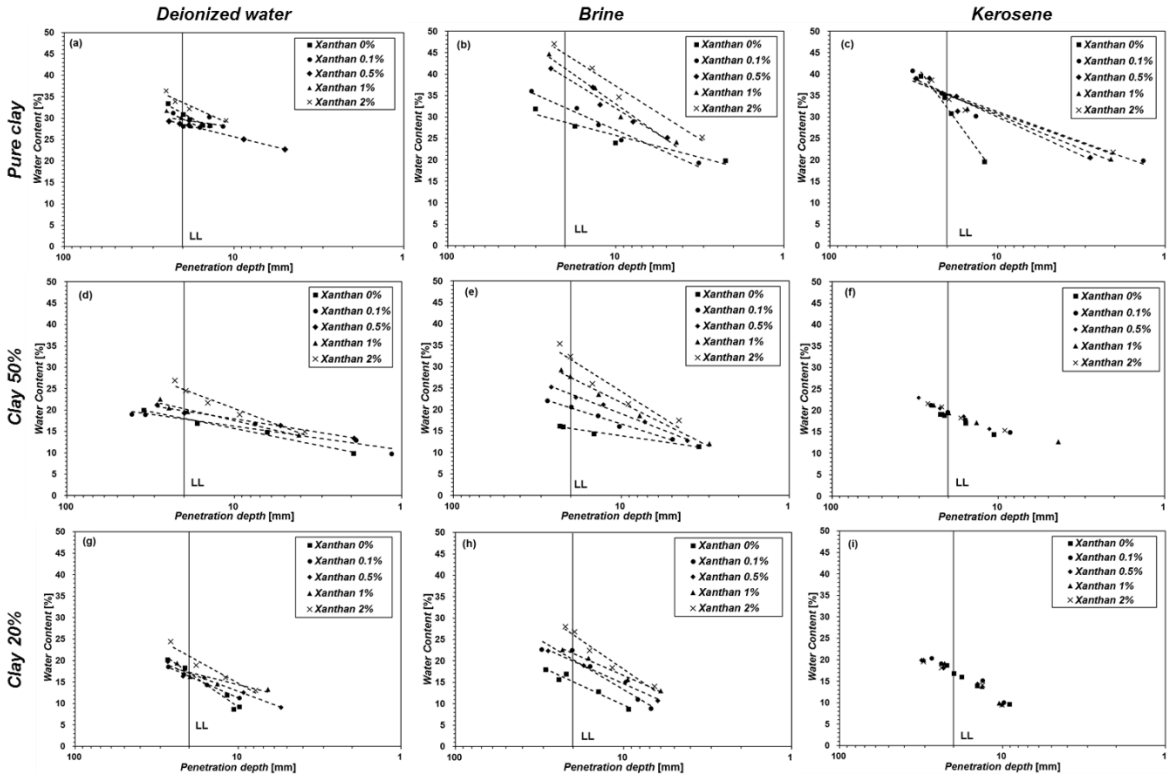

Figure 3.6 Penetration depth against water content relationship for pure clayey silt (a, b & c), 50% clayey silt and 50% jumunjin sand (d, e & f) and 20% clayey silt and 80% jumunjin sand (g, h & i) with deionized water (a, d & g), 2M NaCl brine (b, e & h) and kerosene (c, f & i)

Cone penetration results of montmorillonite-sand mixtures

In the Montmorillonite-sand mixture, a liquid limit was found in water content much higher than other clay minerals (about 5 times compared to kaolinite and about 12 times higher than clayey silt). This is due to the large specific surface area and small particle size of montmorillonite. In the case of brine and kerosene, it was similar to other fine soils. In brine, it was increased by xanthan content (Fig. 3.7 (b), (e) and (h)). In kerosene, it was not affected by xanthan concentration (Fig. 3.7 (c), (f) and (i)). However, when deionized water was injected (Fig. 3.7 (a), (d) and (g)), it showed a tendency different from the above clayey silt and kaolinite. As the Xanthan content increases, the liquid limit tends to decrease.

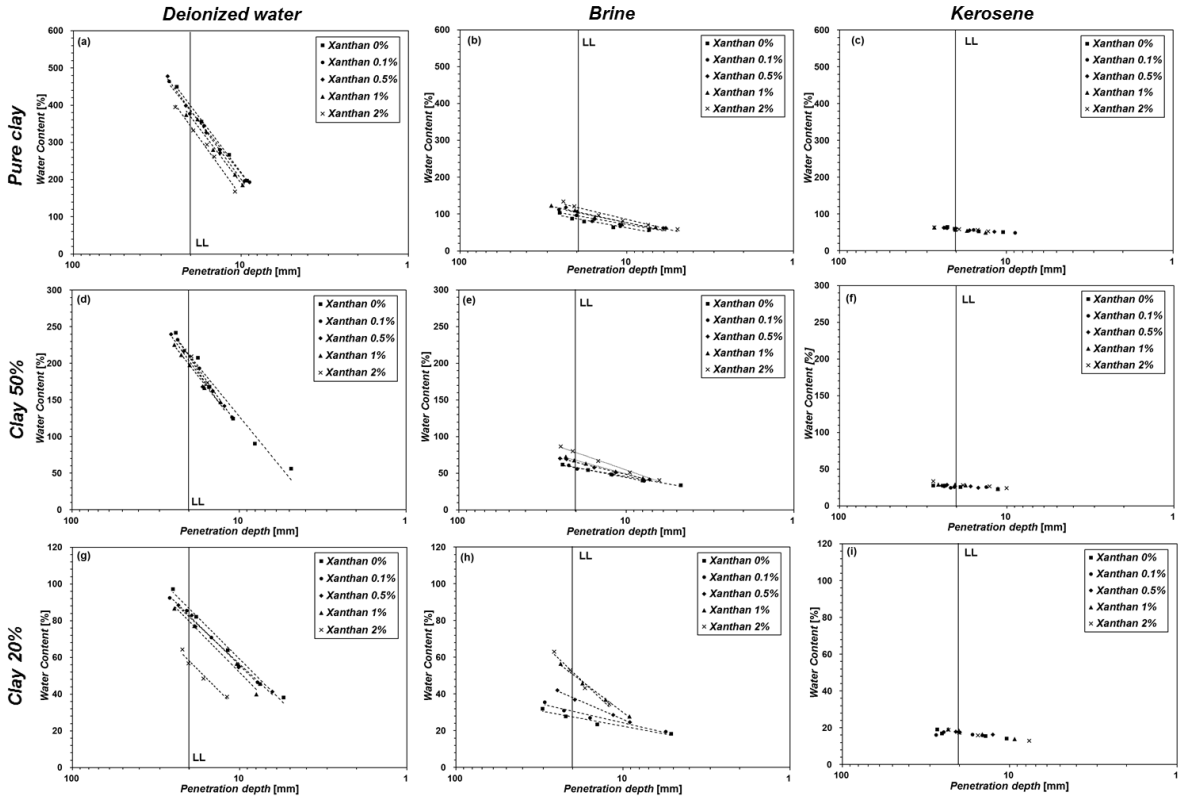

Figure 3.7 Penetration depth against water content relationship for pure montmorillonite (a, b & c), 50% montmorillonite and 50% jumunjin sand (d, e & f) and 20% montmorillonite and 80% jumunjin sand (g, h & i) with deionized water (a, d & g), 2M NaCl brine (b, e & h) and kerosene (c, f & i)

3.3.3 Liquid limits

In order to clearly investigate, the effects of xanthan gum biopolymer to the liquid limit of the soils, the biopolymer content was plotted against the liquid limit of each fine soil-sand mixtures (Fig. 3.5, 6 and 7). Due to the characteristics of xanthan gum, the water absorption capability and the electrical interaction with clay molecules, the behavior of the liquid limit tends to be different depending on the chemical properties of the pore fluid.

Liquid limit variation in 2M NaCl brine

When 2M NaCl brine is injected into a clay bearing a negative charge ((b), (e) in Fig. 2.5, 6 and 7), the Na^+ ions in the brine react with the negative charge on the clay surface to neutralize the total charge. As a result, the water absorption capacity of the clay decreases, the double layer decreases, and the liquid limit decreases (Mansour, Taha and Chik, 2008). When xanthan, anionic biopolymer, is treated with these clays, xanthan reacts with the positive charge of the clay edge and Na^+ ions to enhance

the water absorption capacity of the clay. Additionally, Xanthan absorbs water itself. Therefore, for all clay minerals, the liquid limit in the brine environment (LL_{Brine}) increases steadily with xanthan content.

Liquid limit variation in Kerosene

In the fine soil environment where kerosene is injected, there is little change in the liquid limit according to the content of xanthan gum ((c), (f) in Fig. 3.8, 9 and 10). In order for xanthan to interact with clay molecules, the process of absorbing fluids and gelation must be preceded. Xanthan gum has a highly hydrophilic surface, and it is therefore only gelated in water (Laneuville, Turgeon, Sanchez and Paquin, 2006). However, organic fluids such as kerosene do not react with xanthan molecules because they have low electrical conductivity and permittivity. In this state, the injected xanthan has no function to the fine soil molecules. Therefore, the liquid limit at kerosene injection ($LL_{kerosene}$) is hardly affected by xanthan content.

Liquid limit variation in deionized water

An interesting behavior was observed for deionized water treated soil material ((a), (d) in Fig 3.8, 9 and 10). It has been found that the liquid limit change in deionized water has a different tendency depending on the fine soil types. Clayey silt and kaolinite showed an increase in the liquid limit at the initial low xanthan content and then decreased after the peak (0.5% for kaolinite and 0.1% for clayey silt). Thereafter, the liquid limit tended to increase slightly with increasing xanthan content.

This fluctuation tendency in the initial content ratio is due to the two functions of xanthan gum: 1) to reduce the surface area by narrowing the distance between the molecules by reacting with the clay molecule, 2) to increase the water absorption capacity of the clay by absorbing water. At lower contents than the peak concentration (less than 0.5% for kaolinite, less than 0.1% for clayey silt), the injected xanthan mainly absorbs water because it is not enough to narrow the distance between the clay particles. Therefore, the liquid limit increases in this section. After reaching the peak concentration, however, the injected xanthan begins to form a bridge by attracting clay molecules. This reduces the surface area and thus the liquid limit. After bridge formation is completed, injected xanthan mainly plays a role of absorbing water again, and improves viscosity by gelation. This results in an increase in the liquid limit at higher xanthan content than at the completion of bridge formation. For clayey silt, these interactions

occurs with the clay fractions in clayey silt and thus, the peak concentration was found at low amount of xanthan.

In case of kaolinite, the peak xanthan concentration was found to be 0.5% in all cases when the concentration was changed to clay weight rather than total soil weight. These results support the finding of a previous study that the behavior of xanthan gum is dominated by the content of fine soil rather than coarse soil (Chang and Cho, 2012). However, in the case of clayey silt, this property could not be confirmed because the experiment proceeded with the minimum concentration of 0.1% (peak xanthan concentration of the pure clayey silt). Subsequent studies on liquid limit experiments with 0.1% or less xanthan treated clayey silt are necessary.

However, montmorillonite minerals have completely different tendencies. In the case of montmorillonite mineral, surface charge and water absorption ability are remarkably superior to other molecules. Therefore, the water absorption capacity of xanthan gum in montmorillonite is relatively reduced as compared with that in kaolinite and ilite. Additionally, due to its high surface, xanthan gum interact with bentonite particles rather than with water. The local charge neutralization that occurs at the positive charge of the clay edge and the xanthan bond reduces the double layer thickness. Therefore, it was found that the liquid limit tended to decrease steadily when the content of xanthan was less than 2%. This is found in all clay: sand ratios, and this fact also proves that the behavior of xanthan with the soil is dominated by clay.

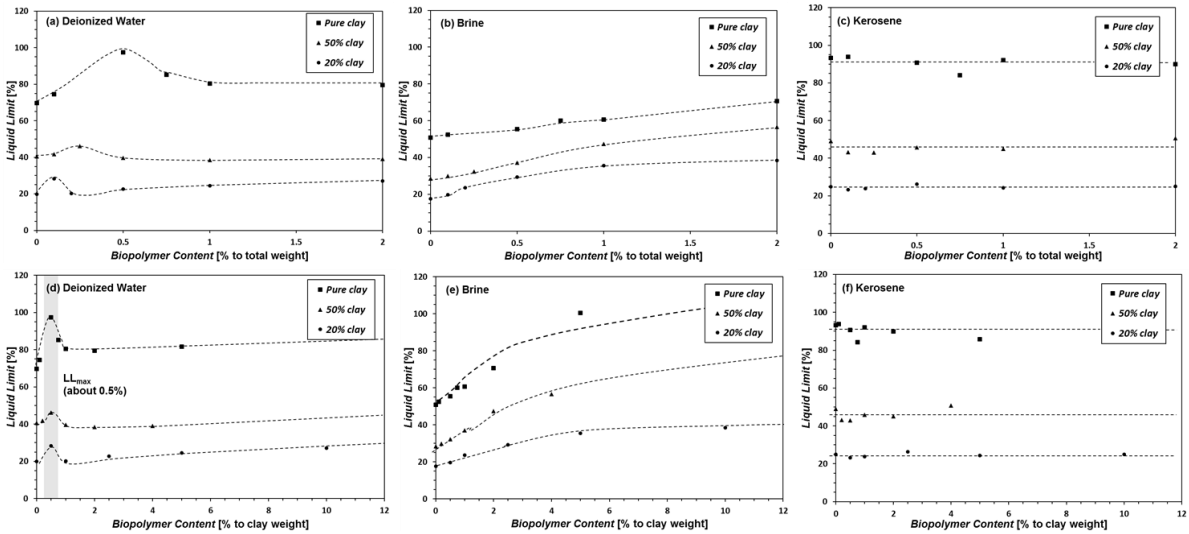

Figure 3.8. Liquid limit of xanthan gum treated kaolinite soils with deionized water (a & d), brine (b & e), and kerosene (c & f). (a, b & c) Liquid limit variation with xanthan gum content to the total mass of soil. (d, e & f) Liquid limit variation with xanthan gum content to the mass of clay

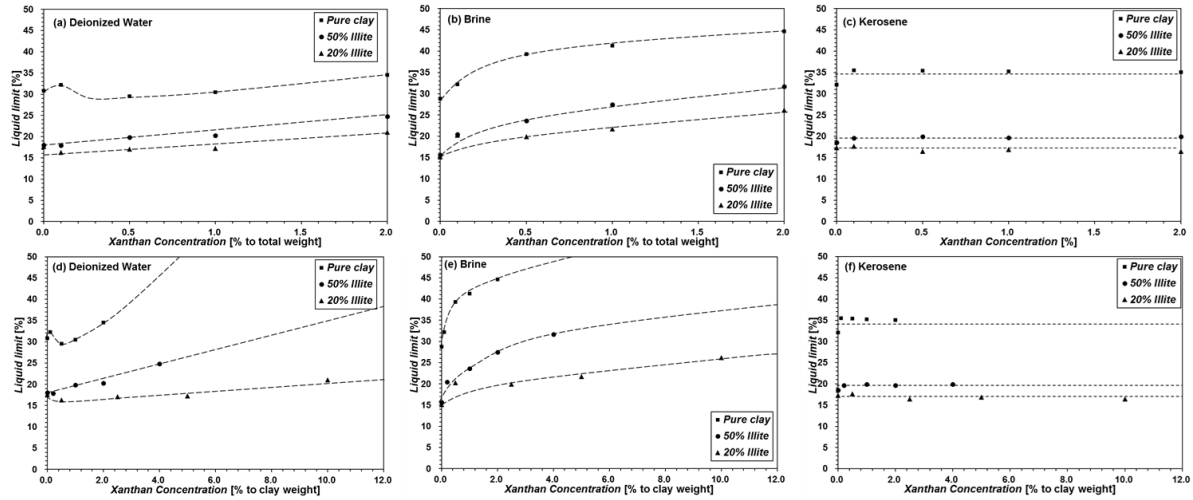

Figure 3.9 Liquid limit of xanthan gum treated clayey silt with deionized water (a & d), brine (b & e), and kerosene (c & f). (a, b & c) Liquid limit variation with xanthan gum content to the total mass of soil. (d, e & f) Liquid limit variation with xanthan gum content to the mass of clayey silt

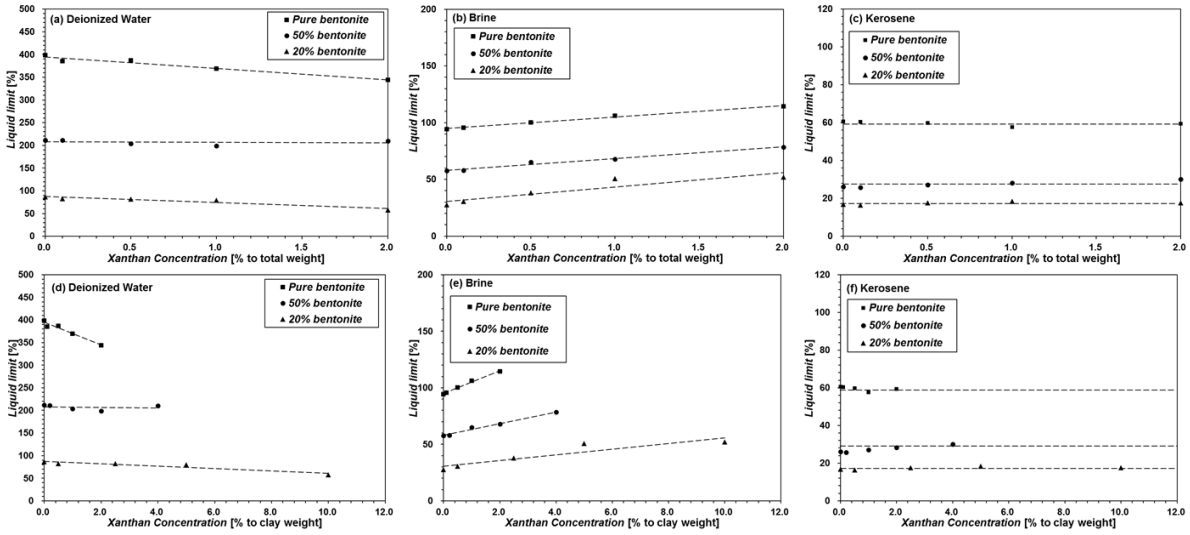

Figure 3.10 Liquid limit of xanthan gum treated montmorillonite soil with deionized water (a & d), brine (b & e), and kerosene (c & f). (a, b & c) Liquid limit variation with xanthan gum content to the total mass of soil. (d, e & f) Liquid limit variation with xanthan gum content to the mass of clay

3.3.4 SEM images

To study the rheology of organic materials in different fluid chemistry visually, scanning electron microscopic (SEM) image analysis were conducted. Figures 3.11, 12 and 13 show SEM images of pure kaolinite, pure clayey silt and pure montmorillonite, respectively. In each image, (a), (b) and (c) are SEM images of untreated fine soils, and (d), (e) and (f) show SEM images of 1% xanthan treated fine soils. SEM Images confirmed that the structure of the fine soils varies depending on the treatment of xanthan and the chemical properties of the pore fluid.

Kaolinite

For untreated kaolinite, images for different pore fluid, brine and deionized water, were very different due to the electrical interactions of the ionic particles (Fig 3.11 (a) and (b)). Due to sodium ions, the soil surfaces were layered with the ions decreasing the plate-to-plate distance of the kaolinite particles. With xanthan gum treated kaolinite, a unique structure was observed for the deionized water. For xanthan gum treated deionized water samples, xanthan gum bridging between the kaolinite particles were observed (Fig 3.11 (c)). This bridging phenomenon is thought to fixate the liquid limit by fixing the plate-to-plate distances in the kaolinite particles, which was observed for xanthan concentrations above 1%. When brine is used as pore fluid, compared to the untreated brine case (Fig 3.11 (b)), the xanthan gum particles seem to overlap on top of the ions (Fig 3.11 (d)). This interaction most likely

affects the electrical charge density of the specimens to some degree allowing for an increase in the adsorbed layer. Additionally, Na^+ ions were added around the Xanthan gum covered kaolinite mixture and additional Xanthan gum also attached around Na^+ ions. Through these procedures, the surface area continuously increases as the xanthan gum injected. Finally, in case of kerosene, its surroundings look similar to the untreated kaolinite with deionized water (Fig 3.11 (e) and Fig 3.11 (f)). This is due to the organic material not interacting with kerosene, and the gelation process being unable to activate. Therefore, the organic material simply mixes into the soil without any significant changes to the fluid chemistry.

Clayey silt

In clayey silt, the shape of xanthan is not well distinguished. Because the electrical charge of clayey silt is lower than that of clay and the binding of xanthan is not so much, clayey silt particle structure is not changed as that of kaolinite. Due to its low clay concentration, it was confirmed that xanthan absorbs water and cover silt particles rather than form bridge between clay particles. Especially in the brine environment (Fig 3.12 (e)), this coverage effect appears to be prominent because the charge that xanthan can react increases due to the existence of Na^+ contained in the brine. In addition, in kerosene, the image of treated and untreated was not changed. This is because xanthan does not activate in kerosene.

Montmorillonite

SEM images of montmorillonite minerals are notably different especially in brine and deionized water. This is because the surface charge of montmorillonite is large and reacts with large amounts of Na+ ions. Xanthan untreated and treated images in deionized water are not much different. Xanthan untreated and treated images in deionized water are not much different. This seems to be because montmorillonite particle has high charge on its surface, xanthan interacts with montmorillonite particles rather than forms xanthan chains and connects clay particles. (Fig. 3.13 (a) and (d)). The xanthan treated montmorillonite in Brine has a rounded surface compared to the untreated case (Fig. 3.13 (b), (e)). This is because the injected xanthan covers the surface of the brine-clay mixture. Finally, it is confirmed that xanthan has no effect in the kerosene environment (Fig. 3.13 (c), (f)).

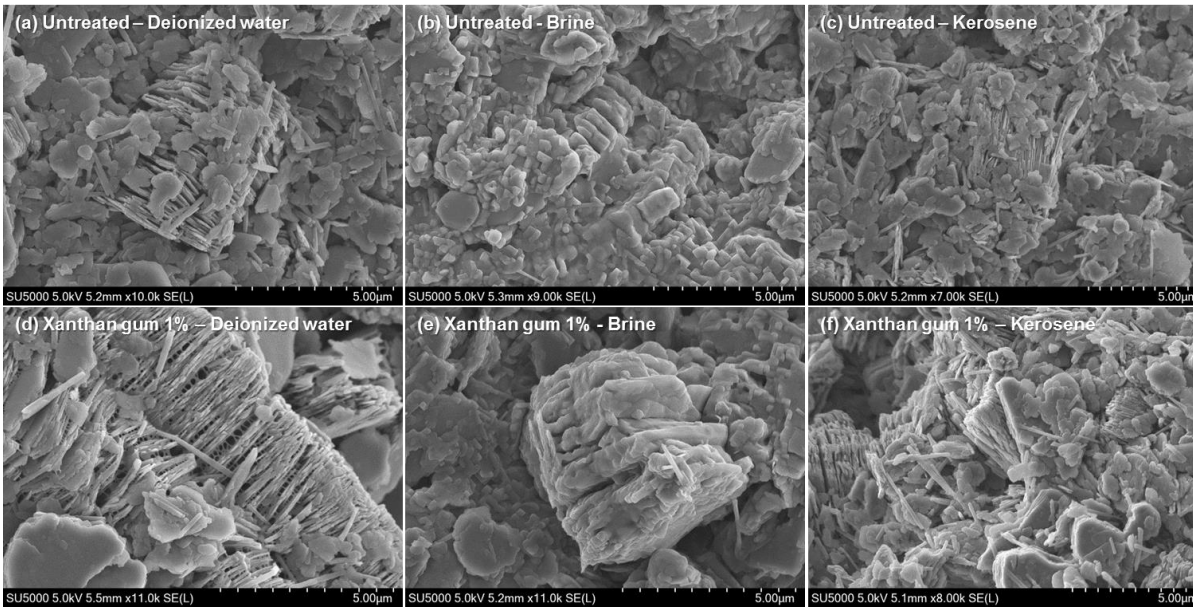

Figure 3.11 SEM images of untreated (a, b & c) and 1% xanthan gum-treated (d, e & f) pure kaolinite at the water content near the liquid limit treated with deionized water (a & d), brine (b & e), and kerosene (c & f), respectively

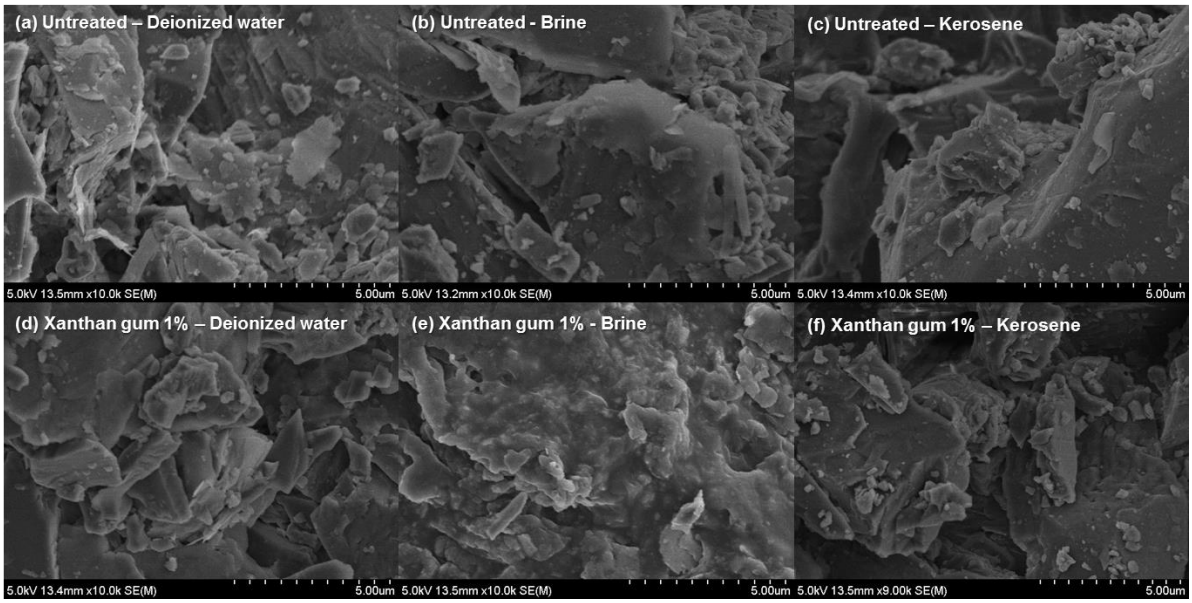

Figure 3.12 SEM images of untreated (a, b & c) and 1% xanthan gum-treated (d, e & f) pure clayey silt at the water content near the liquid limit treated with deionized water (a & d), brine (b & e), and kerosene (c & f), respectively

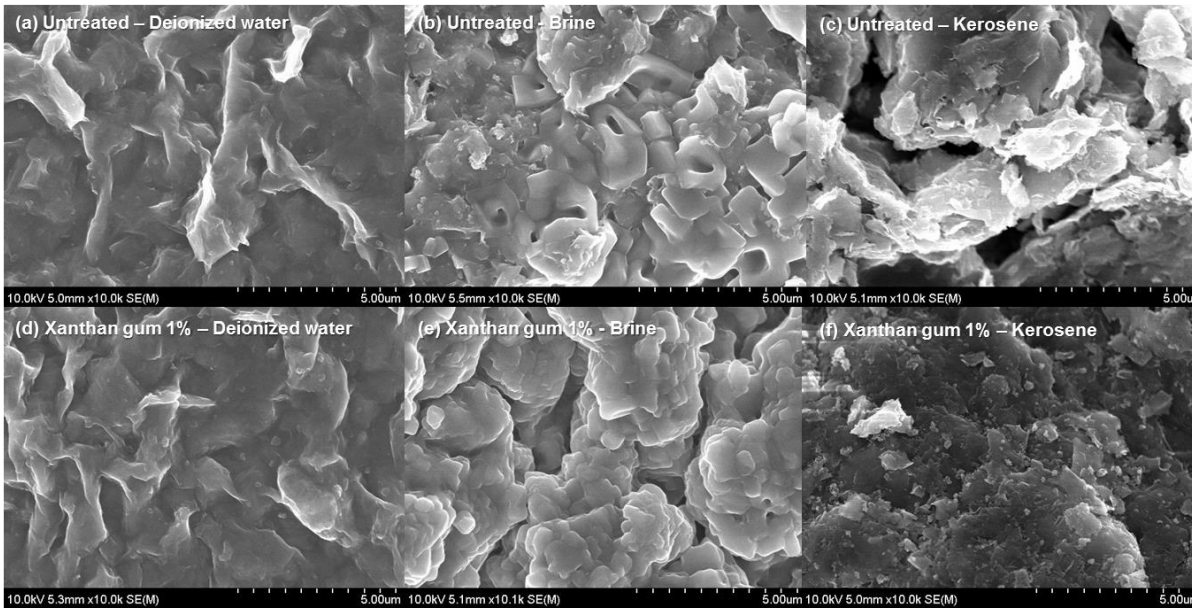

Figure 3.13 SEM images of untreated (a, b & c) and 1% xanthan gum-treated (d, e & f) pure montmorillonite at the water content near the liquid limit treated with deionized water (a & d), brine (b & e), and kerosene (c & f), respectively

3.4 Discussion

3.4.1 The rheology of xanthan gum treated soils by pore fluid chemistry

Through the experimental datum, several factors could be determined about the rheology of xanthan gum mixed soils with varying pore fluids. First, it was observed that the xanthan gum, which holds an electrical charge, generally increased the LL due to its high absorbability and interactions with water molecules. However, xanthan gum has the gelation activation process only in water, and as such when kerosene was used as the pore fluid, any addition of xanthan gum into the soil did not significantly alter the $LL_{kerosene}$ of the soils.

For kaolinite and clayey silt, the increase of the LL with the addition of xanthan gum was especially noticeable for the brine mixtures. However, for the deionized water it was observed that there was a direct increase in the LL up till peak xanthan gum concentration, but above peak concentration, the LL reduced to a somewhat steady state. Then, it was seen that there is slight increase to the LL due to the fluid viscosity enhancement. This tendency is believed to be due to xanthan gum's capability to electrically interact with the ionic charges on the clay surfaces, and through this interaction, fix the spacing between the platy particles by forming structures of bridges to hold the particles together (Fig. 3.14 (c)). However, before there is sufficient xanthan gum particles to fully form this structure (i.e. < 1% in kaolinite) the water absorption capabilities are more dominant than the attraction forces that form

the bridge structures thereby increasing the water content (Fig. 3.14 (b)). Through this process, the LL will increase up until peak concentration and as the attraction forces become dominate over the water absorption forces, the overall LL reduces back down until it has stabilized (seen in Fig. 3.14 (c)).

For montmorillonite, things are different. Montmorillonite particles have a much larger surface charge than other clay minerals and have thick double layer thicknesses (Fig. 3.14 (g)). In this environment, when xanthan is injected, it mainly interacts with the positive charge of the montmorillonite surface. This reaction causes local charge neutralization, which tends to reduce the double layer thickness (Fig. 3.14 (h)). Therefore, in montmorillonite mineral, liquid limit is steadily decreased by xanthan injection.

For the brine samples, the presence of the Na+ ions greatly affect the behavior of the negatively charged xanthan particles. With these ions present in the pore fluids, the xanthan gum biopolymers have a larger tendency to interact with the Na+ ions than the surfaces of the clay particles. In contrast to the deionized treated specimen, bridge structures are rarely observed with the addition of xanthan gum in brine state (seen in Fig 3.14 (c) and (d)). Without the formation of these structures that fix the platy particles, the LL of the samples simply increase with the addition of negatively charged xanthan gum biopolymers which, in this case, help increase the water holding capacity of the soil mixture.

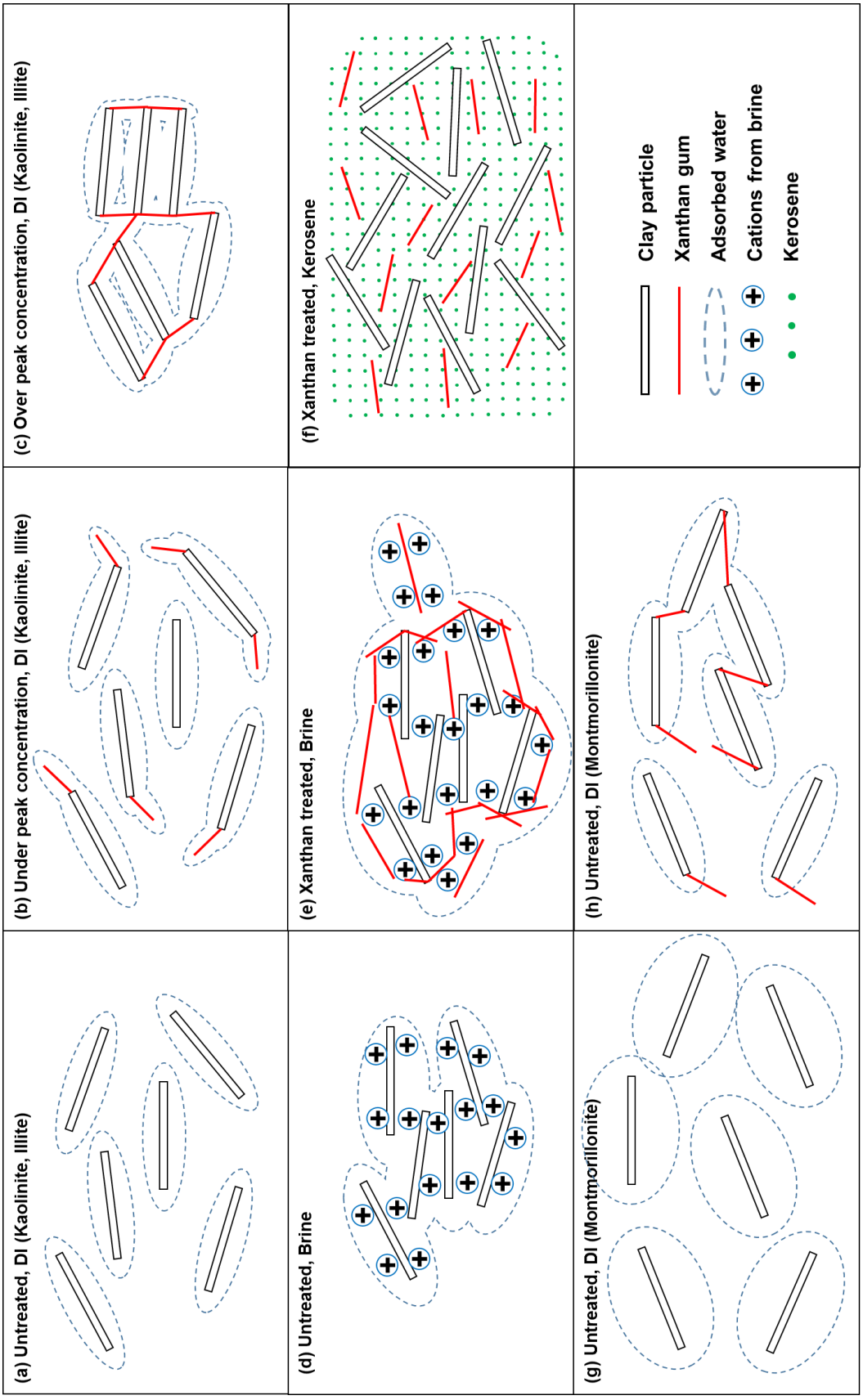

Figure 3.14 Reaction pattern between xanthan gum and clay molecules due to changes in pore fluid chemical properties

3.4.2 The limitation to apply xanthan treated fines for the classification based on USCS

To classify the xanthan treated fine soils based on the united soils classification system (USCS), liquid limit variation by plasticity index were plotted in Figure 3.15. In USCS, fine soils are classified for the soil with the 50% of passing No. 200 sieve. Thus, the pure and 50% specimen were classified. Based on the USCS, the clay was defined as the soil which 50% or more passes No. 200 sieve and above "A" line. However, by the effect of the xanthan gum, some of the clay specimens were observed below "A" line, especially for kaolinite clay. However, fines below "A" line was classified as silt. Additionally, some clayey silt samples were classified as CL (Clay with low plasticity). Thus, it's inappropriate to classify the xanthan gum treated fines based on the USCS.

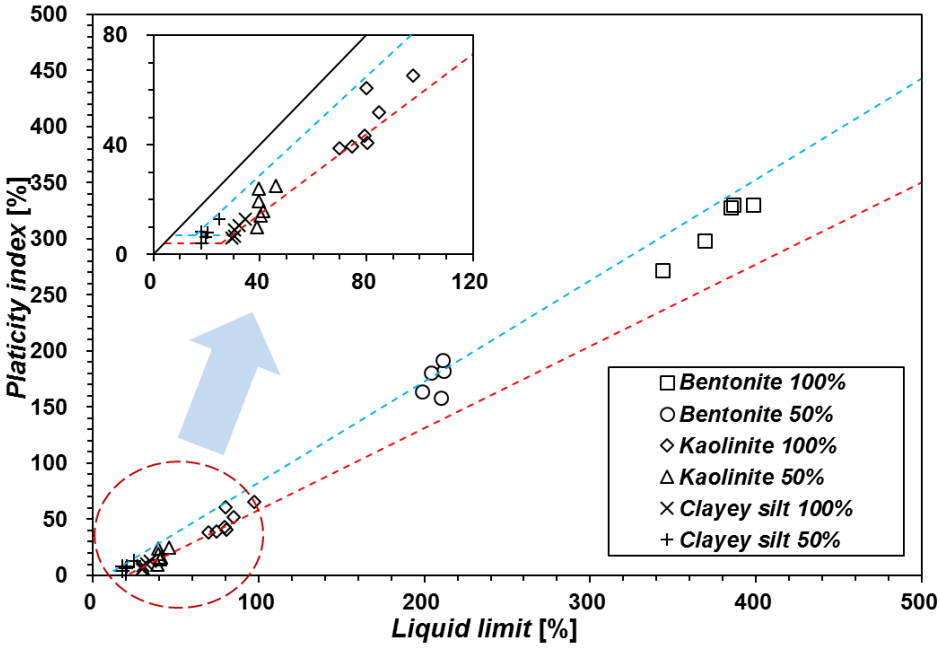

Figure 3.15 Classification of fine soils based on the unified soils classification systems

3.4.3 Electrical Sensitivity

To estimate the response of soil and xanthan gum in fluid chemistry, the liquid limit ratios were plotted using method suggested by Jang and Santamarina (Jang and Carlos Santamarina, 2015). First, the liquid limits obtained with kerosene and brine were corrected to reflect the different fluid properties, specific gravity, and ionic concentrations. Then, the liquid limits measured in the deionized water condition (LL_{DW}) and kerosene condition (LL_{ker}) were divided by the liquid limits measured in brine condition (LL_{brine}). If the divided values were less than 1.0, the reciprocal ratios were used. Those values were plotted on the LL_{DW}/LL_{brine} versus $LL_{kerosene}/LL_{brine}$ quadrants (Fig 3.16). The indication symbols were summarized in table 3.3. This plot shows the common trend where an increase in organic xanthan gum increases the LL_{brine} more than the LL_{DW} and $LL_{kerosene}$. This means that the xanthan gum

supplements in brine conditions increases the water absorption capability of the clay particles through the attachment of exchangeable ions in pore fluids with clay surface, even LL_{brine} became larger than LL_{DW} and $LL_{kerosene.}$

When this plot is observed, the distance of each point from the origin (1, 1) measures the electrical sensitivity of the soil sample, with the point (1, 1) being the point at which there are no effects of the pore fluid chemistry on liquid limits. As shown, the electrical sensitivities show a nearly linear trend for the electrical sensitivity with the addition of xanthan gum in the soils (Fig. 3.16).

As the content of xanthan gum increased for all samples, it tended to change from the upper right (Higher $LL_{kerosene}$, LL_{DW}) to the lower left (Higher LL_{brine}). In case of kaolinite, for small amount of xanthan gum, the electrical sensitivity decreases as it approaches the origin. However, the electrical sensitivity stops decreasing with the further addition of xanthan gum past the critical point, 0.2% for 20% clay, 1% for 50% clay and over 5% for pure clay. Past the critical point, the electrical sensitivity starts to increase again, however in the opposite direction. This point is where the LL_{brine} becomes larger than $LL_{kerosene}$ or LL_{DW}. For clayey silt, due to its low surface charge characteristics, most samples were placed inside the red circle (low electrical sensitivity line). It can be seen that all samples are located on quadrant 4 (LL_{DW}> LL_{brine}> $LL_{kerosene}$). This is due to the high water absorption capability of montmorillonite. Therefore, the liquid limit in kerosene in which no double layer is formed is lower than that in brine, and the effect of double layer thickness reduction due to Na + ion is remarkable compared to other fine soil, and thus it is located on quadrant 4. In all cases, conductivity decreases and permittivity increases. Additionally, all montmorillonite points are located outside the blue circle (high electrical sensitivity line).

From the figure 3.16, it was shown than the addition of xanthan gum has a tendency to neutralize the electrical sensitivity of the samples first, and with further addition, increase the electrical sensitivity only with the opposite charge. The electrical sensitivity value and LLBrine are used for new classification method reflecting pore fluid chemistry, which was proposed by Jang and Santamarina (Jang and Carlos Santamarina, 2015).

Fig 3.17 are contour plot of electrical sensitivity by xanthan gum and fine soil content. Kaolinite forms line symmetry around xanthan 0.5% -clay 20%, xanthan 1% -clay 50% and xanthan 2% -clay 100% lines (fig 3.17 (a)). This is because the cationic charge of xanthan neutralizes the negative charge

of the untreated clay (left of the line) and the treated xanthan increases the total charge after the charge is neutralized (right of the line).

In the case of clayey silt (fig 3.17 (b)), there is almost no surface charge of the silt, and there is only a slight negative charge of the clay fraction included in the clayey silt. Therefore, it can be seen that the injected xanthan neutralizes the total charge at a relatively low concentration and the electrical sensitivity increases steadily as the injection of xanthan increases. In clayey silt case, the electrical sensitivity depends on the xanthan content since silt is the majority (Increase in x-direction).

Since Montmorillonite has a high surface charge, even 2% xanthan treatment does not neutralize the total charge. Therefore, electrical sensitivity decreases steadily with xanthan injection and clay content (fig 3.17 (c)).

Table 3.3 Indication symbols of soil samples used in the experiment

	0	0.1	0.2	0.25	0.5	0.75	1	2	5
Pure Kaolinite	❶	❷			❸	❹	❺	❻	❼
50% Kaolinite	❽	❾		❿	⓫		⓬	⓭	
20% Kaolinite	⓮	⓯	⓰		⓱		⓲	⓳	
Pure clayey silt	①	②			③		④	⑤	
50% clayey silt	⑥	⑦			⑧		⑨	⑩	
20% clayey silt	⑪	⑫			⑬		⑭	⑮	
Pure Bentonite	1	2			3		4	5	
50% Bentonite	6	7			8		9	10	
20% Bentonite	11	12			13		14	15	

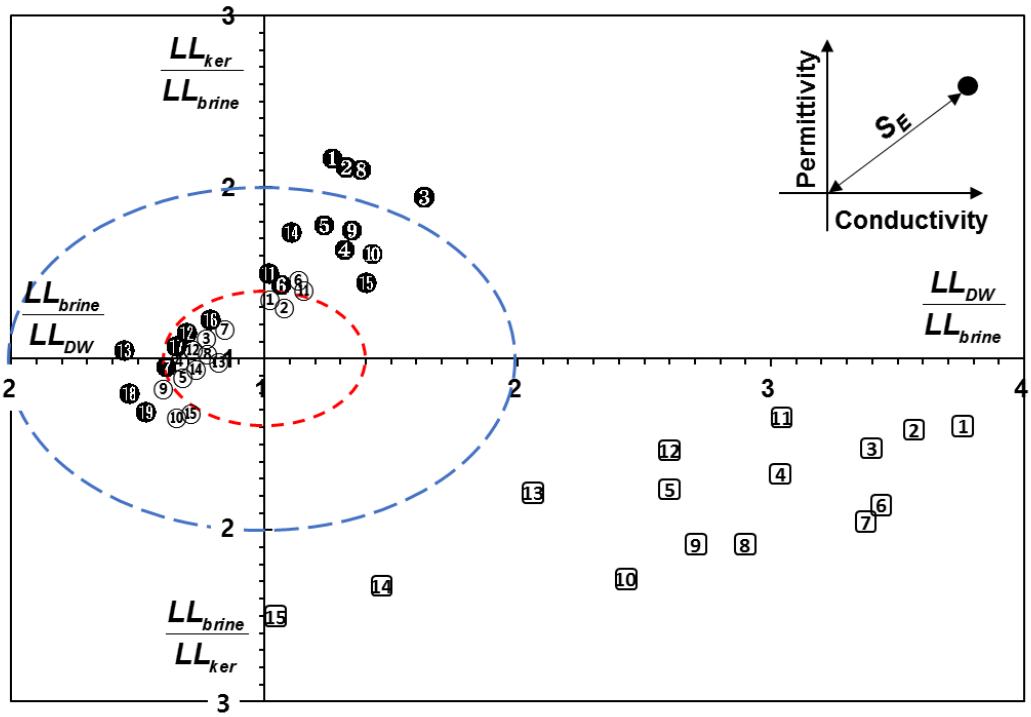

Figure 3.16 The variation of the liquid limit ratios by the change of xanthan gum concentration for various composition of fine soil and sand; The experimental liquid limit values are plotted by the ratio of liquid limits obtained with different types of fluid. X- and Y- axis depends on the conductivity and the permittivity respectively. The distance of each point from the origin is defined as electrical sensitivity

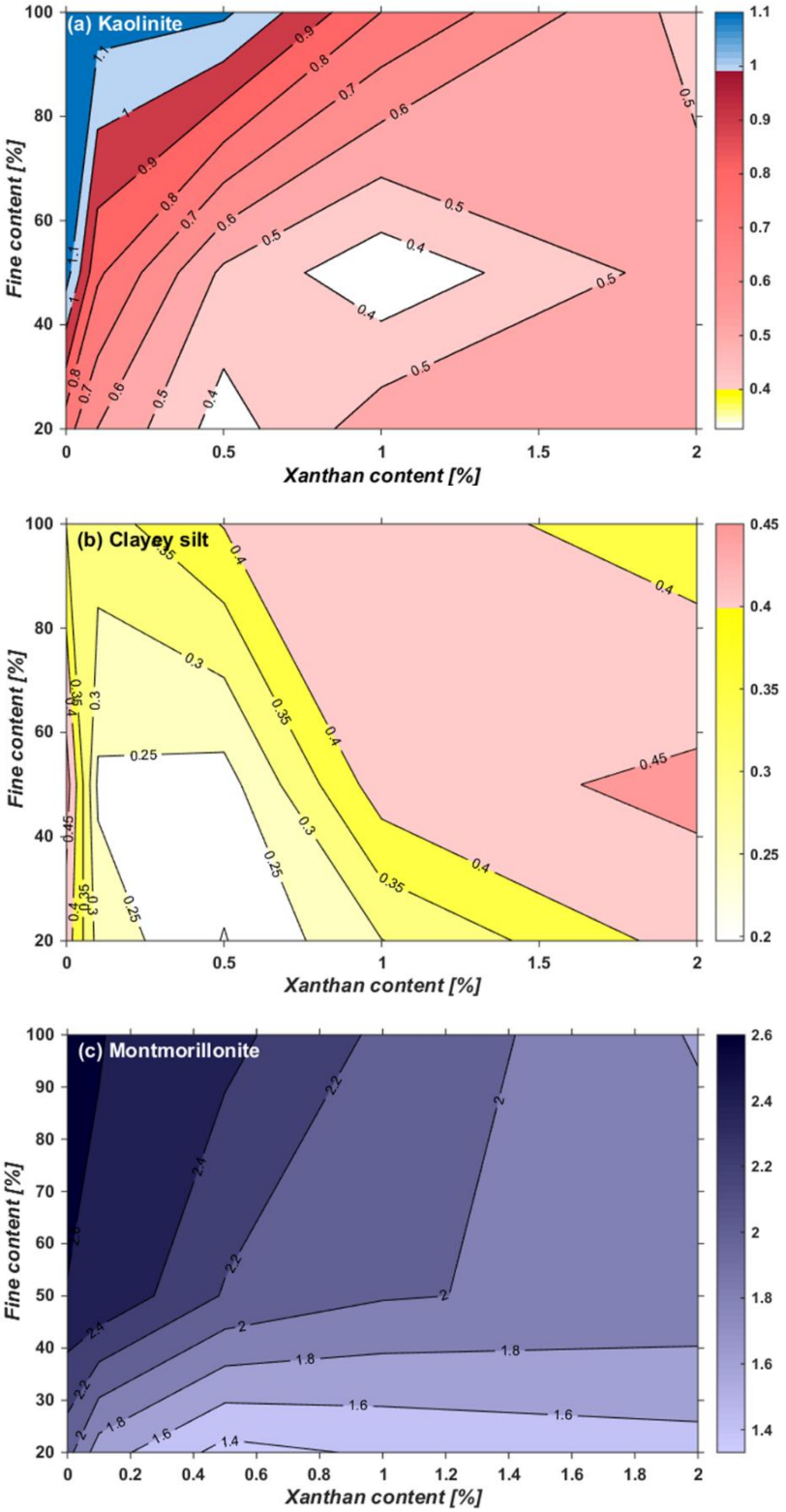

Figure 3.17 Changes in electrical sensitivity with xanthan content and (a) kaolinite, (b) clayey silt and (c) montmorillonite concentration

3.4.4 Soils classification based on sensitivity to pore fluid chemistry

Jang and Santamarina (2015) suggested the classification of fine grains based on pore fluid chemistry (Jang and Carlos Santamarina, 2015). This classification system classifies fine soils by the electrical and plasticity characteristics, and with such as system, the classification can better reflect the soil characteristics, especially with respect to fine soils. From the electrical sensitivity and liquid limits measured with brine, fine soils are classified. From liquid limits with brine, the plasticity of the soils is identified as from no plasticity to high plasticity, and the electrical sensitivity is identified as from low electrical sensitivity to high sensitivity.

Soils with higher clay contents show both higher plasticity and electrical sensitivity. With xanthan gum treatment, plasticity of soils increases due the increase of liquid limit as well as inter-particle bonding of soils induced by hydrophilic adsorption and ionic-bonding characteristics of xanthan gum biopolymer. However, the electrical sensitivities of soils gradually decrease with the xanthan gum treatment to certain bottom point and then rebounds to slightly increase with further xanthan gum contents. For kaolinite clay = 20%, 50%, and 100% soils, the minimum SE values occur at Xanthan gum = 0.5%, 1%, and 2%, respectively. Those values were not for clay materials but for silica or diatom. The minimum SE values become quite similar in a narrow range as 0.3 to 0.4 regardless of soil type. Moreover, in aspects to clay minerals, the lowest SE conditions occur at similar Xanthan gum to clay contents as 2.5%, 2%, and 2%, in order of clay 20%, 50%, and 100% soils. If sand particles are regarded as low electrical sensitivity materials, the 2~2.5% of Xanthan gum to clay content indicates the condition where Xanthan gum and clay particles are fully bonded and form face-to-face packed conglomerates as shown in Figs. 3.11 (a).

For clayey silt, plasticity also increases as xanthan gum content increases. However, electrical sensitivity is remained almost at low electrical sensitivity area. However, due to the charges of xanthan gum, it increases as xanthan gum content increases. For pure clayey silt and 50% clayey silt, electrical sensitivity reaches peak, intermediate electrical sensitivity at 1% treatment and for 20% clayey silt, maximum electrical sensitivity was found at 2% xanthan gum treatment.

For montmorillonite, plasticity increases as xanthan gum increases due to the continuous increase of liquid limit in brine state. Electrical sensitivity decreases until xanthan gum to clay ratio reaches 4% for all montmorillonite mixed soil cases. Then, above 4% of xanthan gum to clay ratio, it starts to increase as shown in figure 3.18. It occurred only in 20% montmorillonite.

Those mechanisms indicated that the xanthan gum content changes the classification extensively, from no plasticity to high plasticity and low electrical sensitivity to high plasticity (shown in Fig. 3.18). The classification clearly shows that xanthan gum, even in small proportions, can drastically change the properties of the soil.

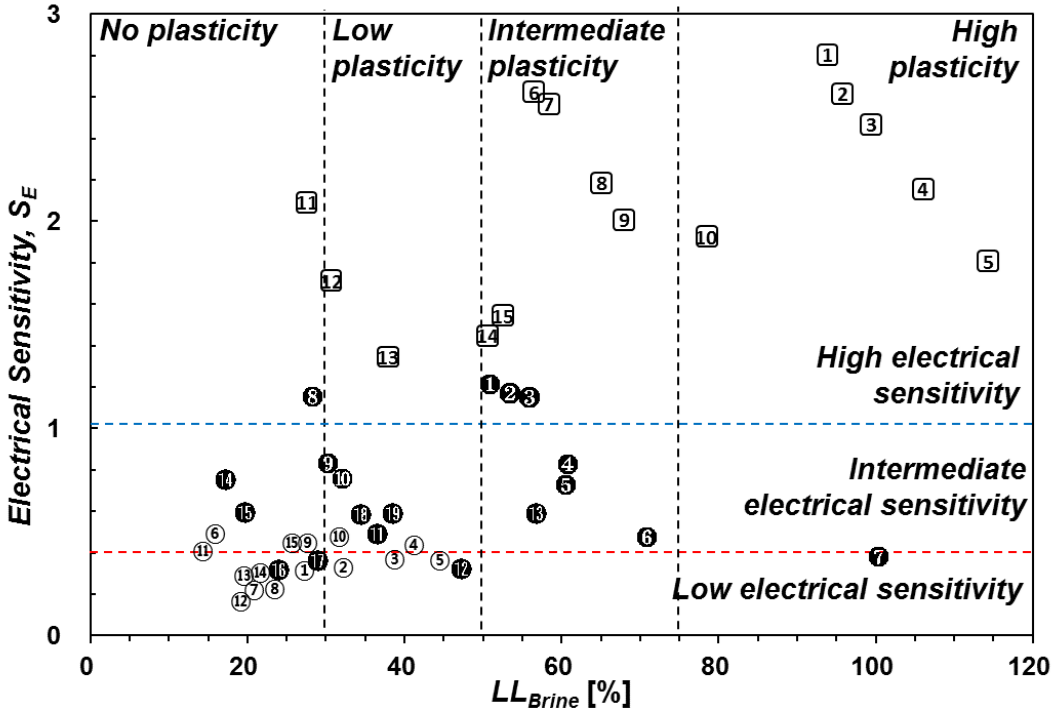

Figure 3.18 Soils classification based on sensitivity to pore fluid chemistry

3.5 Conclusions

Liquid limits of xanthan treated soils are measured with different types of pore fluid chemistry. From the result, it is proved that rheology of xanthan gum, organic biopolymer, shows remarkable differences depending on pore fluid chemistry. Clay fabrics can be changed whether xanthan gum is gellated or not. If xanthan gum is not gellated, it does not react with clay particles and does not make bridges between clay particles. With kerosene, xanthan gum is not gellated. In contrast, xanthan gum is dissolved and gellated in water. Therefore, the structure of xanthan mixed soils in water and kerosene is totally different. Existence of exchangeable cations also changes xanthan gum rheology. Due to larger interaction force of ions with clay than xanthan gum, exchangeable cations is combined with clay particle first. After, xanthan gum interacts with the remaining charge of the ions surrounding clay-sodium ions mixture.

From the result, it is proved that xanthan gum has conflicting effects on liquid limits of soil. In other words, xanthan gum can increase and decrease water absorption capability of soil. First, due to the reaction of xanthan gum and clay particle, its surface area decreases. Decreasing surface area drops the absorption capability of soil particles and causes liquid limit decline. Second, xanthan gum itself can absorb water. Lastly, xanthan gum can supplement decreased water absorption capability due to ions on the clay surface. Thus, xanthan gum increases liquid limit. Because of these complex phenomena, the classification of xanthan gum treated fine soils varies from no plasticity to high plasticity and no electrical sensitivity to high electrical sensitivity.

Chapter 4. The effect of biopolymer on the coagulation of clay suspensions

4.1 Introduction

According to the World Resources Institute, 54% of the Indian subcontinent is currently facing high to extremely high water stress (Fig 4.1), 70% of its surface water is polluted, and more than 100 million people are living in areas of poor water quality (WBCSD, 2015). The data clearly show that increasing water demand along with a serious decline in freshwater sources poses a major challenge to the management and reuse of groundwater. These conditions are also motivating researchers to improve and develop new water treatment technique, such as filtering (Kasim, Mohammad and Abdullah, 2016, Rajapakse, Gallage, Dareeju, Madabhushi and Fenner, 2015).

To reduce potential pollutants from groundwater, biological, chemical, and physical methods are widely used. Bioremediation is a method that uses natural biological activity to biologically degrade or destroy various organic contaminants (Vidali, 2001). Chemical treatment involves the application of agents to promote the degradation of hazardous substances; for example, oxidation-reduction reactions such as ozonation, chlorination, and UV irradiation are applied to bread down organic substances (Marco, Esplugas and Saum, 1997). Meanwhile, physical treatments use physical means to remove contaminants and other hazards, using methods such as electro kinetics (Khoiruddin, Hakim and Wenten, 2014), soil washing and thermal desorption, air sparging/air stripping, and incineration (Shackelford and Jefferis, 2000). In chemical and physical methods, coagulation, flocculation, and sedimentation are processes commonly used to improve the effectiveness of water treatment (Matilainen, Vepsäläinen and Sillanpää, 2010). Furthermore, coagulation and sedimentation are essential procedures in land reclamation, for example, to construct artificial islands through sedimentation processes (Chang and Cho, 2010).

The mechanism for removing waste materials from groundwater involves the transformation of a stable clay colloidal suspension into coagulated or flocculated systems, by neutralization of the repulsive forces on the clay surface (Sengco, Li, Tugend, Kulis and Anderson, 2001). In order to accelerate the coagulation process of a clay suspension, specific coagulants are used in the suspension. Synthetic polymers, polyacrylamide, and mineral additives (aluminum sulfate, ferric chloride, ferric sulfate, and polyaluminum chloride) are the most commonly used coagulants (Csempesz, 2000, Aguilar,

Sáez, Lloréns, Soler, Ortuno, Meseguer and Fuentes, 2005, Tatsi, Zouboulis, Matis and Samaras, 2003, Amuda and Alade, 2006, Pierce, Henry, Higham, Blum, Sengco and Anderson, 2004).

However, these coagulants can pose serious health problems. For instance, while polyacrylamide is known to be an effective conditioner for stabilizing soil aggregates, reducing soil erosion and increasing water infiltration (Seybold, 1994) or water and nutrient movements in soils (Kim, Song, Kim, Kim, Kim, Choi and Seo, 2015) and itself is non-toxic to humans, animals, fish, and plants, its residual acrylamide monomer content is a neurotoxin to humans (Seybold, 1994). Therefore, the residual content needs to be controlled at levels lower than 0.05% (Theodoro, Lenz, Zara and Bergamasco, 2013).

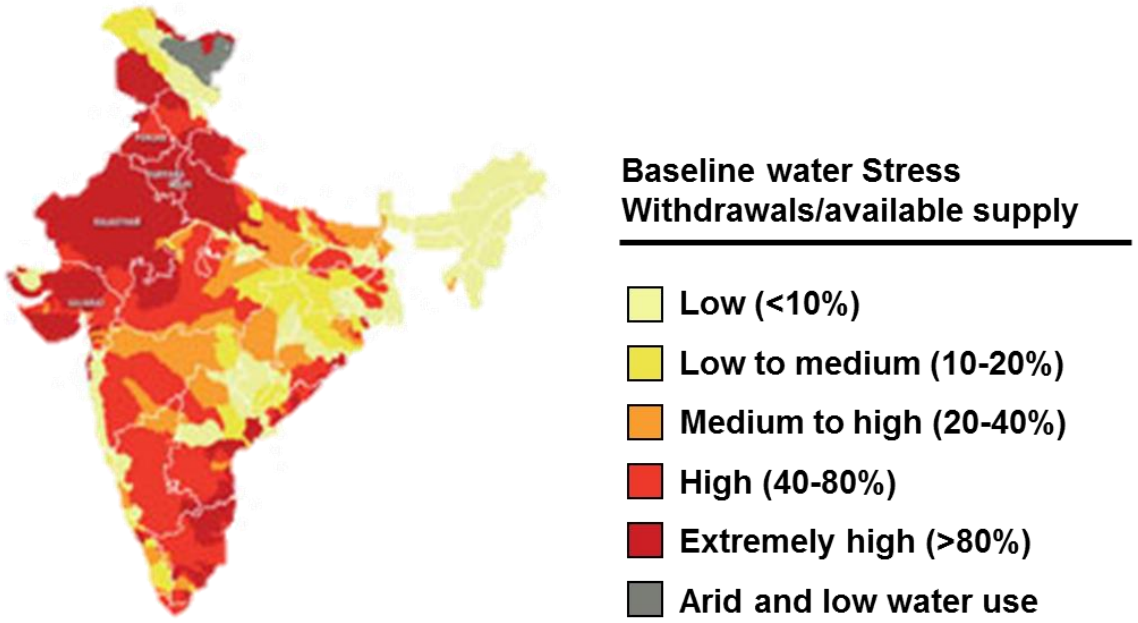

Figure 4.1 Water stress in India (WBCSD 2015)

Recently, organic biopolymers are actively attempted in various environmental and geotechnical engineering purposes (Chang, Prasidhi, Im and Cho, 2015, Chang and Cho, 2012, Chang and Cho, 2014, Chang, Im and Cho, 2016, Chang, Im and Cho, 2016, Chang, Im, Prasidhi and Cho, 2015, Chang, Jeon and Cho, 2015, Chang, Prasidhi, Im, Shin and Cho, 2015). Chitosan, an amino-biopolymer, has received a great deal of attention as a bio-flocculants in water treatment processes (Pan, Huang, Chen and Chung, 1999, Pan, Zhang, Chen, Zou and Yan, 2006, Roussy, Van Vooren and Guibal, 2005, Chatterjee, Chatterjee, Lee, Lee and Woo, 2009). However, because the amino groups of chitosan do not protonate at high pH, chitosan is insoluble in aqueous or alkali solvents. Therefore, the efficiency of chitosan

decreases at high pH, and is restricted even at a neutral pH of 7.0 (Chatterjee, Chatterjee, Chatterjee, Das and Guha, 2005). Furthermore, one kilogram of chitosan costs US $750- 1,0001. Therefore, the practical use of chitosan as a water treatment agent is challenging from an economic point of view.

To overcome the aforementioned limitations of chitosan, this study proposes ε-polylysine, a food grade biopolymer, as a new alternative. In sedimentation aspect, the activity of ε-polylysine is not affected by pH or even the presence of high concentrations of salt (1.0M NaCl) (Chheda and Vernekar, 2014). Furthermore, ε-polylysine is less expensive than chitosan, being just US $10 ~ 3002 per kilogram. In addition, ε-polylysine is a completely non-harmful material, and was approved by the Japanese Ministry of Health, Labor and Welfare as a preservative in food in the late 1980s (Chheda and Vernekar, 2014). Nonetheless, despite these advantages, there have been few studies on the application of ε-polylysine as a coagulant to precipitate soil suspensions.

In this study, a series of sedimentation experiments with varying concentrations of ε-polylysine was conducted. This study provides a detailed explanation of the interaction between ε-polylysine and clay. Furthermore, the effects of ε-polylysine in the sedimentation process are clarified.

[1] Material price quoted by Sigma-Aldrich Co., LLC. (www.sigmaaldrich.com) in 2016
[2] Material price quoted by Zhengzhou Bainafo Bioengineering Co., Ltd. (http://en.bnfsw.com) in 2016

4.2 Methods and materials

4.2.1 Materials

4.2.1.1 ε-Polylysine

ε-Polylysine is a type of polylysine, a lysine homopolymer that contains bonds between the carboxyl and ε-amino groups. It is produced by the fermentation of bacteria, Streptomyces albulus. At pH 7, ε-polylysine has positive charges due to positively charged hydrophilic amino groups at the L-lysine. The typical molecular formula for ε-polylysine is $C_{180}H_{362}N_{60}O_{31}$.

ε-Polylysine has both hydrophobic and hydrophilic characteristics. Methylene groups on the molecule are hydrophobic and carboxyl and amino groups are hydrophilic. This structure can prevent microbial activity and the decomposition of food. ε-Polylysine acts as a cationic surface-active compound and can constrain the proliferation of microorganisms such as yeast, fungi, and bacteria species. Therefore, it can be used as a food preservative (Hiraki, Ichikawa, Ninomiya, Seki, Uohama, Seki, Kimura, Yanagimoto and Barnett, 2003). Additionally, the cationic charges of ε-polylysine can interact with the negatively charged surfaces on a cell, a drug or fine clay. Because of this electrical interaction, polylysine can be used as a coating agent for tissues or drugs in biotechnology (Hiraki, Ichikawa, Ninomiya, Seki, Uohama, Seki, Kimura, Yanagimoto and Barnett, 2003, Mazia, Schatten and Sale, 1975, Park, Jeong and Kim, 2006).

In this study, ε-polylysine was used to accelerate the coagulation and flocculation of clay particles, due to the electrical interaction between the negatively charged facial surfaces of clay particles and the positively charged ε-polylysine. This interaction induces the clay suspension to form flocs, which sediment to the bottom. This phenomenon can be used to remove waste materials in groundwater.

Commercial ε-polylysine (BNF CO., LTD, CAS No. 28211-04-3) was chosen as the surfactant to coagulate clay particles in this study. Its molecular weight is 3,500 – 4,500 Da, and it is effective over a wide range of pH values, from about 4 - 10.

4.2.1.2 Chitosan

Chitosan is a linear polysaccharide produced from chitin, the second most abundant polysaccharide. Chitosan is extracted from the outer skeletons of crustaceans, shrimp, and lobsters (Dutta, Dutta and Tripathi, 2004). It is randomly composed of β-1,4-D-glucosamine ($C_6H_{13}NO_5$) and N-acetlyglucosamine ($C_8H_{15}NO_6$). The amino group (N^-) in chitosan has a positive charge and is more or less soluble in acidic to neutral solutions depending on pH (Goosen, 1997).

Chitosan is a highly biodegradable material (Hirano, Koishibara, Kitaura, Taneko, Tsuchida, Murae and Yamamoto, 1991) and is currently widely used in ecologically friendly fertilizers and biopesticides in agriculture and horticulture (Linden, Stoner, Knutson and Gardner-Hughes, 2000). Furthermore, because of its biocompatible, antibacterial, and polyelectrolytic characteristics (Kobayashi, Kiyosada and Shoda, 1996), chitosan is used in various other industrial applications including water treatment, chromatography, as additives for cosmetics, textile treatment for antimicrobial activity (Shin, Yoo and Min, 1999), novel fibers for textiles, photographic papers, biodegradable films, biomedical devices, and microcapsule implants for the controlled release in drug delivery (Sezer and Akbuga, 1999, Bartkowiak and Hunkeler, 1999, Suzuki, Mizushima, Umeda and Ohashi, 1999)

In civil engineering, chitosan has been used to remove wastes in groundwater by flocculation (Pan, Huang, Chen and Chung, 1999, Pan, Zhang, Chen, Zou and Yan, 2006, Chatterjee, Chatterjee, Lee, Lee and Woo, 2009) or in coating processes (Gupta, Yunus and Sankararamakrishnan, 2013). Chitosan binds fine particles in suspension, and also removes phosphorus, heavy metals, and oils from water. Thus, it is important for water filtration (Juang and Shiau, 2000). In particular, chitosan is suitable for the adsorption of metals, such as Cd^{2+}, Zn^{2+}, Cu^{2+}, Pb^{2+}, etc., due to its chelating property (Liu, Tokura, Haruki, Nishi and Sakairi, 2002).

This study used commercial chitosan with low molecular weight, 50,000 – 190,000 Da, (Sigma-Aldrich, CAS No. 9012-76-4). Its viscosity is 20 – 300 cP at 1% weight to 1% acetic acid.

4.2.1.3 Kaolinite Clay

In this study, kaolinite clay, which has the mineral composition Al_2O_3-$2SiO_2$, was chosen as a representative clay material. The kaolinite used in this study was mined in Indonesia and the kaolinite was used in powdered form with 3% moisture content. It was first mined and then crushed into a powder. Kaolinite has a mean particle size D_{50} = 0.22 μm, specific gravity (Gs) of 2.65, and is classified as a clay of high plasticity, CH via USCS (Unified Soil Classification System).

4.2.2 Experimental Set up

4.2.2.1 Sedimentation

To estimate and compare the coagulation efficiency of ε-polylysine and chitosan, sedimentation tests of clay suspensions were conducted. During the experiments, the temperature and relative humidity were controlled as 22 ± 2°C and 25%, respectively, while the pH of the deionized water was near 6.5. For each experimental trial, 16 g of kaolinite clay and 80 g of deionized water were injected into a 100 ml graduated cylinder. The water content was determined as the point where the suspension could be mixed well by an electric stirrer machine (Kolaian and Low, 2013). The effect of gravity on sedimentation is greater than that of the coulombic attraction when the water content of kaolinite slurry is below 500% (Imai, 1980). Thus, the initial water content was fixed as 500% to render sufficient interaction between clay minerals and biopolymer additives. Previous researches also determined 500% water content for experiments (Kondo and Torrance, 2005, Imai, 1981). The inside diameter of the graduated cylinder was 26.5 mm, and was larger than the “yield diameter”, which is the diameter at which settling cannot occur due to the wall effect, which was about 13 mm for this experiment (Michaels and Bolger, 1962). As a result, the graduated cylinder is large enough to observe any accelerated sedimentation effect caused by the biopolymers. The volume, pH, and turbidity of the suspension were assumed the same since the same initial water content of 500% was set for each cylinder. Clay suspensions were then prepared by mixing kaolinite and deionized water in the graduated cylinder.

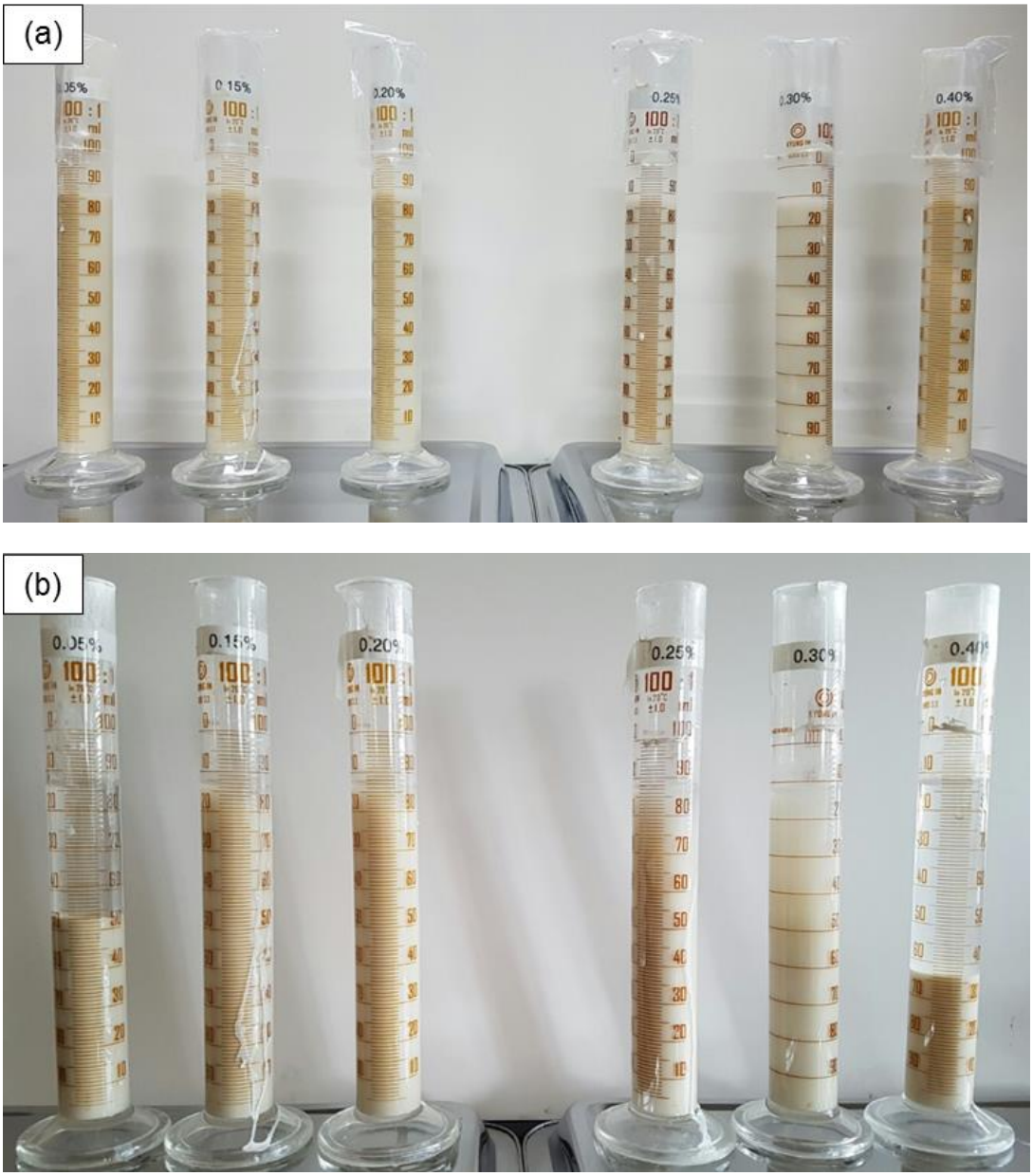

Figure 4.2 sedimentation volume after (a) 0 minutes and (b) 760 minutes from initial time

The cylinders were turned upside down about 20 times to uniformly spread clay particles throughout the suspension. Afterwards, chitosan and ε-polylysine were poured into each suspension with various biopolymer weight to water weight ratios, of 0%, 0.1%, 0.2%, 0.5%, 1%, and 2%, and then thoroughly mixed. For ε-polylysine, additional experiments were conducted at 0.05%, 0.15%, 0.25%, 0.3%, and 0.4% content to estimate the sedimentation effect at lower content more accurately.

After the mixing of the biopolymer and clay suspensions was completed (Fig 4.2a), the volume of clay sediments was measured until the sediment volume change became constant (Fig 4.2b). Then,

the measured volumes were divided by the initial volume to generalize the variation in sedimentation volume, determined as the sediment ratio (instant height ratio to the initial height, %).

$$R_{Sed} = \frac{V_i}{V_i} \times 100\ [\%] \tag{1}$$

where R_{sed} is the sediment ratio, V_t is the sediment volume at time t and V_i is the initial sediment volume.

4.2.2.2 Spectrophotometer

Using spectrophotometry, the light reflection or transmission properties of a target material can be quantitatively measured. There have been many attempts to measure the clarification and turbidity of a supernatant to determine the flocculation and sedimentation of clay suspensions using spectrophotometric experiments (Petzold, Mende, Lunkwitz, Schwarz and Buchhammer, 2003, Li, Zhou, Zhang, Wang and Zhu, 2008, Kurane, Hatamochi, Kakuno, Kiyohara, Hirano and Taniguchi, 1994). By comparing the absorbance values for each case, the clay particles remaining suspended in the supernatant can be evaluated. The amount of light absorbed during the propagation is expressed as a dimensionless value, absorbance. Absorbance (A) is the logarithmic ratio of the radiant flux received (ϕ_e^i) over the material to the radiant flux transmitted (ϕ_e^t).

$$A = \log_{10}(\frac{\phi_e^i}{\phi_e^t}) \tag{2}$$

The absorbance property represents the amount of clay particles floating in the liquid. Therefore, higher absorbance means the sedimentation procedure has low efficiency.

After the sedimentation process was finished, 1000 µl volume of the uppermost layer was sampled with the use of a micropipette (Eppendorf Research® plus). The sample was then poured into a disposable cuvette (Eppendorf® UVette®) to fit into the spectrophotometer. The center height of the cuvette is 8.5 mm, the chamber volume is 2000 µL, and light in the wavelength range of 200-1600 nm can penetrate the cuvette. Afterwards, the cuvette was installed in the spectrophotometer (DR 5000TM UV-Vis Spectrophotometer) and visible light with a 640 nm wavelength, that is, red light, was used to measure the absorbance of each sample. Through the light penetration procedure, the effect of the biopolymer concentration on the absorbance variation was measured.

4.2.2.3 Microscopic Observation

Microscopic observations were performed to identify the interaction behavior between kaolinite particles in the suspension and the ε-polylysine biopolymer. After the final constant sedimentation volume was measured, the clay aggregates at the bottom of the cylinders were sampled and smoothly spread out on carbon conductive tabs (Pelco TabsTM) attached on an SEM mount (diameter 25 mm). The remaining moisture in the samples was eliminated using a manual air dryer for a minute. To improve the imaging of the specimen, osmium coating of the SEM mount was conducted using an osmium plasma coater (OPC 60-A). Using a scanning electron microscope (SEM; SU5000), high-resolution images were taken, and they showed inter-particle bridges and structures between the clay and ε-polylysine particles.

4.3 Results and analysis

4.3.1 Sedimentation test

The sedimentation behavior of soils is governed by 1) type of clay mineral; 2) type of dissolved electrolytes; 3) initial water content (water to solid ratio in mass); and 4) ionic concentration in water. Generally, gravitational force becomes dominant when the initial water content and ionic concentrations are relatively low, while inter-particle flocculation governs the sedimentation behavior when both water and ionic contents increase (Imai, 1980).

Different sedimentation behaviors are exhibited based on the electrolyte concentration. The sedimentation behaviors of kaolinite clay suspensions can be divided into three categories, flocculation-sedimentation, accumulation-sedimentation and mixed-sedimentation (Ma and Pierre, 1992). Mixed sedimentation can be observed when accumulation sedimentation occurs for heavy solid matters at the beginning, while flocculation occurs sequentially with remaining light suspensions. However, it is hard to distinguish pure accumulation and mixed (accumulation and flocculation) sedimentation behaviors clearly. Thus, we avoided mixed sedimentation behavior in this study. The left side of Fig 4.3 (a) and (b) shows flocculation-sedimentation.

In flocculation sedimentation, two layers, the flocculated sedimentation and the clear supernatant liquid, are clearly distinguishable. The flocculated sedimentation volume gradually drops down as sedimentation proceeds. This means that the density of the sediment continuously increases until reaching a final constant volume.

The right side of Fig 4.3 (a) and (b) shows accumulation-sedimentation. With accumulation sedimentation, there is a transition zone that remains in a suspended state. Accordingly, the division between the layers is less clear than in the case of flocculation sedimentation. Accumulation-sedimentation occurs due to the gravimetric settling of clay particles. Thus, the height of the interface between the accumulation-sedimentation zone and the transition zone continuously increases from the beginning to the end of sedimentation.

In general, flocculation sedimentation induces uniform sediment due to the identical settling behavior (e.g. similar size and gravimetric force) of each individual floc, while sediments formed via accumulation sedimentation shows gradual grain size distribution depending on the different size and density of distinguished solid matters. In the experiments, both flocculation and accumulation sedimentation behaviors were observed analyzed for ε-polylysine-treated kaolinite clay.

4.3.1.1 ε -polylysine

Sedimentation Volume

The variation in sedimentation volume when ε-polylysine was used as a coagulant is shown in Fig 4.4. The results show that for most ε-polylysine concentrations, the sedimentation follows flocculation sedimentation behavior. However, from 0.15% to 0.25%, accumulation sedimentation became the dominant sedimentation mechanism. Each sedimentation type shows a different tendency in volume variation. For flocculation sedimentation, the total volumes of flocs decline together. Thus, the sedimentation volume is continuously decreased. In contrast, with accumulation sedimentation of 0.15% to 0.25%, clays were accumulated at the bottom of the cylinder from the heaviest particle. Therefore, the sediment volume increased until the volume became constant.

Flocculation sedimentation volumes are shown for ε-polylysine concentrations of 0.0%, 0.1%, 0.5%, 1%, and 2% in Fig 4.4 (a). For the flocculation sedimentation cases, even 0.1% injection of ε-polylysine produced a reduction in final sedimentation volume, by 74%, compared to the final volume at 0.0% injection. The lowest sedimentation volume, 27.5% of the initial sediment volume, occurred with an injection of 0.5% concentration ε-polylysine. The final sediment volume increases again as the ε-polylysine concentration exceeds 0.5%, but this value is smaller than that of the untreated clay suspension.

According to the DLVO theory (Pierre, 1992), counter ions, cations for kaolinite clay, on the ε-polylysine surface neutralize the suspension charges and lower the repulsive forces between the colloidal particles. Therefore, the double layer around the clay particles is compressed and the clay particles collide more frequently. This rheology in the clay suspension flocculates the clay suspension and constitutes sedimentation.

Acceleration of the sedimentation velocity is also observed in Fig 4.4 (a). The slope of the graph for the ε-polylysine treated suspension is steeper than that of the untreated case. This indicates that the injection of ε-polylysine in the clay suspensions accelerates the sedimentation process.

For the 0.15%, 0.20%, and 0.25% ε-polylysine concentrations, the dominant sedimentation mechanism was accumulation sedimentation (Fig 4.4 (b)). ε-Polylysine breaks the floc structure and reconstitutes the floc structure by bonding clay particles face to face. However, for this case, the concentration of injected ε-polylysine was not sufficient to form bridges between clay particles. Hence, the dominant role of ε-polylysine was destroying clay structures and charge neutralization, and the heavy particles dropped by gravimetric force.

The volumes of accumulation sedimentation at 0.15%, 0.20%, and 0.25% are plotted in Fig 4.4 (b). Compared to the flocculation sedimentation, accumulation sedimentation became constant more rapidly. Flocculation sedimentation became constant after more than 1000 minutes, and accumulation sedimentation became constant at about 300 to 400 minutes. Additionally, the final sedimentation volume reached the lowest level of 0.20% and this indicates that at a ε-polylysine concentration of around 0.20%, most particles were separated and floating individually in the clay suspensions.

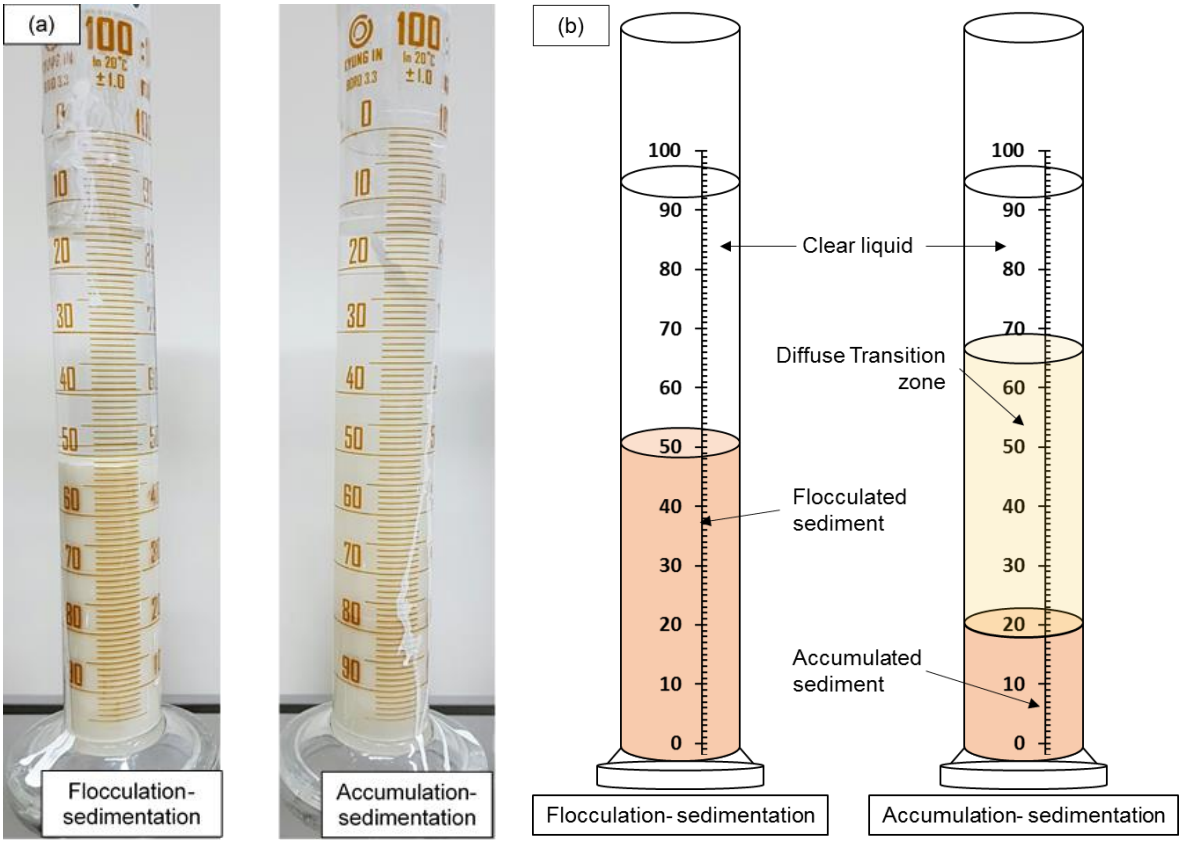

Figure 4.3 Comparison of flocculation and sedimentation (a) pictures after 8640 minutes settling; (b) schematic diagram

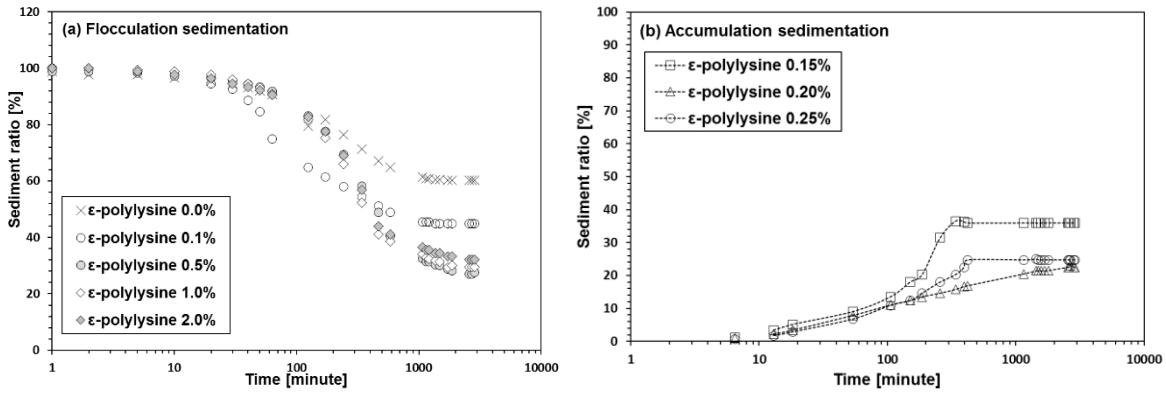

Figure 4.4 Variation in sedimentation volume of ε-polylysine treated suspension for (a) flocculation sedimentation and (b) accumulation sedimentation

Sedimentation Properties

During the sedimentation process, changes occur in the soil void ratio. Clay particles in the suspended state are not in contact and the repulsive forces between the clay particles are large enough to disperse the clay particles. Therefore, the void ratio is large, over 1000%. After sedimentation proceeds, the clay particles interact with each other and create denser structures, and hence the void ratio decreases. The decrease in void ratio increases the dry unit weight.

The void ratio was derived using Eqs. (3),

$$e = \frac{V_{sed}}{Gs \times \gamma_{water} \times W_{soil}} - 1 \tag{3}$$

Where e is the void ratio, V_{sed} is sediment volume, Υ_{water} is the unit weight of water, W_{soil} is the weight of the soil.

For the flocculation sedimentation, changes in the sedimentation property by time were calculated, because it can be assumed that all the clay particles settled together. However, in the case of accumulation sedimentation, it could not be assumed that the accumulated volume contains all the clay particles in the suspension. Therefore, only the flocculation sedimentation cases were compared. Flocculated sediment settles down together and so the volume of the sediment continues to shrink. Shrinkage in volume continuously decreased the void ratio (Fig 4.5). The existence of ε-polylysine assisted the formation of flocs and accelerated the variation in sedimentation properties. Additionally, structures in the flocculation sedimentation differed according to the ε-polylysine concentration. Because low ε-polylysine treated sediments had looser structures than high ε-polylysine treated sediments, the final void ratio decreases as ε-polylysine concentration decreases.

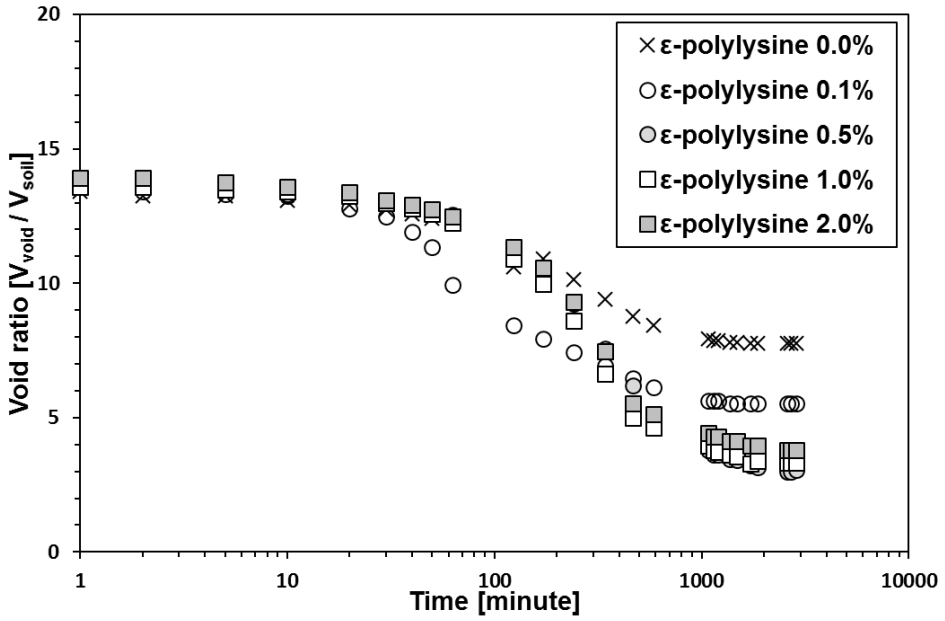

Figure 4.5 Variation in void ratio of ε-polylysine treated suspensions

4.1.2 Chitosan

Sedimentation Volume

Chitosan is one of the most commonly used, environmentally friendly coagulants for reducing pollutants in groundwater (Roussy, Van Vooren and Guibal, 2005, Zou, Pan, Chen and Yuan, 2006, Ghaee and Zerafat, 2016). To compare the sedimentation effects of chitosan and ε-polylysine, the same sedimentation experiment procedure was followed.

Unlike the ε-polylysine treated suspension, the use of chitosan increases the final sedimentation volume. This occurs due to the higher molecular weight of chitosan compared to ε-polylysine. Generally, high molecular weight coagulants form bridge flocculation. Bridge flocculation renders larger flocs than those formed by ionic destabilization (e.g. via salts). However, although bridge flocculation forms large flocs, flocs have empty voids along bridge connections which results in overall strength reduction (Yukselen and Gregory, 2004).

Compared to the final sediment volume of the untreated sample, the largest final volume, 118 %, occurred with the 2.0% chitosan treated suspension. This indicates that the chitosan formed looser floc structures and the density of the sediment gradually decreased.

Additionally, chitosan used in this study has a higher molecular weight (50,000-190,000 g/mol) than that of ε-polylysine (3,200-4,500 g/mol). Thus, chitosan induces bridge flocculation between

kaolinite particles regardless of chitosan concentration, while shows higher final void ratios (lower density) compared to ε-polylysine treatment. Therefore, flocculation sedimentation was observed for every experimented chitosan concentration, 0.0%, 0.1%, 0.2%, 0.5%, 1.0%, and 2.0%. Variation in sedimentation volume by time is plotted in Fig 4.6.

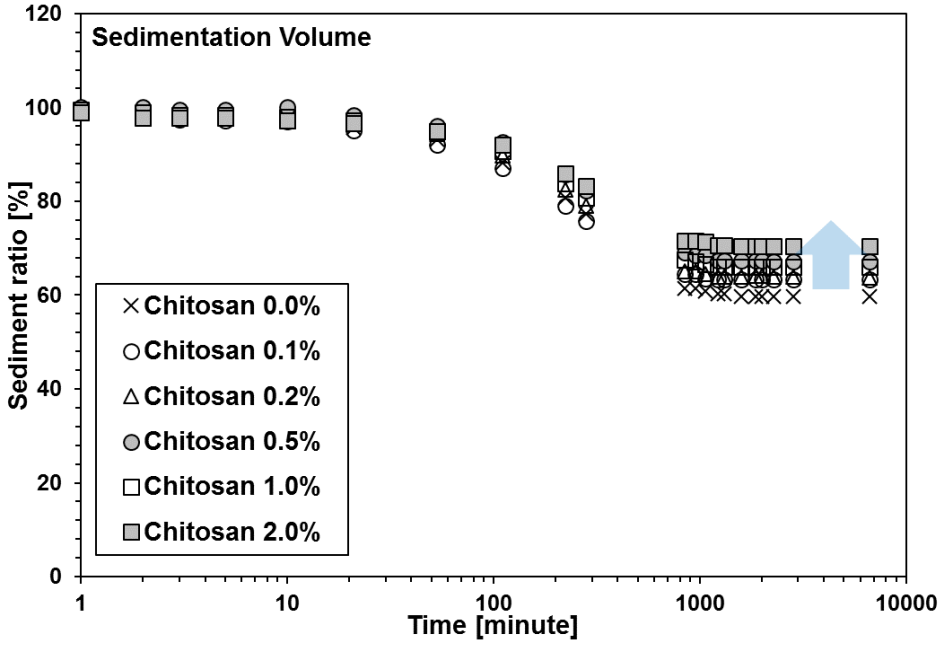

Figure 4.6 Variation in flocculation-sedimentation volume of chitosan treated suspensions

Sedimentation Properties

Sedimentation void ratio is plotted in Fig 4.7. The void ratio was increased by increasing chitosan concentration.

The lowest final void ratio was also obtained for the untreated case, and the maximum, which was 120.4% larger than that of the untreated sample, was obtained for the 2.0% treated case. The results show that the structure of the chitosan treated sedimentation is looser than the ε-polylysine treated sediments, and even pure clay floc structures.

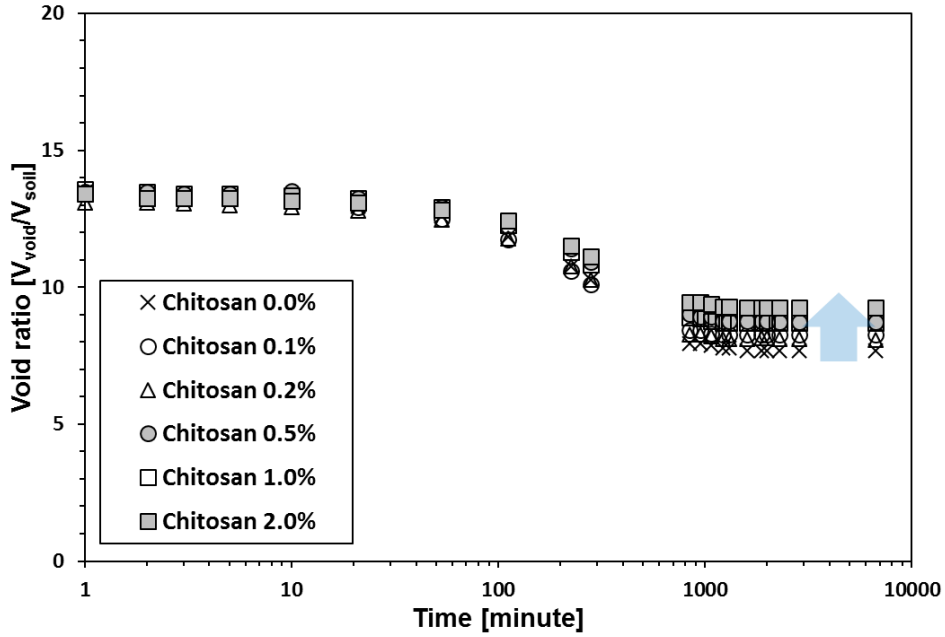

Figure 4.7 Variation in sedimentation properties of chitosan treated suspensions; void ratio

4.2 UV Penetration

Laboratory sedimentation tests were proceeded for 8,640 minutes (6 days), since sediment heights converged after 1,000 minutes in most cases. Thus, 6 days were enough to collect uppermost supernatant fluid, which is totally separated from solid particles. The spectral absorbance values of the uppermost supernatant were measured with a spectrophotometer to determine the clarity of the supernatant. Absorbance refers to the amount of light that is absorbed while penetrating a media. It is expressed as the common logarithm of the ratio of incident to transmitted spectral power. For this study, the UV penetration method was used to measure the remaining clay particles in the upper liquid. After constant sedimentation volumes were observed, the uppermost part of the remaining liquid was

collected using a micropipette and cuvette. Then, the spectrophotometer measured the amount of light penetrating the cuvette.

For the ε-polylysine treated clay suspension (Fig 4.8 (a)), the absorbance value increases at low concentration of ε-polylysine and it reaches the highest absorbance at 0.25% ε-polylysine concentration, which is 0.134. At this stage, the injected ε-polylysine detach kaolinite particles. Therefore, only heavy particles are submerged and light particles float in a suspended state.

Among the experimental conditions, the most clay particles remained at 0.25%. Additionally, the remaining liquid had a greater amount of impurities in the accumulation sedimentation state. Then, as addition concentrations of ε-polylysine were injected, the overall amount of ε-polylysine becomes sufficient to form ε-polylysine – kaolinite flocs which reduces suspensions in the supernatant with gradual absorbance reduction with higher ε-polylysine concentration.

The lowest values were measured at 1% and 2% ε-polylysine concentration. Both absorbance values were 0.005. From the UV penetration results, it was verified that higher ε-polylysine injection improves the clay removal efficiency.

In the case of the chitosan treated clay suspension (Fig 4.8 (b)), the highest absorbance value, 0.085, was obtained at 0.5% concentration and the lowest value, 0.022, at 0.2% concentration. However, even the lowest value was not much higher than the absorbance value of the untreated case, 0.024. Additionally, the absorbance values of chitosan treated sediment is higher than that of ε-polylysine. This shows that the effect of chitosan on the clarity of the supernatant was smaller than that of ε-polylysine.

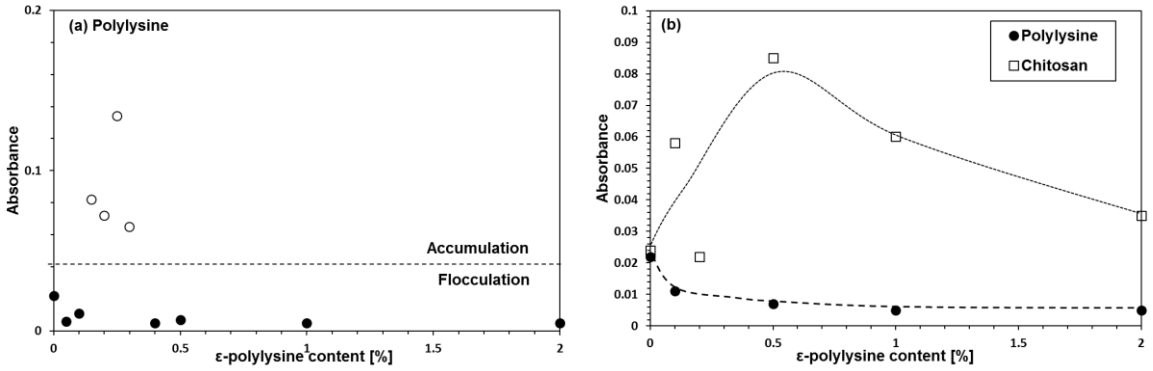

Figure 4.8 Variation in absorbance with biopolymer concentration; (a) ε -polylysine and (b) comparison between ε -polylysine (flocculation sedimentation) and chitosan

4.3 SEM images

A scanning electron microscopic analysis was conducted to compare the sediment structure of low concentration ε-polylysine treated specimens, high concentration ε-polylysine treated specimens, and chitosan treated sediments. Representative sedimentation samples of 0.05% concentration ε-polylysine and 0.40% ε-polylysine treated suspensions were selected. The SEM images for those samples are presented in Fig 4.9, and they indicate different sedimentation structures, altered by different concentrations and coagulants.

First, the effect of the ε-polylysine concentration on the sediment structure is compared in Fig 4.9 (a), (b) and Fig 4.9 (c), (d). At low concentration, 0.05%, the amount of ε-polylysine was not enough to transform the edge to face structures into face to face structures. Thus, the main role of ε-polylysine was breakage of the edge-to-face contacts. In Fig 4.9 (a), (b), face-to-face aggregated particles are not observed in notable quantities. At high concentration, 0.40%, the injected ε-polylysine amount was enough to bond clay particles and form face-to-face contacts (Fig 4.9 (c), (d)).

Face-to-face structures were more abundantly observed than in the case of lower concentration. Additionally, ε-polylysine formed clay conglomerates by bonding clay particles, and the surface of the higher concentration ε-polylysine suspension was coarser than that of the lower concentration treated specimen. The microstructure of the chitosan treated sediment was also different from that of the ε-polylysine treated samples. The surface of the chitosan treated sediment in Fig 4.9 (e), (f) indicates that the face-to-face structures are indirectly bonded.

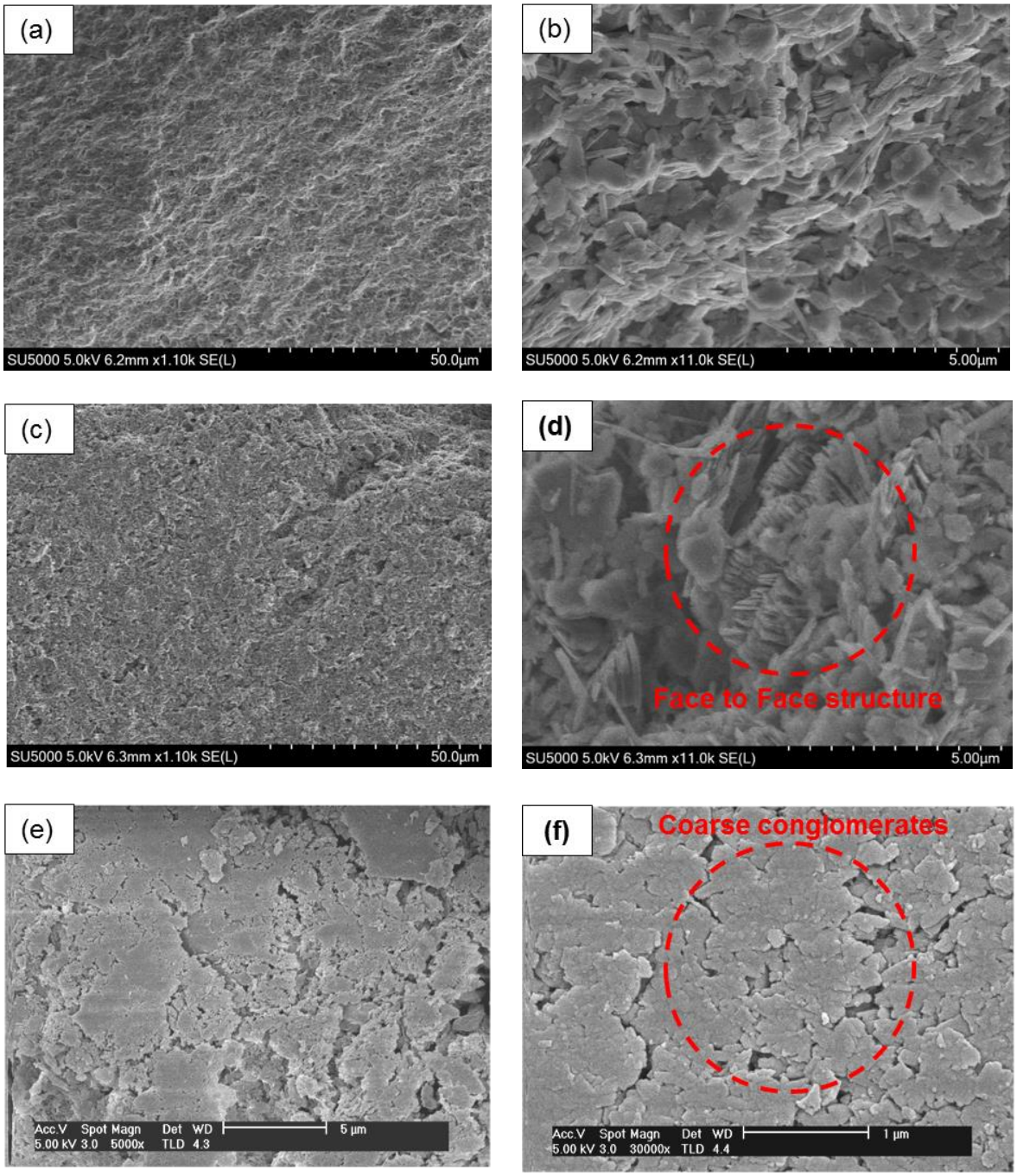

Figure 4.9 SEM images of 0.05% ε-polylysine treated suspension; (a) and (b), flocculation sedimentation of 0.40% ε-polylysine treated suspension; (c) and (d) and chitosan treated specimen (e) and (f)

4.4 Discussions

Floc structure affects the final sedimentation thickness and densities (Sidik, Canakci, Kilic and Celik, 2014). At small concentrations of ε-polylysine, the dominant structure of flocs was an edge to face structure. Naturally, clay has negative charges on its face and positive charges on its edges. Therefore, the edges of the clay particles bond with the faces of the clay particles and these edge to face (EF) bonding structures form flocs (Rand and Melton, 1977). Normally, the EF structure has higher porosity than other types of structures. Thus, the final sedimentation volume is the highest in the untreated case.

Fig 4.10 presents possible inter-particle interaction mechanisms between clay particles and ε-polylysine with ε-polylysine content variation, as obtained from this study. When ε-polylysine is initially injected into a clay suspension, its positive charges break the EF bonds between clays and reconstitute clay particles by bonding the particles. If the injected amount of ε-polylysine is not enough to bridge or bond clay particles, the dominant effect of ε-polylysine in the floc structure is the breakage of EF bonding. During this stage, clay particles are separated and float in the suspension individually and accumulate from the heaviest particles. Hence, the accumulated particles of this stage became coarse. Light particles remain in suspension and these particles increase the absorption value. Therefore, the clarity of the supernatant was the lowest in the 0.25% ε-polylysine treated suspension. Additionally, the injected ε-polylysine decreases the liquid double layer and the distance between clay particles. Due to the larger amount of remaining clay particles and the compressed liquid double layer, the final sedimentation volume reached the smallest value at 0.20%.

At ε-polylysine content above 0.25%, the amount of ε-polylysine is sufficient to form bonds between clay particles. ε-Polylysine interacts with negative charges on the clay face and connects clay particles by face-to-face (FF) structures. Thus, FF flocs are the dominant floc structure at this stage. As the ε-polylysine content increases, injected ε-polylysine bonds with clay particles forming face-to-face structures, and this bonding effect increases the clay floc size. Floc density decreases when the floc size increases (Tambo and Watanabe, 1979). Therefore, the final sedimentation volume is increased by the ε-polylysine concentration at this stage.

In the case of sedimentation tests performed with ε-polylysine, both accumulation and flocculation sedimentation were observed. For chitosan treated suspensions, only flocculation sedimentation was discovered. Additionally, ε-polylysine decreased the final sedimentation thickness,

whereas chitosan increased the final sedimentation thickness. These phenomena occurred due to the molecular size difference between ε-polylysine and chitosan. Chitosan has a 10-50 times higher molecular weight than ε-polylysine. Therefore, flocs formed by chitosan have higher molecular weight than flocs formed in the ε-polylysine treated suspension. Floc size and floc density have an inverse proportional relation. Small floc density resulted in a large final sedimentation volume.

ε-polylysine and chitosan can be applied for different purposes, to form different sediments. With low concentration ε-polylysine, accumulation sedimentation occurs, and sediments have low final volume while the supernatant liquid is turbid. For this reason, it is inappropriate for waste removal in contaminated groundwater, but could be applied in the reclamation industry, such as for artificial island construction.

The supernatant liquids that remained after flocculation sedimentation had lower absorbance values than those in the case of accumulation sedimentation. This means that the clay and the liquid were more effectively separated in the suspension with flocculation sedimentation. This characteristic is suitable for the contaminant removal field.

Additionally, the injection of ε-polylysine decreased the final sedimentation thickness. For chitosan, the final sedimentation volume increased. This volume difference indicates that ε-polylysine and chitosan produce final sediments with different densities. Lower sediment volume indicates that settled materials can be more effectively removed.

In conclusion, higher concentrations of ε-polylysine were more effective than chitosan for the removal of floating matter in suspension, kaolinite in this study. However, it should be noted that the results in this study are based on the use of deionized water. In practical implementations, ground water in field contains numerous ions such as calcium, magnesium, sodium, potassium, bicarbonate, carbonate, sulphate, chloride, and so on. Higher ionic concentration should promote inter-particle flocculation due to enhanced ionic bonds. In this study, deionized water was used to evaluate the pure effect of biopolymer additives on the sedimentation behavior of kaolinite clay regardless of additional ions. However, further considerations with ground water and seawater are required before empirical applications.

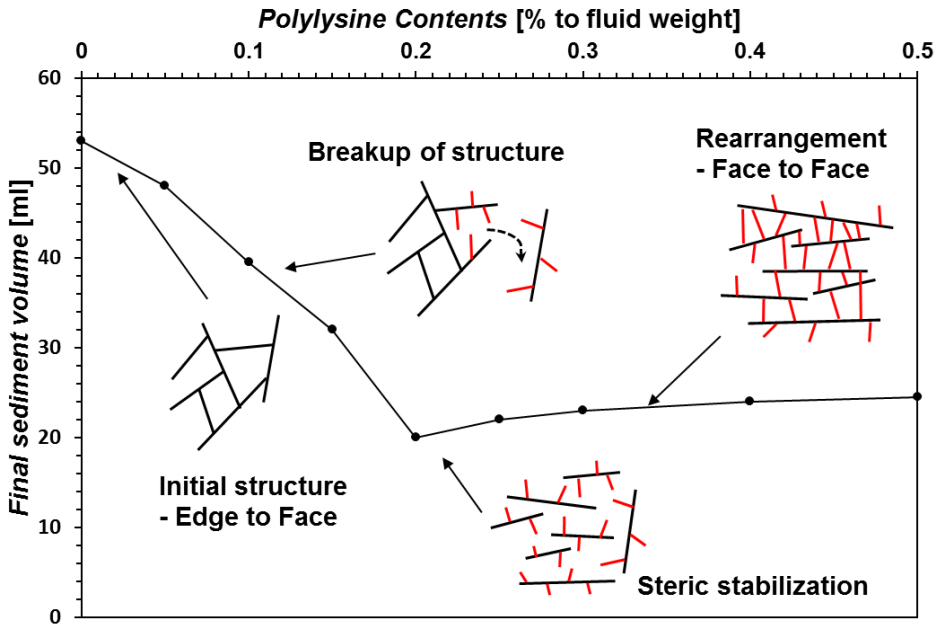

Figure 4.10 Interaction mechanisms of clay suspension by the varying the ε-polylysine content

4.5 Conclusions

In this study, ε-polylysine was proposed as a new environmentally friendly coagulant to remove pollutants in contaminated groundwater. The rheology and the properties for each situation were analyzed using sedimentation experiments and SEM image analysis. The amount of clay particles remaining in the fluid were measured by the spectrophotometer. Additionally, the performance of ε-polylysine as a coagulant was compared with the performance of chitosan.

ε-Polylysine detaches clay flocs at low concentrations and reconstitutes clay flocs at high concentrations. Based on the structural changes, the sedimentation mechanisms of the kaolinite clay suspensions were classified into two types, accumulation sedimentation and flocculation sedimentation. The final sedimentation volume for ε-polylysine was smaller than that of chitosan. This indicates that more highly compacted sediments were obtained for ε-polylysine treated sedimentation. Therefore, ε-polylysine sedimentation has greater applicability to clay removal.

For accumulation sedimentation, separation between the clay and liquid was not clear because light clay particles remained in the suspension. Thus, accumulation sedimentation is not appropriate for clay removal.

This study can be a guideline for designing the injection concentration of ε-polylysine coagulant. From the results of this study, the concentration of coagulant that is appropriate for the given purpose can be determined.

Chapter 5. The effect of biopolymer on the stabilization of tidal flat soil

5.1 Introduction

Among the sedimentary soils, sediments with high fine soil content such as clay are classified as soft ground. Soft grounds consist of soft soil, such as unconsolidated clay, loose sand, and organic soil. These grounds are formed naturally in wetlands in plains, coastal and mountainous canyons. Soft ground is also formed in artificially formed embankments and landfills (Ahn, Um, Lee and Kim, 1994).

Among soft ground, tidal flats, also known as mud flats are large flat wetlands on the beach or by the river created by the tides. The area of Korea 's tidal flat is 2,489.4 km^2, 2,080 km^2 (83.5%) on the west coast and 409.4 km^2 (16.4%) on the south coast (excluding Jeju Island and East Coast)

Construction on coastal sediments such as tidal flats suffers from various problems caused by unconsolidated sediments formed during sedimentation. Such problems include: 1) destruction of foundation ground subsurface; 2) Uneven settlement; 3) Negative skin friction; 4) Liquefaction; and 5) Lateral flow.

In order to solve the above problems in soft clay soil, geotechnical engineering uses methods such as promotion of consolidation through dehydration, substitution to replace clay tidal flat with sandy soil. Two kinds of consolidation promotion method are widely used: 1) a drain construction method that promotes the consolidation and strength increase effect by shortening the drainage distance by using sand pile or cardboard and 2) preloading method which accelerates settlement by accumulating soil higher than planned height. A chemical consolidation promoting method is also used: 1) Penetration method to absorb moisture of clay by increasing osmotic pressure by injecting solution with high concentration; 2) quicklime piling method to enhance strength through reaction with clay and to accelerate dewatering; 3) Electrodeposition method for dehydrating pore water using electrodes.

The substitution method includes 1) a method of excavating a soft soil and substituting it with a high quality soil, 2) a method of forcibly consolidating a soft layer by its own weight by backfill and 3) a bombardment substitution method in which the soft layer is bombarded to consolidate and replace the soft layer.

In order to effectively carry out the soft soil improvement method, a method for ensuring trafficability of the construction equipment such as a truck, a crane, a putter, a generator, and an air compressor is required on the surface of the tidal flat. As a conventional surface treatment method for

soft ground, bottom mat, surface solidification treatment method and the like were used. In the case of bottom mat method, it is comparably cheap, but it is possible to apply only to sandy soil and it may cause flow breakage and ground failure at the time of backfill formation, excessive use of soil material, and longtime natural dehydration consolidation.

In addition, the surface hardening treatment method is a chemical treatment method in which a special solidifying agent is injected into a viscous soil having a high water content and agitated to improve ground condition. It is a way to enable passage of people or equipment by solidifying the depth of 0.5-2.0m in the surface layer. Because this method is not necessary to consolidate through natural dehydration, it is possible to shorten the construction period. By the chemical interaction between fine soil and solidifying agent, silt and clay are changed to be used as a construction material. However, up to now, it is difficult to use due to high cost of construction.

In this chapter, the possibility of using biopolymer as an environment friendly and economic surface solidification treatment material for tidal flat reinforcement is studied. Through the interaction with biopolymer and clay, it was found that biopolymer could directly increase the strength of the tidal flat soil or promote the tidal flat sediment.

This chapter uses xanthan gum and polylysine biopolymer to enhance surface trafficability of tidal flat. Xanthan interacts with clay molecules. This interaction aggregates clay particles, reduces the amount of water the tidal flat molecule itself hold. These responses can enhance the strength of the tidal flats. Polylysine improves sedimentation of the tidal flats by flocculating suspended clay molecules. The flocculation effect will accelerate the sedimentation of the tidal flat and increases its strength. This chapter aims to examine the above performance of biopolymers through various experiments.

Changes in the liquid limit and plastic limit of the xanthan treated tidal flats were observed and laboratory vane shear tests were performed to examine undrained shear strength variation. In addition, sedimentation experiments of tidal flats treated with polylysine were carried out. The unconfined compressive strength test of the biopolymer treated tidal flat soil was carried out to observe the compressive strength. Finally, scanning electron microscope (SEM) analysis were conducted to visually examine the interaction between biopolymer and tidal flat soil. Through a series of experimental analyzes, the possibility of biopolymer as a solidification material for surface layer stabilization of tidal flat was confirmed.

5.2 Materials and Procedure

5.2.1 Materials

5.2.1.1 Soils: Tidal flat

Korean tidal flat soil is widely distributed soil material spread in the west coast and the south coast of Korean peninsula. Tidal flats have different composition depending on the area. Clay or silty tidal flats are tidal flats with a low percentage of sand (usually within 20-30%) and many fine components (70-80%). Sandy tidal flats are tidal flats with more than 70% sand. Intermediate tidal flat is a tidal flat where sand and fine soil are mixed together.

The tidal flat soil used in this study is obtained from Yeo-su, Korea, which has one of the representative tidal flat area in Korea. The natural Korean tidal flat soils was dried in the oven at 60^{o}C to prevent the organic materials in soil to be burn. The particle size distribution of Korean tidal flat soils were summarized in figure 5.1. Additionally, basic geotechnical properties of Korean tidal flat soils are summarized in table 5.1. It has mean particle size, D 50, of 0.018 mm. Thus, it can be classified as silt that has grain size between 0.002 mm and 0.075 mm based on the AASHTO classification (Das, 2013). Tidal flat used have the coefficient of uniformity, Cu, of 11.75 and the coefficient of curvature of 1.31. It has a liquid limit of 56.02 % and the plastic limit of 31.43 %. Thus, Tidal flat soil in Yeosu area can be classified as organic clay or silt with high plasticity (OH) based on the unified soils classification system (Astm, 2011).

Table 5.1 Geotechnical properties of Yeosu tidal flat soil

D50 [mm]	Cu	Cc	Atterberg limits [%]			USCS
			LL	PL	PI	
0.018	11.75	1.31	56	31	25	MH

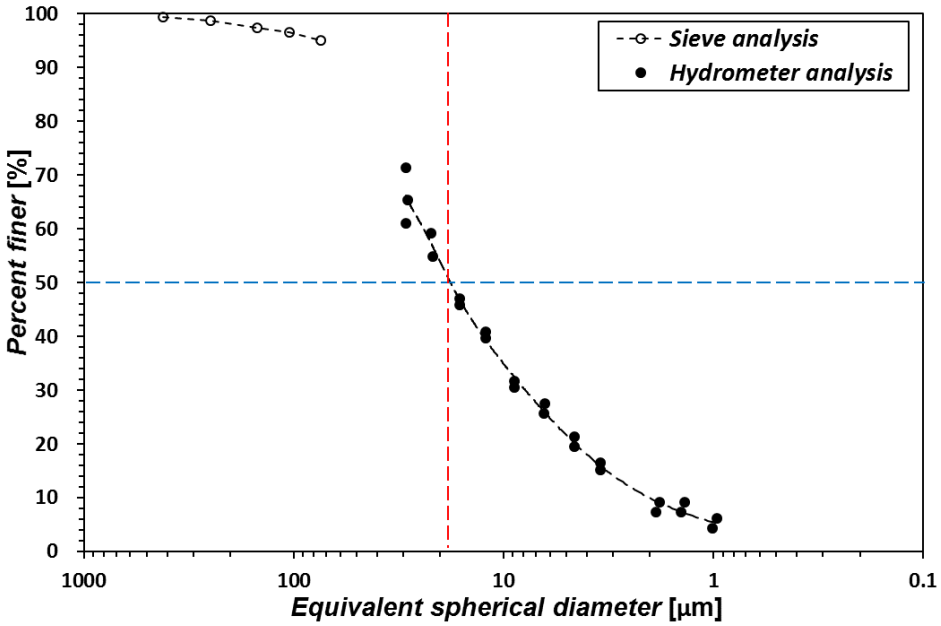

Figure 5.1 Particle size distribution of Yeosu tidal flat soils

5.2.1.2 Biopolymers: Xanthan gum and ε-Polylysine

Xanthan gum

Xanthan gum biopolymer was chosen as the organic material for this study in order to estimate the interaction of xanthan gum with tidal flat. Xanthan gum is an anionic bipolymer that is produced by the *Xanthomonas compestris* bacterium. Due to its high viscosity when dissolved in water, xanthan gum solution is widely used as a thickener in food, farming, and oil industries (Garcıa-Ochoa, Santos, Casas and Gomez, 2000). Recent researchs have attempted to apply xanthan gum in geotechnical area as a soil strengthening agents (Chang, Im, Prasidhi and Cho, 2015). Studies have shown that xanthan gum interacts with clay particles forming a structured matrix between the clay particles, and these increased interactions have been shown to be capable of increasing the strength of the clay material and undrained shear strength (Chang, Im, Prasidhi and Cho, 2015). Other researches have focused on the decrease of soil permeability by forming impervious barriers (Martin, Yen and Karimi, 1996). The research observed that the permeability was decreased by a factor of 100 or greater. This research used commercially produced xanthan gum from Sigma-Aldrich Co. LLC., CAS No. 11138-66-2. It has a faint yellow to yellow to beige color appearance and powder form. The viscosity of 1% pure xanthan solution has a brookfield viscosity of 800 – 1200 cps.

ε-Polylysine

ε-Polylysine is a type of polylysine, a lysine homopolymer that contains bonds between the carboxyl and ε-amino groups. It is produced by the fermentation of bacteria, Streptomyces albulus. At pH 7, ε-polylysine has positive charges due to positively charged hydrophilic amino groups at the L-lysine. The typical molecular formula for ε-polylysine is $C_{180}H_{362}N_{60}O_{31}$.

ε-Polylysine has both hydrophobic and hydrophilic characteristics. Methylene groups on the molecule are hydrophobic and carboxyl and amino groups are hydrophilic. This structure can prevent microbial activity and the decomposition of food. ε-Polylysine acts as a cationic surface-active compound and can constrain the proliferation of microorganisms such as yeast, fungi, and bacteria species. Therefore, it can be used as a food preservative (Hiraki, Ichikawa, Ninomiya, Seki, Uohama, Seki, Kimura, Yanagimoto and Barnett, 2003). Additionally, the cationic charges of ε-polylysine can interact with the negatively charged surfaces on a cell, a drug or fine clay. Because of this electrical interaction, polylysine can be used as a coating agent for tissues or drugs in biotechnology (Hiraki, Ichikawa, Ninomiya, Seki, Uohama, Seki, Kimura, Yanagimoto and Barnett, 2003, Mazia, Schatten and Sale, 1975, Park, Jeong and Kim, 2006).

In this study, ε-polylysine was used to accelerate the coagulation and flocculation of clay particles, due to the electrical interaction between the negatively charged facial surfaces of clay particles and the positively charged ε-polylysine. This interaction induces the clay suspension to form flocs, which sediment to the bottom. This phenomenon can be used to remove waste materials in groundwater.

Commercial ε-polylysine (BNF CO., LTD, CAS No. 28211-04-3) was chosen as the surfactant to coagulate clay particles in this study. Its molecular weight is 3,500 – 4,500 Da, and it is effective over a wide range of pH values, from about 4 - 10.

5.2.2 Experimental Program

5.2.2.1 Soil-BP Mixture preparation

In this chapter, xanthan gum and ε-polylysine were used as representative biopolymers to treat in tidal flats. Most of the experiments were performed with a water content ratio of 100%, which is the most similar to the field environment. However, in the case of dried unconfined compressive strength (UCS) experiment, drying was started at a water content of 60%, which is higher than the liquid limit, and the sample was prepared at a water content of 0%.

Biopolymer treated tidal flat samples was formed by the following procedure. First, the tidal flats were dried at 30 °C for more than 48 hours to vaporize all the fluids contained in the tidal flats. The temperature of 30 °C is to prevent burning of organic matter contained in the tidal flats. The dried tidal flats were crushed to form soil powder. This procedure was performed to make a sample of uniform water content. Then, biopolymer and water are mixed to make an aqueous solution that activates the biopolymer molecule. Aqueous solution and dry tidal flats were mixed to form a biopolymer treated tidal flats with in situ water content.

5.2.2.2 Soil consistency

Liquid limit and plastic limit of clay are important factors to grasp various characteristics such as soil condition and strength, and measurement is required in most works related to clay soil. In this chapter, the process of obtaining the consistency was carried out to analyze the change of the soil condition and the shear strength characteristics using the xanthan.

Plastic limit of soils were determined using thread rolling test. Plastic limit-Rolling device produced based on the ASTM D 4318-05 was used to increase the reliability of results (ASTM). A device made of acryl was depicted in figure 2.1. Unglazed papers attached to the top and bottom plate absorb the fluid in soil and does not add foreign substance. Top plates were moved back and forth to decrease the water content of soil until the thread were broken at the thread thickness of 3.2mm and the water content at this state was determined as plastic limit. Same procedure was repeated twice to reduce the error.

The liquid limits were determined by the fall cone tests instead of the ‘casagrande cup’ method, due to its high reliability (Koumoto and Houlsby, 2001, Casagrande, 1958). The fall cone equipment used for this study conforms to the British Standard BS 1377 (BS1377, 1990). A cone with a weight of 80g and an angle of 30° was allowed to penetrate soil specimens for 5 seconds at various water contents. The penetration depth was measured using a dial gauge with a precision within 0.01mm. Liquid limits for each sample were determined as the water content when the cone penetrated 20mm into the soil sample. For one soil sample, an average of 12 different measurements, 4 different water content and 3 repeated penetration at same water content, were taken to obtain credible penetration depth-water content line.

5.2.2.3 Undrained shear strength

The undrained shear strength of each soil specimens at the field water content of 100% were measured using the laboratory vane shear equipment (D4648, 2000).

Vane shear experiments were performed to measure undrained shear strength of cohesive fine soils. There are two methods of vane shear experiment, field vane test and laboratory vane test. The field vane test is affected by the weight of upper load. Therefore, there is a difficulty in obtaining uniform data because the strength changes depending on the depth. To overcome the weakness of field vane shear test, laboratory vane shear test was developed (D4648, 2000). The laboratory vane shear test has advantages of being able to perform the re-shaping of the sample and applicable to soft and sensitive clay with a shear strength of less than 20 kPa .

This study was carried out in accordance with ASTM D-4648 standard. A blade with a length of 12.7 mm and a width of 12.7 mm was used (Fig. 5.2), and the sample tube was φ 38 mm. The undrained shear strength was measured by rotating the blade at a rate of 1 degree per second using a spring suitable for clay (k = 1.862 Nmm / degrees) and measuring when the pointer stopped.

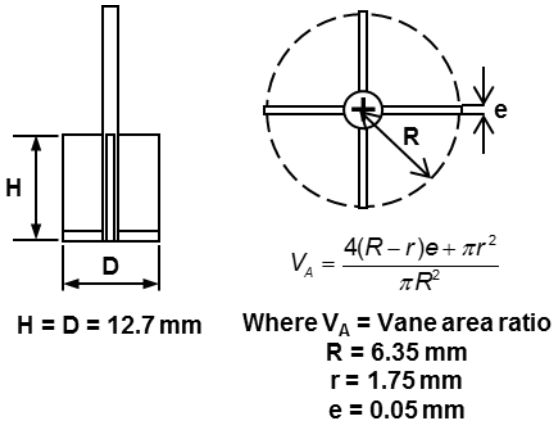

Figure 5.2 Miniature vane blade geometry

However, at low biopolymer concentration, the undrained shear strength was obtained using the liquidity index of each soil because its undrained shear strength is too low to measure with vane shear equipment. The soil at the liquid limit state has the undrained shear strength of 1.7-2.0 kPa. The undrained shear strength is affected by the water content. Thus, at the same water content, the soil with higher liquid limit has higher undrained shear strength than the soil with lower liquid limit (Watts,

Tolhurst, Black and Whitmore, 2003). It indicates that the liquidity index of soil is important factor for shear resistance of soil. The biopolymer treatment in soil enhances the liquid limit of soil by the viscosity increase of pore fluid and the bonding characteristics of biopolymer with soil particles.

Wroth and Wood, 1978 proposed the relationship between undrained shear strength and liquidity index (Wroth and Wood, 1978). Assuming that the undrained shear strength ratio of the soil at the plastic limit and the liquid limit is 1: 100 and the undrained shear strength at the liquid limit is 1.7 kPa, equation 5.1 is derived. Undrained shear strength values of the low biopolymer concentration (0-2% to soil weight) treated tidal flat were obtained using the equation 5.1.

$$c_u = 1.7 \times 100^{(1-I_L)} \tag{5.1}$$

Where C_u is undrained shear strength, I_L is liquidity index.

5.2.2.4 Sedimentation

To estimate the coagulation efficiency of ε-polylysine, sedimentation tests of tidal flat suspensions were conducted. During the experiments, the temperature and relative humidity were controlled as 22 ± 2°C and 25%, respectively, while the pH of the deionized water was near 6.5. For each experimental trial, 4 g of kaolinite clay and 100 g of deionized water were injected into a 100 ml graduated cylinder. The water content was determined as the point where the suspension could be mixed well by an electric stirrer machine (Kolaian and Low, 2013). The effect of gravity on sedimentation is greater than that of the coulombic attraction when the water content of kaolinite slurry is below 500% (Imai, 1980). Thus, the initial water content of 2500% is sufficient to render interaction between tidal flat and biopolymer additives. The inside diameter of the graduated cylinder was 26.5 mm, and was larger than the “yield diameter”, which is the diameter at which settling cannot occur due to the wall effect, which was about 13 mm for this experiment (Michaels and Bolger, 1962). As a result, the graduated cylinder is large enough to observe any accelerated sedimentation effect caused by the biopolymers. The volume, pH, and turbidity of the suspension were assumed the same since the same initial water content of 2,500% was set for each cylinder. Clay suspensions were then prepared by mixing kaolinite and deionized water in the graduated cylinder.

The cylinders were turned upside down about 20 times to uniformly spread clay particles throughout the suspension. Afterwards, ε-polylysine were poured into each suspension with various biopolymer weight to water weight ratios, of 0%, 0.1%, 0.25%, 0.5%, 1%, and 2%, and then thoroughly

mixed. After the mixing of the biopolymer and clay suspensions was completed, the volume of clay sediments was measured until the sediment volume change became constant. Then, the measured volumes were divided by the initial volume to generalize the variation in sedimentation volume, determined as the sediment ratio (instant height ratio to the initial height, %).

$$R_{Sed} = \frac{V_i}{V_i} \times 100\ [\%] \tag{5.2}$$

Where R_{sed} is the sediment ratio, V_t is the sediment volume at time t and V_i is the initial sediment volume.

5.2.2.5 Unconfined Compressive Strength

Cube (50 mm × 50 mm × 50 mm) shaped tidal flat samples were prepared with untreated, 1% xanthan treated and 1% polylysine treated tidal flat. Unconfined uniaxial compressive testing was performed using a master loader (Humboldt Mgf. Co., HM-5030.3F) device. The axial strain rate was controlled at 0.5 mm/min (i.e., 1 % strain / min). The maximum strength and the stress-strain behaviors were obtained by averaging three different measurements for a single condition. The experimental setup can be seen in Fig. 5.3.

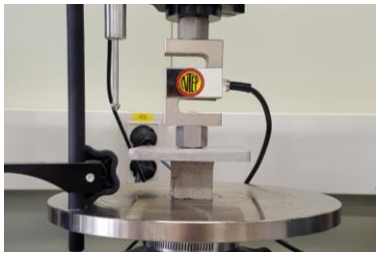

Figure 5.3 Unconfined uniaxial compression test setup

5.2.2.6 Microscopic observation (Scanning Electron Microscopy: SEM)

Microscopic observations using the scanning electron microscope (SEM; S4800) was performed to visually analyze the behavior of biopolymer (i.e. xanthan gum, polylysine) in tidal flats. Untreated tidal flats, xanthan gum 1% treated mud flat samples at liquid limit condition, and polylysine 1% treated tidal flat samples after sedimentation were naturally dried. SEM images were obtained by attaching the soil with insulating tape on the sample plate and then osmium coating for 15 seconds to obtain sufficient conductivity.

5.3. Results and Analysis

5.3.1 The variation of soil consistency by xanthan gum concentration

The results of the fall cone test, thread rolling experiment and classification result of tidal flat soils in xanthan treated tidal flats are summarized in Table 5.2 and Figure 5.4.

As shown in Figure 5.3 (a), the slope of the penetration depth graph with increasing water content tends to increase as the content of xanthan gum increases. It indicates that the penetration depth decreases with increasing xanthan gum content in the same water content. It can be seen that the role of xanthan gum is absorbing water or increasing double layer thickness. This trend was also found in the liquid limit variation in Figure 5.3 (b). The liquid limit is steadily increased according to the content of xanthan gum. In case of untreated tidal flat, the cationic charge of brine contained in the tidal flat electrically interacts with the anionic charge of the clay on the tidal flat surface and decreases double layer thickness. When xanthan gum biopolymer is treated in tidal flat, xanthan gum with the negative charge interacts with the brine and increases water absorption capacity of tidal flat. In addition, xanthan gum absorbs water directly by itself. These two phenomena increase liquid limit of xanthan treated tidal flat.

In fig 5.4 (b), plastic limit variation shows that the plastic limit is smaller than untreated when low concentration of xanthan is treated (compared to pure tidal flat and 0.1% treated tidal flat) and then increases again with increasing xanthan content is. Because the thread rolling test proceeds while lowering the water content, activated xanthan gum aggregate soil particles and hold the form of thread until low water content. If the content of xanthan is increased, the plastic limit is increased by the effect of double layer expansion due to the increase of total net charge and water content absorbed by xanthan. However, xanthan's effect on plastic limit is less than that on the liquid limit. Plasticity index is steadily increased due to liquid limit and plastic limit behavior.

Based on the obtained soil properties, classification of the xanthan treated tidal flat based on the unified soils classification system (USCS) was performed. According to the results, it was confirmed that tidal flats are classified as silt with high plasticity (MH) or clay with high plasticity (CH) according to xanthan contents.

Table 5.2 Mechanical properties of xanthan gum treated tidal flat

Xanthan content [% to soil weight]	Liquid limit [%]	Plastic limit [%]	Plasticity index [%]	Classification [based on USCS]
0.0 %	56.0	31.4	24.6	MH
0.1 %	56.5	29.0	27.5	CH
0.5 %	62.7	29.3	33.4	CH
1.0 %	70.0	32.4	37.6	CH
2.0 %	75.3	37.5	37.8	MH

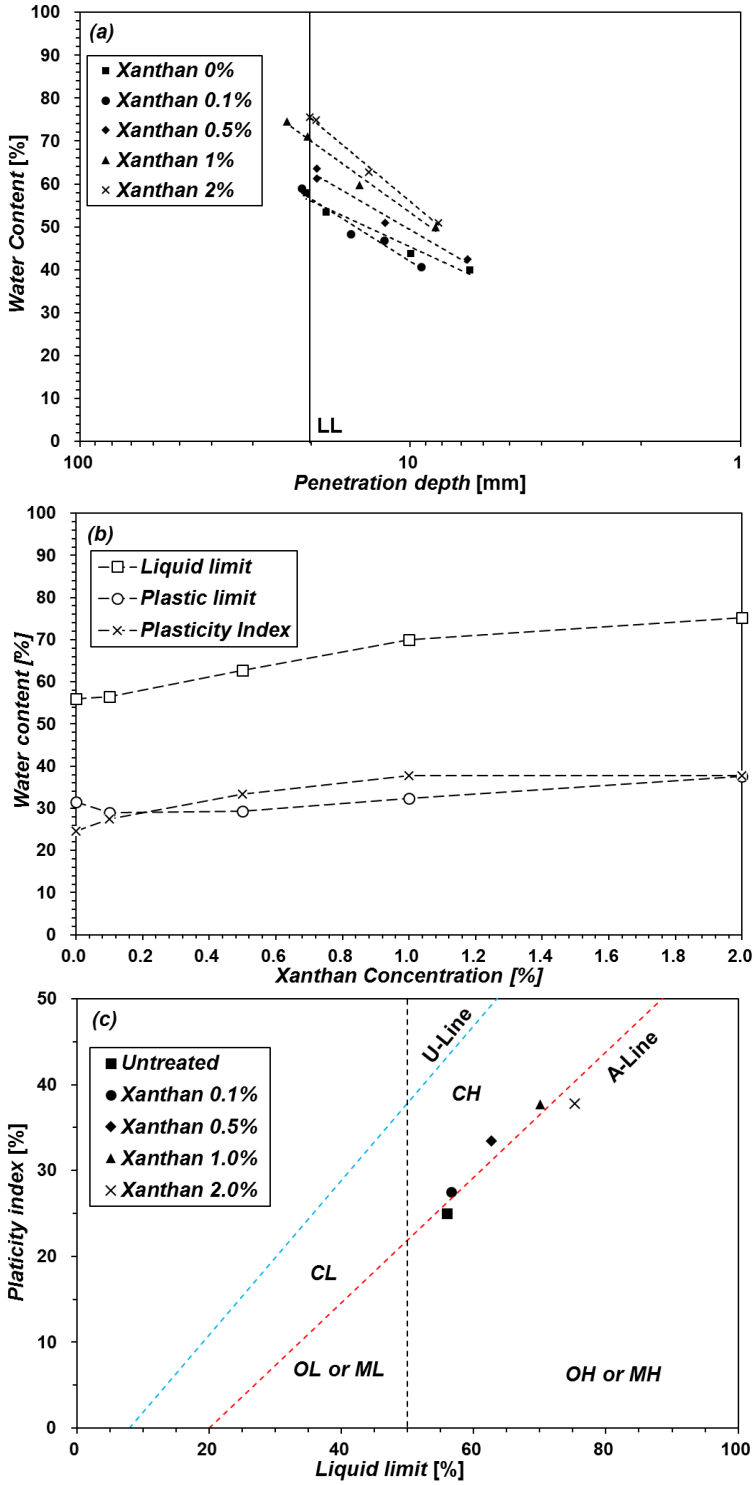

Figure 5.4 The effect of biopolymer on the consistency of tidal flat: (a) Variation of penetration depth according to water content with xanthan content; (b) the variation of liquid limit, plastic limit and plasticity index by xanthan content and (c) the classification of xanthan treated tidal flat based on the unified soil classification system

5.3.2 Undrained shear strength

The change in undrained shear strength with the content of xanthan gum is summarized in Figure 5.5 (a). The undrained shear strength results under 2% xanthan gum content was derived from the relationship between liquidity index and undrained shear strength, and the undrained shear strength above 2% xanthan gum content was obtained using a laboratory vane shear test.

The untreated tidal flat, which is 100% water content, is almost liquid state. This is because the void ratio is 2 or more assuming a fully saturated state. Therefore, in this case, the undrained shear strength is close to zero and does not meet the shear strength required to ensure the trafficability of the construction equipment. On the other hand, as the Xanthan content increases, the injected xanthan bonds with the tidal flat to aggregate the particles, and xanthan absorbs the voids to increase the viscosity of the voids. Due to this effect, the state of the tidal flat changes into a gel shape like a glue. This leads to an increase of undrained shear strength and an increase of 2 kPa.

The undrained shear strength was converted to the maximum loadable equipment weight by a series of calculation. As shown in Figure 5.6, it was assumed that xanthan is treated on the tidal flats at a thickness of 50 cm. On this xanthan treated tidal flat, the weight of the equipment (assuming that the construction equipment is grounded 1 m length and 1 m width) that can be loaded is obtained from equations 5.1, 5.2 and 5.3. As a result, it was confirmed that about 2 tons of equipment can be loaded at 10% xanthan treated tidal flat. This occurs because the shear strength is increased due to the xanthan gum effect of viscosity increase and the clay bonding. Thus, this study confirmed the effect of xanthan treatment for trafficability.

$$q_u[kPa] = 5.14 \times c_u \tag{5.1}$$

$$q_d[kPa] = \frac{9.8 \times W[kN]}{(A + 2 \times H \times \tan\theta) \times (B + 2 \times H \times \tan\theta)[m^2]} \tag{5.2}$$

$$FS = \frac{q_u}{q_d} \tag{5.3}$$

Where q_u is ultimate bearing capacity, c_u is undrained shear strength, W is equipment weight and FS is the factor of safety.

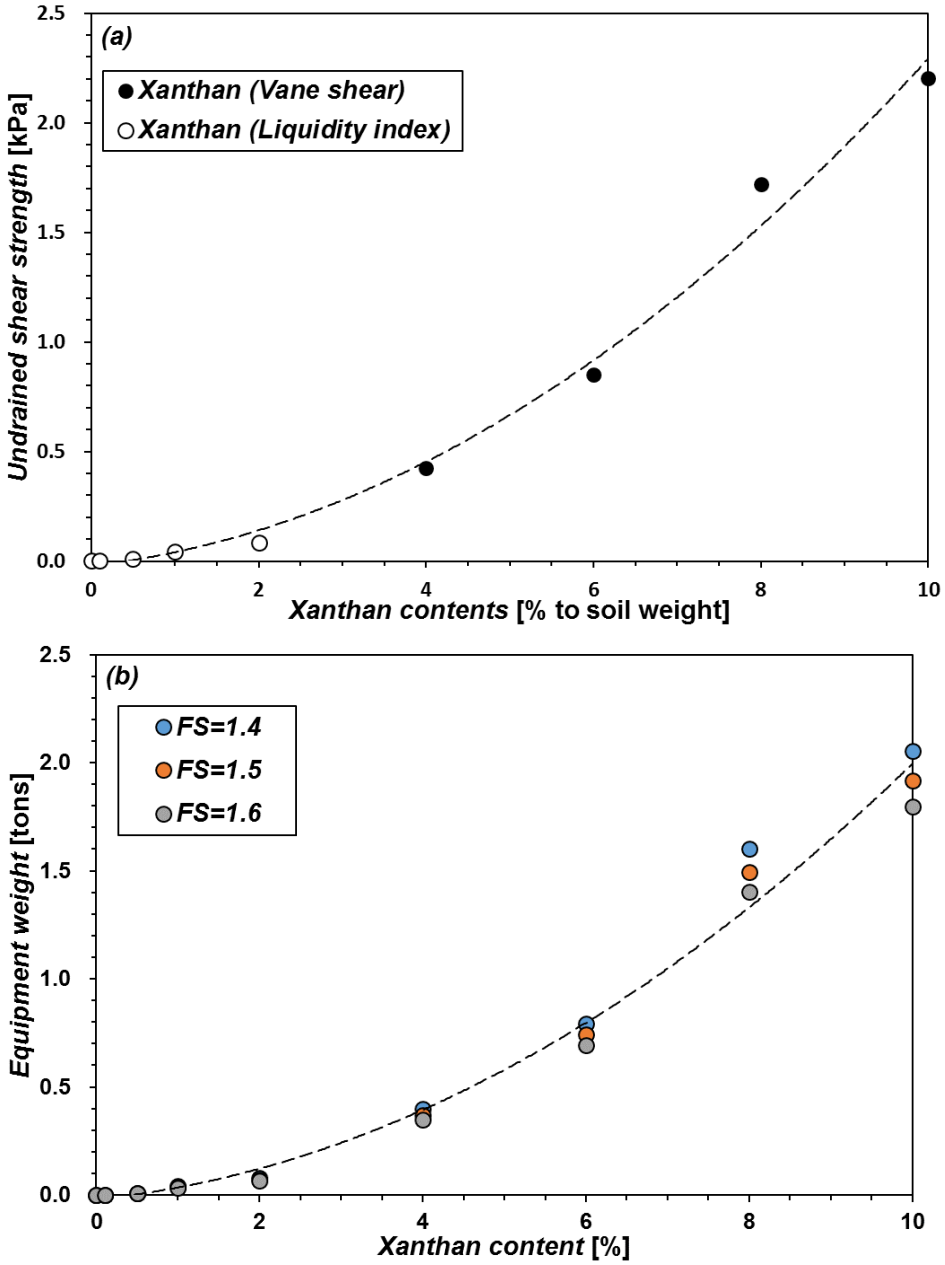

Figure 5.5 The effect of xanthan gum on the undrained shear strength of tidal flats; (a) Undrained shear strength, (b) Maximum loadable equipment weight

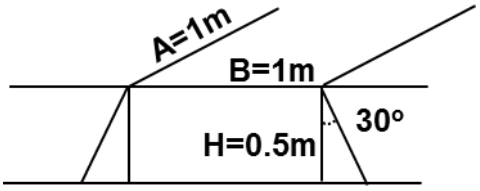

Figure 5.6 Geometry of xanthan gum treated tidal flats

5.3.3 Sedimentation effect of polylysine

The variation in sedimentation volume when ε-polylysine was used as a coagulant is shown in fig 5.7. Due to its higher particle size than clay particles, the sedimentation follows flocculation sedimentation behavior for all polylysine content.

As sedimentation progresses, all soil particle settles together as time passes, thus the pore between the soil decreases and the dry density steadily increases. The final sediment properties at the end of the sediment show a tendency that the final sediment ratio, void ratio decreases and dry density increase continuously until the content of polylysine is 0.25%. Above 0.25% concentration, the final sediment ratio and void ratio are increased and the dry density is decreased up to 1% concentration. However, the efficiency is higher than untreated tidal flat even in this case. Since then, the minimum final sediment ratio and void ratio have been observed at 2%, and the maximum dry density occurs at same concentration.

However, no significant change in final sediment properties is seen above 0.25%. On the other hand, it can be seen that there is a marked difference in sediment velocity according to the polylysine content . In 2% treated tidal flat, sedimentation was completed in 24 minutes, but in untreated tidal flat in 1437 minutes. Thus, the effect of polylysine was mainly found in the increase of sediment velocity. This is attributed to the particle flocculation effect of polylysine, which results in the increase of particle weight. On the other hand, in the case of polylysine treatment of 0.25% or more, a bridge is formed between the particles and maintain a distance of more than a certain distance, so that the final sediment ratio and void ratio are increased and the dry density is decreased. However, since this experiment was conducted on a small scale, further application of an in-depth study reflecting the scale effect is required for practical application.

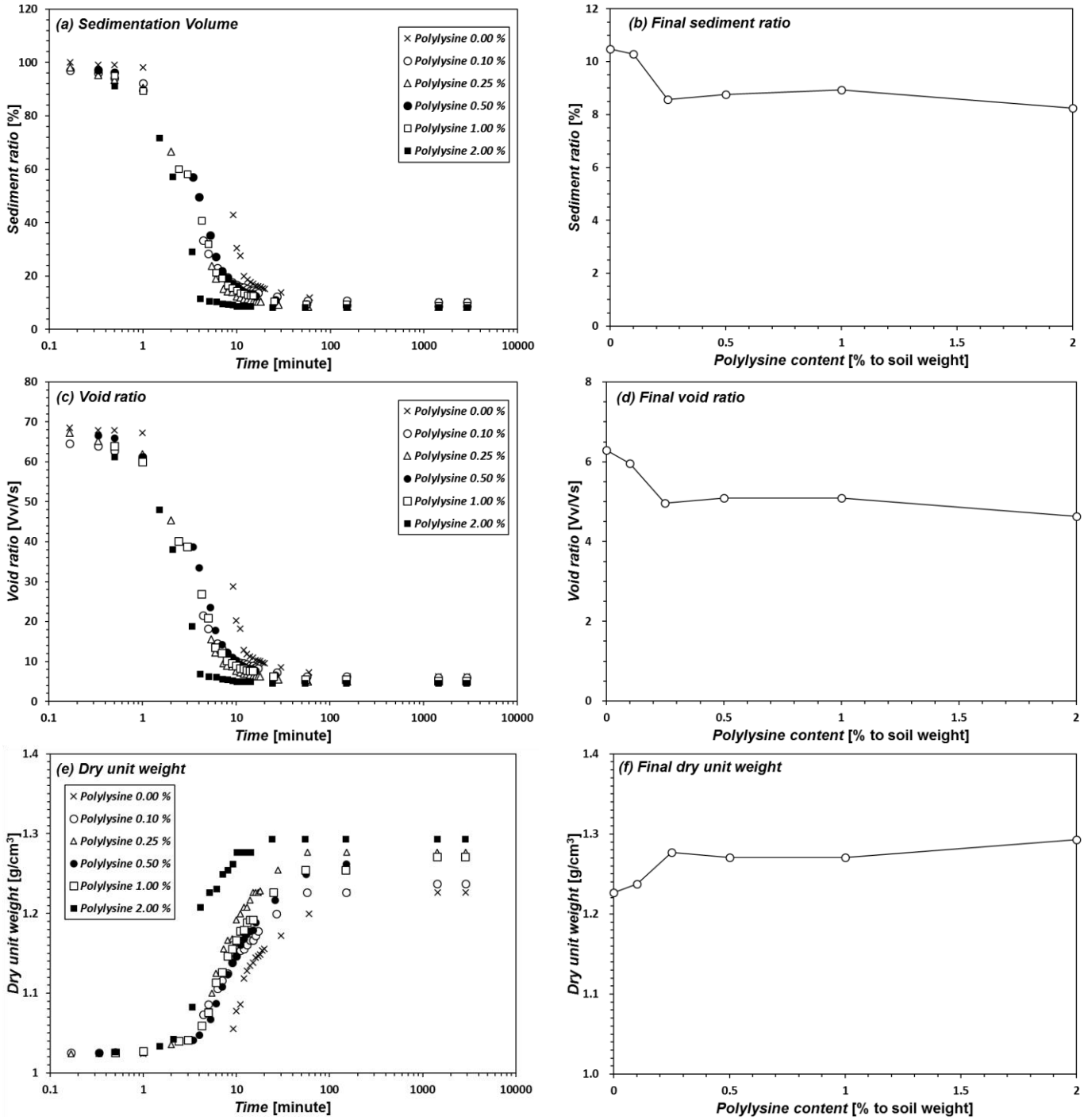

Figure 5.7 Variation in sedimentation properties of chitosan treated suspensions: (a),(c) and (e) indicate the sedimentation property, sediment ratio, void ratio and dry unit weight respectively, variation by time, (b), (d) and (f) indicate the final sedimentation property, sediment ratio, void ratio and dry unit weight respectively, variation by polylysine contents

5.3.4 Unconfined uniaxial compression strength

The effects of xanthan and polylysine on uniaxial compression strength for tidal flat can be observed in fig 5.8. As can be seen, the strength of the samples tend to increase as curing time increases. This is because the sample is continuously dried rather than the effect of the curing time. In addition, the strength of xanthan treated tidal flat samples increased by 1.63 times (48 hours) and 2.4 times (7 days) compared to that of untreated tidal flat. It was confirmed that the strength enhancement effect of xanthan through electrical interaction and fluid viscosity enhancement was confirmed. In addition, as the curing time increases, the effect of increasing the strength of xanthan treated tidal flat is enhanced. This reflects that the water absorbed by xanthan takes longer to dry. On the other hand, in the case of tidal flat sample treated with polylysine, the strength decreased by 0.37 times and 0.78 times compared to untreated. This seems to be because polylysine aggregates tidal flats and reduces the binding between the conglomerates. Therefore, it can be confirmed that xanthan treatment is better in improving the compressive strength than polylysine.

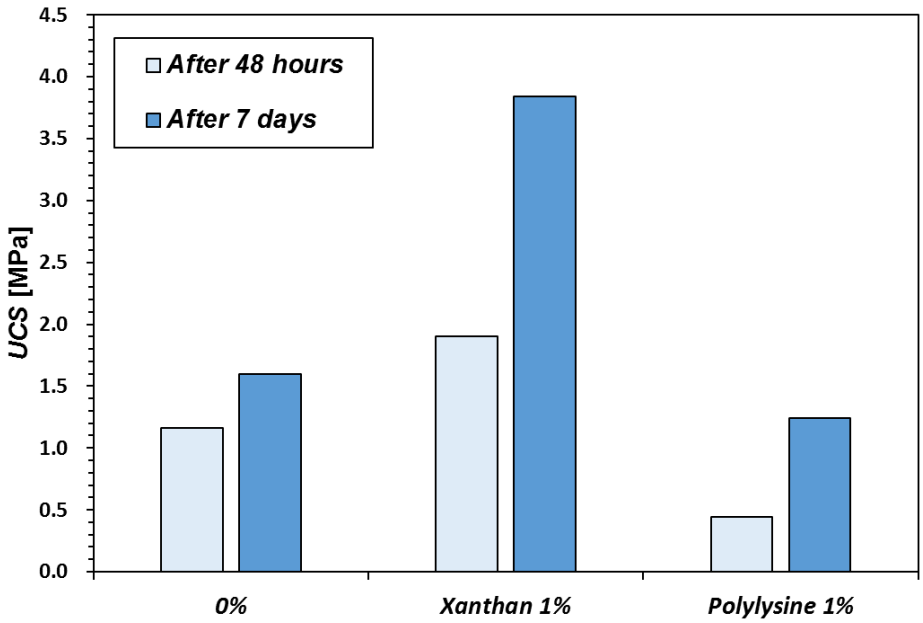

Figure 5.8 Unconfined uniaxial compression strength variation by curing time and biopolymer types

5.3.5 SEM images

SEM images (5000 magnification, 10000 magnification, 25000 magnification) of untreated tidal flat, 1% xanthan treated tidal flat and 1% polylysine treated tidal flat are shown in figure 5.9.

In the case of the untreated tidal flat, the ions contained in the brine are interact with the charge of the clay in the tidal flat particles and cover the surface of the clay (Fig. 5.9 (a), (b) and (c)). In this case, the electrical charge and double layer thickness of the clay decrease, and the liquidity index decreases as a whole. When the xanthan gum is treated on the tidal flat, the xanthan gum absorbs the fluid and expands. This effect increases soil viscosity. Fig. 5.9 (d), (e) and (f) show smoothed particle shape because xanthan interacted with cations of soil particles and brine by activation after absorbing water. Finally, when polylysine is applied, it is confirmed that there is almost no salt molecule on the surface. This is because the surface charge of polylysine is higher than that of brine, so it dissolves and reacts directly with the soil. In addition, the clay flocculation effect of polylysine indicates that particles are aggregated and thus have a coarse structure compared to other images.

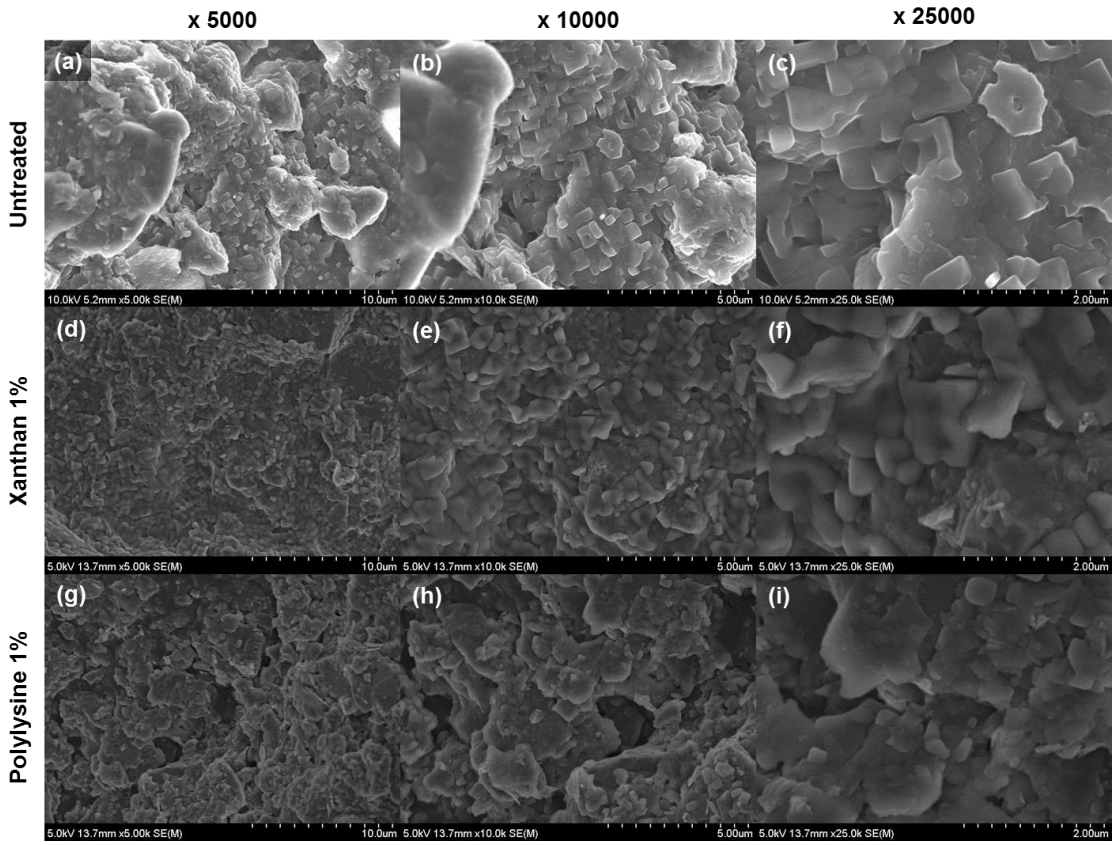

Figure 5.9 SEM images of untreated (a, b & c), 1% xanthan gum-treated (d, e & f) and 1% polylysine-treated (g,h & i) tidal flats with 5,000 times magnification (a, d & g), 10,000 times magnification (b, e & h), and 25,000 times magnification (c, f & i), respectively

5.4 Conclusions

In this chapter, we analyzed the applicability of biopolymer to the stabilization of tidal flat, which is a representative site soft ground. Xanthan treatment has the effect of increasing the liquid limit of the tidal flat, improving the undrained shear strength and compressive strength. Therefore, it is suitable for rapid cementing for securing the trafficability to enter the construction equipment. On the other hand, polylysine was not excellent in strength enhancement, but it was confirmed that sedimentary acceleration effect of tidal flat was excellent. This result shows that the polylysine is a biopolymer suitable for the reclamation or dredging of tidal flat soil. As a result of this experiment, it can be seen that biopolymer is an eco-friendly reinforcing material for tidal flat improvement.

Chapter 6. Conclusion and Further study

6.1 Conclusion

In this study, the behavior between biopolymer and fine soil was investigated, and the possibility of geotechnical application of biopolymer was analyzed based on this behavior. The results of the analysis are summarized in table 6.1. The biopolymer forms a direct electrical bond with the fine soil, especially in the clay, which changes the structure and characteristics of the fine soil. Therefore, the new classification system that can clearly distinguish the biopolymer treated fine soil by reflecting the electrical characteristics of the clay can be the foundation stone for further in-depth study of biopolymer treated fine soil. In addition, the increase of fluid viscosity of biopolymer and the clay particle bonding effect result in the enhancement of strength. Thus, it is applicable to stabilize soft ground. The sedimentation effect of biopolymer is applicable to reclamation, soft ground strengthening by consolidation substitution, and clay removal in groundwater.

6.2 Further study

Further research items proposed in this study are as follows. First, it is necessary to compare the liquidity behavior changes of silt and coarse soil used in the experiment. Silt is a kind of fine soil, but unlike clay, it has no charge on the surface. Thus, liquidity behavior is expected to be similar to coarse sand rather than clay. To demonstrate this experimentally, the liquidity behavior between silt and coarse soil must be compared.

Second, the amount of clay particles remaining in the supernatant was indirectly analyzed by the absorbance value. The correlation between clay quantity and absorbance value are required. Additionally, sedimentation tests have been conducted in small scale, but practical applications are performed on a large scale, so further studies on scale effects must be performed.

Finally, it is necessary to confirm the relationship between undrained shear strength and liquidity index, and confirm whether biopolymer application changes the linear relationship between undrained shear strength and liquidity index.

Table 6.1 Overall summary of the Key Findings in this study.

	Key Finding
Behavior of biopolymer treated fine soil by fluid chemistry	• Silt and Sand have no electrical bond with biopolymer, so liquidity behavior is dominated by clay • In deionized water, both water absorption and clay molecular bonding of biopolymer act simultaneously and liquid limit increase or decrease according to dominant factors. • In brine, biopolymer plays a role in increasing the liquid limit of a fine soil reduced by Na +. • In kerosene, no effect was found because biopolymer is not activated.
Classification based on pore fluid chemistry	• Classification changes in broad category according to Xanthan content and fine type. • This classification method was proved as proper classification because it reflects electrical interaction between xanthan and fine soil.
Sedimentation tests	• The sediment structure changes from edge to edge structure to face-to-face structure according to ε-polylysine concentration. • Accumulation-type sedimentation was found at around 0.2% due to the change in sediment structure. • In the case of accumulation sedimentation, it is not applicable to remove clay particles because a large amount of suspended solids is not suitable. • The final sedimentation density of the ε-polylysine treated suspension is higher than the sedimentation density of the chitosan-treated suspension. • ε-Polylysine treated suspension has less supernatant than chitosan treated clay suspension. • ε-Polylysine proved its performance as clay coagulants to remove clay particles in ground water.
The application of biopolymer on the tidal flat	• The liquid limit tends to steadily increase as xanthan concentration increases due to the interaction among tidal flat, brine and xanthan. • Undrained shear strength increased up to 2 kPa by xanthan treatment. • UCS of xanthan gum treated tidal flat increased 2.4 times compared to untreated samples. • This is because xanthan increases fluid viscosity and combines with the clay contained in the tidal flat. • It was found that polylysine treatment had sedimentation acceleration effect. This confirms that it is possible to apply for reclamation of dredging.

Bibliography

[1] Potts, D. T. (1997). *Mesopotamian civilization: The material foundations*, A&C Black.

[2] Yang, F., Zhang, B., and Ma, Q. (2010). "Study of sticky rice– lime mortar technology for the restoration of historical masonry construction." *Accounts of chemical research*, 43(6), 936-944.

[3] Ayeldeen, M. K., Negm, A. M., and El Sawwaf, M. A. (2016). "Evaluating the physical characteristics of biopolymer/soil mixtures." *Arabian Journal of Geosciences*, 9(5), 1-13.

[4] Chang, I., Prasidhi, A. K., Im, J., and Cho, G.-C. (2015). "Soil strengthening using thermo-gelation biopolymers." *Construction and Building Materials*, 77, 430-438.

[5] Blezard, R. G. (1998). "The history of calcareous cements." *Lea's chemistry of cement and concrete*, 4, 1-23.

[6] Turekian, K. K., and Wedepohl, K. H. (1961). "Distribution of the elements in some major units of the earth's crust." *Geological Society of America Bulletin*, 72(2), 175-192.

[7] Poon, C.-S., Azhar, S., Anson, M., and Wong, Y.-L. (2001). "Comparison of the strength and durability performance of normal-and high-strength pozzolanic concretes at elevated temperatures." *Cement and concrete research*, 31(9), 1291-1300.

[8] Chen, C., Habert, G., Bouzidi, Y., and Jullien, A. (2010). "Environmental impact of cement production: detail of the different processes and cement plant variability evaluation." *Journal of Cleaner Production*, 18(5), 478-485.

[9] Larson, A. (2011). *Sustainability, innovation, and entrepreneurship*.

[10] Initiative, C. S. (2009). "Cement Industry Energy and CO2 Performance,"Getting the Numbers Right"." *World Business Council for Sustainable Development*.

[11] Humphreys, K., and Mahasenan, M. (2002). *Toward a Sustainable Cement Industry: Climate Change. Substudy 8*, World Business Council for Sustainable Development.

[12] Hills, L., and Johansen, V. (2007). "Hexavalent chromium in cement manufacturing: literature review."

[13] Richman, D. L., Tucker, C. L., and Koehler, P. G. (2006). "Influence of Portland cement amendment on soil pH and residual soil termiticide performance." *Pest management science*, 62(12), 1216-1223.

[14] Doerr, W. (1952). "Pneumoconiosis caused by cement dust." *Virchows Archiv: an international journal of pathology*, 322(4), 397-427.

[15] Humans, I. W. G. o. t. E. o. C. R. t., Cancer, I. A. f. R. o., and Organization, W. H. (1997). *Silica, some silicates, coal dust and para-aramid fibrils*, World Health Organization.

[16] Khatami, H. R., and O'Kelly, B. C. (2012). "Improving mechanical properties of sand using biopolymers." *Journal of Geotechnical and Geoenvironmental Engineering*, 139(8), 1402-1406.

[17] Latifi, N., Horpibulsuk, S., Meehan, C. L., Abd Majid, M. Z., Tahir, M. M., and Mohamad, E. T. (2016). "Improvement of Problematic Soils with Biopolymer—An Environmentally Friendly Soil Stabilizer." *Journal of Materials in Civil Engineering*, 04016204.

[18] Chang, I., and Cho, G.-C. (2012). "Strengthening of Korean residual soil with β-1, 3/1, 6-glucan biopolymer." *Construction and Building Materials*, 30, 30-35.

[19] Vanapalli, S., Fredlund, D., Pufahl, D., and Clifton, A. (1996). "Model for the prediction of shear

strength with respect to soil suction." *Canadian Geotechnical Journal*, 33(3), 379-392.
[20] Watts, C., Tolhurst, T., Black, K., and Whitmore, A. (2003). "In situ measurements of erosion shear stress and geotechnical shear strength of the intertidal sediments of the experimental managed realignment scheme at Tollesbury, Essex, UK." *Estuarine, Coastal and Shelf Science*, 58(3), 611-620.
[21] Nugent, R., Zhang, G., and Gambrell, R. (2009). "Effect of exopolymers on the liquid limit of clays and its engineering implications." *Transportation Research Record: Journal of the Transportation Research Board*(2101), 34-43.
[22] Chen, R., Zhang, L., and Budhu, M. (2013). "Biopolymer stabilization of mine tailings." *Journal of Geotechnical and Geoenvironmental Engineering*, 139(10), 1802-1807.
[23] Chang, I., and Cho, G.-C. (2014). "Geotechnical behavior of a beta-1, 3/1, 6-glucan biopolymer-treated residual soil." *Geomechanics and Engineering*, 7(6), 633-647.
[24] Kim, E. C. (2013). "주요 7개국 시멘트산업 동향 분석/보고."KCA (Korea cement association).
[25] Chang, I., Jeon, M., and Cho, G.-C. (2015). "Application of microbial biopolymers as an alternative construction binder for earth buildings in underdeveloped countries." *International Journal of Polymer Science*, 2015.
[26] Astm, D. (2011). "2487, Standard Classification of Soils for Engineering Purposes (Unified Soil Classification System)." *Annual Book of ASTM Standards*, 4, 206-215.
[27] Schroth, B. K., and Sposito, G. "Surface charge properties of kaolinite." *Proc., MRS Proceedings*, Cambridge Univ Press, 87.
[28] Sposito, G., Skipper, N. T., Sutton, R., Park, S.-h., Soper, A. K., and Greathouse, J. A. (1999). "Surface geochemistry of the clay minerals." *Proceedings of the National Academy of Sciences*, 96(7), 3358-3364.
[29] Sridharan, A., and Jayadeva, M. (1982). "Double layer theory and compressibility of clays." *Geotechnique*, 32(2), 133-144.
[30] Di Maio, C., Santoli, L., and Schiavone, P. (2004). "Volume change behaviour of clays: the influence of mineral composition, pore fluid composition and stress state." *Mechanics of materials*, 36(5), 435-451.
[31] Van de Velde, K., and Kiekens, P. (2002). "Biopolymers: overview of several properties and consequences on their applications." *Polymer Testing*, 21(4), 433-442.
[32] Congress, U. S. (1993). "Biopolymers: Making Materials Nature's way." *Office of Technological Assessement*, 51-62.
[33] Saha, D., and Bhattacharya, S. (2010). "Hydrocolloids as thickening and gelling agents in food: a critical review." *Journal of Food Science Technology*, 47(6), 587-597.
[34] Lorenzo, G., Zaritzky, N., and Califano, A. (2012). "Rheological analysis of emulsion-filled gels based on high acyl gellan gum." *Food Hydrocolloids*, 30, 672-680.
[35] Velde, K. V. d., and Kiekens, P. (2002). "Biopolymers: overview of several properties and consequences on their applications." *Polymer Testing*, 21, 433-442.
[36] Orts, W. J., Roa-Espinosa, A., Sojka, R. E., Glenn, G. M., Imam, S. H., Erlacher, K., and Pedersen, J. S. (2007). "Use of synthetic polymers and biopolymers for soil stabilization in agricultural,

construction, and military applications." *Journal of materials in civil engineering*, 19(1), 58-66.
[37] Ferruzzi, G. G., Pan, N., and Casey, W. H. (2000). "Mechanical Properties of Gellan and Polyacrylamide Gels With Implications for Soil Stabilization." *Soil Science*, 165(10), 778-792.
[38] Orts, W. J., Sojka, R. E., and Glenn, G. M. (2000). "Biopolymer additives to reduce erosion-induced soil losses during irrigation." *Industrial Crops and Products*, 11(1), 19-29.
[39] Chang, I., Im, J., Prasidhi, A. K., and Cho, G.-C. (2015). "Effects of Xanthan gum biopolymer on soil strengthening." *Construction and Building Materials*, 74, 65-72.
[40] Awad, Y. M., Blagodatskaya, E., Ok, Y. S., and Kuzyakov, Y. (2012). "Effects of polyacrylamide, biopolymer, and biochar on decomposition of soil organic matter and plant residues as determined by 14 C and enzyme activities." *European Journal of Soil Biology*, 48, 1-10.
[41] Jang, J., and Carlos Santamarina, J. (2015). "Fines Classification Based on Sensitivity to Pore-Fluid Chemistry." *Journal of Geotechnical and Geoenvironmental Engineering*, 142(4), 06015018.
[42] Bear, F. E. (1964). "Chemistry of the Soil." *Soil Science*, 98(1), 70.
[43] Devidal, J.-L., Dandurand, J.-L., and Gout, R. (1996). "Gibbs free energy of formation of kaolinite from solubility measurement in basic solution between 60 and 170 C." *Geochimica et Cosmochimica Acta*, 60(4), 553-564.
[44] Sondi, I., Bišćan, J., and Pravdić, V. (1996). "Electrokinetics of pure clay minerals revisited." *Journal of Colloid and Interface Science*, 178(2), 514-522.
[45] Hensen, E. J., and Smit, B. (2002). "Why clays swell." *Journal of Physical Chemistry B*, 106(EPFL-ARTICLE-200697), 12664-12667.
[46] Garcıa-Ochoa, F., Santos, V., Casas, J., and Gomez, E. (2000). "Xanthan gum: production, recovery, and properties." *Biotechnology advances*, 18(7), 549-579.
[47] Martin, G., Yen, T., and Karimi, S. "Application of biopolymer technology in silty soil matrices to form impervious barriers." *Proc., 7th Australia New Zealand Conference on Geomechanics: Geomechanics in a Changing World: Conference Proceedings*, Institution of Engineers, Australia, 814.
[48] ASTM, D. "4318-05 (2005)." *Standard test methods for liquid limit, plastic limit, and plasticity index of soil*.
[49] Koumoto, T., and Houlsby, G. (2001). "Theory and practice of the fall cone test." *Géotechnique*, 51(8), 701-712.
[50] Casagrande, A. (1958). "Notes on the design of the liquid limit device." *Geotechnique*, 8(2), 84-91.
[51] BS1377 (1990). "Methods of test for soils for civil engineering purposes." *British Standards Institution, London*.
[52] Carter, D., Mortland, M., and Kemper, W. (1986). "Specific surface."
[53] Hang, P. T., and Brindley, G. (1970). "Methylene blue absorption by clay minerals. Determination of surface areas and cation exchange capacities (clay-organic studies XVIII)." *Clays and clay minerals*, 18(4), 203-212.
[54] Mansour, Z., Taha, M. R., and Chik, Z. (2008). "Fresh-brine water effect on the basic engineering properties of Lisan marl-dead sea-jordan." *Journal of Applied Sciences*, 8(20), 3603-3611.

[55] Laneuville, S. I., Turgeon, S. L., Sanchez, C., and Paquin, P. (2006). "Gelation of native β-lactoglobulin induced by electrostatic attractive interaction with xanthan gum." *Langmuir*, 22(17), 7351-7357.
[56] WBCSD (2015). "The indian Water Tool version 2 (IWT 2.1)." <http://www.indiawatertool.in/>. (Oct. 12, 2016).
[57] Kasim, N., Mohammad, A. W., and Abdullah, S. R. S. (2016). "Performance of membrane filtration in the removal of iron and manganese from Malaysia's groundwater." *Membrane Water Treatment*, 7(4), 277-296.
[58] Rajapakse, J. P., Gallage, C., Dareeju, B., Madabhushi, G., and Fenner, R. (2015). "Strength properties of composite clay balls containing additives from industry wastes as new filter media in water treatment." *Geomechanics and Engineering*, 8(6), 859-872.
[59] Vidali, M. (2001). "Bioremediation. an overview." *Pure and Applied Chemistry*, 73(7), 1163-1172.
[60] Marco, A., Esplugas, S., and Saum, G. (1997). "How and why combine chemical and biological processes for wastewater treatment." *Water Science and Technology*, 35(4), 321-327.
[61] Khoiruddin, K., Hakim, A. N., and Wenten, I. G. (2014). "Advances in electrodeionization technology for ionic separation - A review." *Membrane Water Treatment*, 5(2), 87-108.
[62] Shackelford, C. D., and Jefferis, S. A. "Geoenvironmental engineering for in situ remediation." *Proc., ISRM International Symposium*, International Society for Rock Mechanics.
[63] Matilainen, A., Vepsäläinen, M., and Sillanpää, M. (2010). "Natural organic matter removal by coagulation during drinking water treatment: a review." *Advances in colloid and interface science*, 159(2), 189-197.
[64] Chang, I., and Cho, G.-C. (2010). "A New Alternative for Estimation of Geotechnical Engineering Parameters in Reclaimed Clays by using Shear Wave Velocity." *ASTM Geotechnical Testing Journal*, 33(3), 171-182.
[65] Sengco, M. R., Li, A., Tugend, K., Kulis, D., and Anderson, D. M. (2001). "Removal of red-and brown-tide cells using clay flocculation. I. Laboratory culture experiments with Gymnodinium breve and Aureococcus anophagefferens." *Marine ecology progress series*, 210, 41-53.
[66] Csempesz, F. (2000). "Enhanced flocculation of colloidal dispersions by polymer mixtures." *Chemical Engineering Journal*, 80(1), 43-49.
[67] Aguilar, M., Sáez, J., Lloréns, M., Soler, A., Ortuno, J., Meseguer, V., and Fuentes, A. (2005). "Improvement of coagulation–flocculation process using anionic polyacrylamide as coagulant aid." *Chemosphere*, 58(1), 47-56.
[68] Tatsi, A., Zouboulis, A., Matis, K., and Samaras, P. (2003). "Coagulation–flocculation pretreatment of sanitary landfill leachates." *Chemosphere*, 53(7), 737-744.
[69] Amuda, O., and Alade, A. (2006). "Coagulation/flocculation process in the treatment of abattoir wastewater." *Desalination*, 196(1), 22-31.
[70] Pierce, R. H., Henry, M. S., Higham, C. J., Blum, P., Sengco, M. R., and Anderson, D. M. (2004). "Removal of harmful algal cells (Karenia brevis) and toxins from seawater culture by clay flocculation." *Harmful Algae*, 3(2), 141-148.

[71] Seybold, C. (1994). "Polyacrylamide review: Soil conditioning and environmental fate." *Communications in Soil Science & Plant Analysis*, 25(11-12), 2171-2185.
[72] Kim, M., Song, I., Kim, M., Kim, S., Kim, Y., Choi, Y., and Seo, M. (2015). "Effect of Polyacrylamide Application on Water and Nutrient Movements in Soils." *Journal of Agricultural Chemistry and Environment*, 4(03), 76.
[73] Theodoro, J. D. P., Lenz, G. F., Zara, R. F., and Bergamasco, R. (2013). "Coagulants and natural polymers: perspectives for the treatment of water." *Plastic and Polymer Technology*, 2(3), 55-62.
[74] Chang, I., and Cho, G.-C. (2012). "Strengthening of Korean residual soil with β-1,3/1,6-glucan biopolymer." *Construction and Building Materials*, 30(0), 30-35.
[75] Chang, I., and Cho, G.-C. (2014). "Geotechnical behavior of a beta-1,3/1,6-glucan biopolymer-treated residual soil." *Geomechanics and Engineering*, 7(6), 633-647.
[76] Chang, I., Im, J., and Cho, G.-C. (2016). "Introduction of microbial biopolymers in soil treatment for future environmentally-friendly and sustainable geotechnical engineering." *Sustainability*, 8(3), 251.
[77] Chang, I., Im, J., and Cho, G.-C. (2016). "Geotechnical engineering behaviors of gellan gum biopolymer treated sand." *Canadian Geotechnical Journal*, 53(10), 1658-1670.
[78] Chang, I., Im, J., Prasidhi, A. K., and Cho, G.-C. (2015). "Effects of Xanthan gum biopolymer on soil strengthening." *Construction and Building Materials*, 74(0), 65-72.
[79] Chang, I., Jeon, M., and Cho, G.-C. (2015). "Application of microbial biopolymers as an alternative construction binder for earth buildings in underdeveloped countries." *International Journal of Polymer Science*, 2015, 9.
[80] Chang, I., Prasidhi, A. K., Im, J., Shin, H.-D., and Cho, G.-C. (2015). "Soil treatment using microbial biopolymers for anti-desertification purposes." *Geoderma*, 253–254(0), 39-47.
[81] Pan, J. R., Huang, C., Chen, S., and Chung, Y.-C. (1999). "Evaluation of a modified chitosan biopolymer for coagulation of colloidal particles." *Colloids and Surfaces A: Physicochemical and Engineering Aspects*, 147(3), 359-364.
[82] Pan, G., Zhang, M.-M., Chen, H., Zou, H., and Yan, H. (2006). "Removal of cyanobacterial blooms in Taihu Lake using local soils. I. Equilibrium and kinetic screening on the flocculation of Microcystis aeruginosa using commercially available clays and minerals." *Environmental Pollution*, 141(2), 195-200.
[83] Roussy, J., Van Vooren, M., and Guibal, E. (2005). "Chitosan for the coagulation and flocculation of mineral colloids." *Journal of dispersion science and technology*, 25(5), 663-677.
[84] Chatterjee, T., Chatterjee, S., Lee, D. S., Lee, M. W., and Woo, S. H. (2009). "Coagulation of soil suspensions containing nonionic or anionic surfactants using chitosan, polyacrylamide, and polyaluminium chloride." *Chemosphere*, 75(10), 1307-1314.
[85] Chatterjee, S., Chatterjee, S., Chatterjee, B. P., Das, A. R., and Guha, A. K. (2005). "Adsorption of a model anionic dye, eosin Y, from aqueous solution by chitosan hydrobeads." *Journal of colloid and interface science*, 288(1), 30-35.
[86] Chheda, A., and Vernekar, M. (2014). "A natural preservative ε-poly-L-lysine: fermentative

production and applications in food industry."
[87] Hiraki, J., Ichikawa, T., Ninomiya, S.-i., Seki, H., Uohama, K., Seki, H., Kimura, S., Yanagimoto, Y., and Barnett, J. W. (2003). "Use of ADME studies to confirm the safety of ε-polylysine as a preservative in food." *Regulatory Toxicology and Pharmacology*, 37(2), 328-340.
[88] Mazia, D., Schatten, G., and Sale, W. (1975). "Adhesion of cells to surfaces coated with polylysine. Applications to electron microscopy." *The Journal of cell biology*, 66(1), 198-200.
[89] Park, T. G., Jeong, J. H., and Kim, S. W. (2006). "Current status of polymeric gene delivery systems." *Advanced drug delivery reviews*, 58(4), 467-486.
[90] Dutta, P. K., Dutta, J., and Tripathi, V. (2004). "Chitin and chitosan: Chemistry, properties and applications." *Journal of scientific and industrial research*, 63(1), 20-31.
[91] Goosen, M. F. A. (1997). *Applications of Chitin and Chitosan*, Technomic Pub., Lancaster, Pa.
[92] Hirano, S., Koishibara, Y., Kitaura, S., Taneko, T., Tsuchida, H., Murae, K., and Yamamoto, T. (1991). "Chitin Biodegradation in Sand Dunes." *Biochemical Systematics and Ecology*, 19(5), 379-384.
[93] Linden, J. C., Stoner, R. J., Knutson, K. W., and Gardner-Hughes, C. A. (2000). "Organic disease control elicitors." *Agro Food Industry Hi-Tech*, 11(5), 32-34.
[94] Kobayashi, S., Kiyosada, T., and Shoda, S. (1996). "Synthesis of artificial chitin: Irreversible catalytic behavior of a glycosyl hydrolase through a transition state analogue substrate." *Journal of the American Chemical Society*, 118(51), 13113-13114.
[95] Shin, Y., Yoo, D. I., and Min, K. (1999). "Antimicrobial finishing of polypropylene nonwoven fabric by treatment with chitosan oligomer." *Journal of Applied Polymer Science*, 74(12), 2911-2916.
[96] Sezer, A. D., and Akbuga, J. (1999). "Release characteristics of chitosan treated alginate beads: II. Sustained release of a low molecular drug from chitosan treated alginate beads." *Journal of Microencapsulation*, 16(6), 687-696.
[97] Bartkowiak, A., and Hunkeler, D. (1999). "Alginate-oligochitosan microcapsules: A mechanistic study relating membrane and capsule properties to reaction conditions." *Chemistry of Materials*, 11(9), 2486-2492.
[98] Suzuki, T., Mizushima, Y., Umeda, T., and Ohashi, R. (1999). "Further biocompatibility testing of silica-chitosan complex membrane in the production of tissue plasminogen activator by epithelial and fibroblast cells." *Journal of Bioscience and Bioengineering*, 88(2), 194-199.
[99] Gupta, A., Yunus, M., and Sankararamakrishnan, N. (2013). "Chitosan-and iron–chitosan-coated sand filters: a cost-effective approach for enhanced arsenic removal." *Industrial & Engineering Chemistry Research*, 52(5), 2066-2072.
[100] Juang, R. S., and Shiau, R. C. (2000). "Metal removal from aqueous solutions using chitosan-enhanced membrane filtration." *Journal of Membrane Science*, 165(2), 159-167.
[101] Liu, X. D., Tokura, S., Haruki, M., Nishi, N., and Sakairi, N. (2002). "Surface modification of nonporous glass beads with chitosan and their adsorption property for transition metal ions." *Carbohydrate Polymers*, 49(2), 103-108.
[102] Kolaian, J. H., and Low, P. F. "Thermodynamic properties of water in suspensions of montmorillonite." *Proc., Clays and Clay Minerals: Proceedings of the Ninth National Conference on*

Clays and Clay Minerals, Elsevier, 71.
[103] Imai, G. (1980). "Settling behavior of clay suspension." *Soils and Foundations*, 20(2), 61-77.
[104] Kondo, F., and Torrance, J. K. (2005). "Effects of smectite, salinity and water content on sedimentation and self-weight consolidation of thoroughly disturbed soft marine clay." *Paddy and Water Environment*, 3(3), 155-164.
[105] Imai, G. (1981). "Experimental studies on sedimentation mechanism and sediment formation of clay materials." *Soils and Foundations*, 21(1), 7-20.
[106] Michaels, A. S., and Bolger, J. C. (1962). "Settling rates and sediment volumes of flocculated kaolin suspensions." *Industrial & Engineering Chemistry Fundamentals*, 1(1), 24-33.
[107] Petzold, G., Mende, M., Lunkwitz, K., Schwarz, S., and Buchhammer, H.-M. (2003). "Higher efficiency in the flocculation of clay suspensions by using combinations of oppositely charged polyelectrolytes." *Colloids and Surfaces A: Physicochemical and Engineering Aspects*, 218(1), 47-57.
[108] Li, W., Zhou, W., Zhang, Y., Wang, J., and Zhu, X. (2008). "Flocculation behavior and mechanism of an exopolysaccharide from the deep-sea psychrophilic bacterium Pseudoalteromonas sp. SM9913." *Bioresource Technology*, 99(15), 6893-6899.
[109] Kurane, R., Hatamochi, K., Kakuno, T., Kiyohara, M., Hirano, M., and Taniguchi, Y. (1994). "Production of a bioflocculant by Rhodococcus erythropolis S-1 grown on alcohols." *Bioscience, biotechnology, and biochemistry*, 58(2), 428-429.
[110] Ma, K., and Pierre, A. C. (1992). "Sedimentation behavior of a fine kaolinite in the presence of fresh Fe electrolyte." *Clays and Clay Minerals*, 40(5), 586-592.
[111] Pierre, A. (1992). "The gelation of colloidal platelike particles." *Journal of the Canadian Ceramic Society*, 61(2), 135-138.
[112] Zou, H., Pan, G., Chen, H., and Yuan, X. (2006). "Removal of cyanobacterial blooms in Taihu Lake using local soils II. Effective removal of Microcystis aeruginosa using local soils and sediments modified by chitosan." *Environmental Pollution*, 141(2), 201-205.
[113] Ghaee, A., and Zerafat, M. M. (2016). "Adsorption mechanism of copper ions on porous chitosan membranes: Equilibrium and XPS study." *Membrane Water Treatment*, 7(6), 555-571.
[114] Yukselen, M. A., and Gregory, J. (2004). "The reversibility of floc breakage." *International Journal of Mineral Processing*, 73(2–4), 251-259.
[115] Sidik, W. S., Canakci, H., Kilic, I. H., and Celik, F. (2014). "Applicability of biocementation for organic soil and its effect on permeability." *Geomechanics and Engineering*, 7(6), 649-663.
[116] Rand, B., and Melton, I. E. (1977). "Particle interactions in aqueous kaolinite suspensions: I. Effect of pH and electrolyte upon the mode of particle interaction in homoionic sodium kaolinite suspensions." *Journal of Colloid and Interface Science*, 60(2), 308-320.
[117] Tambo, N., and Watanabe, Y. (1979). "Physical characteristics of flocs—I. The floc density function and aluminium floc." *Water Research*, 13(5), 409-419.
[118] Ahn, S., Um, Y., Lee, Y., and Kim, J. (1994). "The Evaluation of Engineering Characteristics for Domestic Marine Clay." *Korea Institute of Construction Technology, KICT*, 149.
[119] Das, B. M. (2013). *Advanced soil mechanics*, CRC Press.

[120] D4648, A. (2000). "Standard Test Method for Laboratory Minituare Vane Shear Test for Saturated Fine-Grained Clayey Soil." *Annual Book of ASTM Standards*, 1-7.
[121] Wroth, C., and Wood, D. (1978). "The correlation of index properties with some basic engineering properties of soils." *Canadian Geotechnical Journal*, 15(2), 137-145.

Acknowledgments in Korean

지반 시스템 연구실에서 2년간의 석사 과정은 지반 공학도로 첫 발돋움을 하는 저에게 뜻 깊은 시간이었습니다. 많은 분들의 도움으로 석사학위라는 첫 발걸음을 내딛을 수 있었던 것 같습니다.

먼저 부족한 저에게 지반 공학이라는 학문을 진지하게 임할 수 있도록 이끌어주시고, 끊임없는 격려와 지도, 조언과 가르침을 주신 조계춘 교수님께 깊은 감사의 말씀을 드립니다. 앞으로 시작하게 될 박사학위 과정 중에도 교수님의 가르침 아래 초심을 잃지않고 배우는 자세로 임하겠습니다. 아울러, 학부시절부터 현재까지의 저를 형성하는 데에 있어 많은 조언과 가르침을 주신 이승래 교수님, 김동수 교수님, 권태혁 교수님께 깊은 감사의 말씀을 드립니다. 교수님들께서 보여주신 학문에 대한 열정을 본받아 열심히 연구하는 지반공학도가 되겠습니다.

석사과정 2년간을 돌이켜보면, 좌충우돌했던 것 같습니다. 이러한 제가 제 몫을 할 수 있도록 물심양면 도움을 주신 지반 시스템 연구실의 선배님들, 홍은수 박사님, 정성훈 박사님, 김아람 박사님, 창호형, 요한이형, Tran thi phuong an, 지원이, 케냐, 정태형, 철환이형, 태진이형, 석준이에게 감사의 말씀을 드리고 싶습니다. 또한, 아무것도 모르는 저를 동생처럼, 선생님처럼 물심양면 도와주신 정문숙 선생님께 감사의 말씀을 드립니다. 그리고, 백지장처럼 하얗던 저를 바이오폴리머의 색으로 물들여주신 장일한 박사님께 감사의 말씀을 드립니다.

또한 함께하며 많은 것들을 배우고 공유하게 만들어준 친구들, 길완, 해찬, 남우, 대원, 준희, 익준에게 감사하다고 말하고 싶습니다.

2년 간의 석사 과정이 어느 정도의 성공과 어느 정도의 실패 인지는 아직은 가늠할 수 없습니다. 앞으로 이어지는 박사 과정을 통해 많은 결실을 얻어서, 지나보니 내 석사 과정은 그래도 성공적이었다고 생각할 수 있는 사람이 되고자 노력하겠습니다.

마지막으로, 저를 건강히 낳아주시고 오늘날에 이르기까지 끝없는 사랑으로 응원해주신 아버지, 어머니께 사랑한다는 말씀 드리고 싶습니다. 그리고 이제 곧 결혼을 하게 될 우리 형에게도 감사의 말씀을 전합니다. 끝으로, 항상 힘이 되고 행복이 되는 동반자 은진이에게 감사하고 사랑한다는 말을 전합니다.

Curriculum Vitae in Korean

이　　름: 권 영 만 (權 寧 晩)

생년월일: 1991년 4월 24일

출 생 지: 경상북도 안동시

학 력

2007. 3. - 2010. 2. 한일고등학교

2010. 2. - 2015. 2. 한국과학기술원 건설및환경공학과 (학사)

2015. 8. - 2017. 8. 한국과학기술원 건설및환경공학과 (석사)

학회활동

1. **Kwon, Y. M**., Im, J., Chang, I., & Cho, G. C. (2016). "Polylysine biopolymer for coagulation of contaminated water" The 2016 World Congress on Advances in Civil, Environmental, and Materials Research (ACEM16), Jeju island, Korea.

2. **Kwon, Y. M**., Im, J., Chang, I., & Cho, G. C. (2016). "Characteristics of Xanthan Gum Bio-Polymer: Pore-Fluid Chemistry of Xanthan Treated Soils and Their Different Behaviors." The 29th KKHTCNN symposium on Civil Engineering (KKHTCNN), Hong Kong.

3. **권영만**, 임주영, 조계춘, 정문경, & 장일한. (2016). "미생물 기원 바이오폴리머 함유 흙의 액소성 거동 특성에 관한 실험 연구." 대한토목학회 학술대회, 165-166.

4. **권영만**, 임주영, 장일한, & 조계춘. (2017). "잔탄검 바이오폴리머 처리 흙의 액성한계 거동." 한국지반공학회 봄학술발표회.

연구업적

1. **Kwon, Y. M**., Im, J., Chang, I., & Cho, G. C. (2017). "ε-Polylysine biopolymer for coagulation of clay suspensions." Geomechanics and Engineering, An Int'l Journal Vol. 12 No. 5.

2. 김재현, **권영만**, 박근보, 김영석, & 김동수 (2017). "동남극 테라노바만 흙 시료의 동결 및 비동결 상태에서의 동적특성 평가." 한국지반공학회논문집, 33(3), 37-4